EFFECT OF FRACTIONATION ON THE SORPTION PROPERTIES OF NOM ONTO MODIFIED TiO_2 SURFACES

by

YELİZ ÜLKER

BS. in Chem. Teach., Boğaziçi University, 2005

Submitted to the Institute of Environmental Sciences in partial fulfillment of

the requirements for the degree of

Master of Science

in

Environmental Sciences

Boğaziçi University

2008

EFFECT OF FRACTIONATION ON THE SORPTION PROPERTIES OF NOM ONTO MODIFIED TiO_2 SURFACES

APPROVED BY:

Prof. Dr. Miray Bekbölet ……..
(Thesis Supervisor)

Prof. Dr. Ferhan Çeçen ……..

Prof. Dr. Zekiye Çınar ……..

DATE OF APPROVAL (Day/Month/Year) ……

Dedicated to my mother…

ACKNOWLEDGEMENTS

I am deeply grateful for the overwhelming guidance, support and excellent supervision I have received from Prof. Dr. Miray Bekbölet, Institute of Environmental Sciences, Boğazici University. Her intuition and knowledge have never ceased to amaze me. She provided me with many opportunities for invaluable scientific and personal experiences. She created always a friendly and stimulating atmosphere that made me enjoy my work very much.

I would like to express my appreciation to the members of my thesis jury; Prof. Dr. Ferhan Çeçen, Institute of Environmental Sciences, Boğazici University and Prof. Dr. Zekiye Çınar, Director of Science Institute for their valuable time and comments.

I would also like to thank Dr. Ceyda Senem Uyguner, Institute of Environmental Sciences, Boğazici University, for the nice working atmosphere and the warmhearted helps and valuable discussions. I am also much indebted to her, on whose competent advice and most efficient help I could always rely.

Last but not least, I would like to thank my parents for their love and their unconditioned and never-ending support of whatever will make me happy. No words are sufficient to thank my wonderful friend “Uğur”. The patience, love, sacrifice, encouragement, care and support freely given by his which I experienced during my study were invaluable and made all the difference.

EFFECT OF FRACTIONATION ON THE SORPTION PROPERTIES OF NOM ONTO MODIFIED TiO_2 SURFACES

Natural organic matters (NOM) can be broadly divided into two fractions: hydrophobic (humic substances), and hydrophilic or non-humic substances. Chemical composition of humic substance varies with molecular size and the differences in the chemical composition between size fractions may have significant consequences on the environmental chemistry and geochemistry of humic substances. They have a crucial role in transporting the contaminants in the environment because of their solubility.

Contaminant distribution can be reduced by removing humic substances that have soluble subclass as humic and fulvic acids. Due to the heterogeneity of humic acids in terms of physical and chemical properties, they were fractionated into molecular fractions by using different suitable membranes.

Due to the photocatalytic properties, TiO_2 that is used for the degradation of undesirable chemical contaminants in water has been the focus of many investigations. By comparing the adsorption of the humic acid and its fractions onto bare and surface modified titanium dioxide, this work presented important information for understanding the photocatalytic efficiencies of TiO_2.

This study is conducted to investigate the complex interactions between the surface properties of titanium dioxide and the molecular size dependent fractions of the humic acid in order to provide information in relation to the photocatalytic degradation of humic acids with surface modified TiO_2 powders.

FRAKSİYONLARIN KATKILANDIRILMIŞ TiO_2 YÜZEYLERİNDE DOM ADSORPSİYON ÖZELLİKLERİNE ETKİLERİ

Doğal organik maddeler (DOM) genel olarak iki bölüme ayrılabilir: hidrofobik (hümik maddeler), ve hidrofilik veya gayri-hümik maddeler. Hümik maddenin kimyasal bileşimi, moleküler büyüklükle değişir ve boyut fraksiyonların arasında kimyasal bileşimdeki farklar, çevre kimyasında ve hümik maddelerinin jeokimyasında önemli sonuçlara sahip olabilir. Çözülebilirliğinden dolayı, hümik maddeler çevredeki kirleticileri taşımakta önemli bir role sahiptir.

Kirletici madde dağılımı, hümik ve fülvik asitler olarak çözülebilir alt sınıfa sahip olan hümik maddelerin giderilmesiyle azaltılabilir. Hümik asitlerin fiziksel ve kimyasal özellikler bakımından heterojenliği nedeniyle, farklı uygunlukta membranlar kullanılarak hümik asitler molekül fraksiyonlarına ayrılmıştır.

Fotokatalitik özellikleri nedeniyle, suda istenmeyen kimyasal kirletici maddelerin giderilmesinde kullanılan TiO_2, birçok araştırmanın odağı olmuştur. Bu çalışma, sade ve yüzeyi değiştirilmiş titanyum dioksit üzerindeki hümik asitin ve onun fraksiyonlarının adsorpsiyonu kıyaslanarak, TiO_2'in fotokatalitik verimliliklerini anlamada önemli bilgi sundu.

Bu çalışma, titanyum dioksit tozlarının yüzey değişimiyle hümik asitlerin fotokatalitik giderimine ilişkin bilgiyi sağlamak amacıyla, titanyum dioksitin yüzey özellikleri ve hümik asitin molekül büyüklüğüne bağlı fraksiyonları arasındaki karmaşık etkileşimleri araştırmak için yürütüldü.

TABLE OF CONTENTS

LIST OF FIGURES

LIST OF TABLES

LIST OF SYMBOLS/ABBREVIATIONS

Symbol	Explanation	Units used
AA	Ascorbic Acid	
C	Concentration	mgL^{-1}
C_e	Equilibrium concentration of adsorbate	mgL^{-1} (TOC)
		m^{-1} (UV-vis)
C_i	Initial concentration of adsorbate	mgL^{-1} (TOC)
		m^{-1} (UV-vis)
Cs	Amount of adsorbate adsorbed on adsorbent	mgL^{-1} (TOC)
		m^{-1} (UV-vis)
$Color_{436}$	Absorbance at 436 nm	
$\Delta\lambda$	Bandwidth	nm
DBPs	Disinfection by-Products	
FA	Fulvic Acid	
FI	Fluorescence Intensity	
FTIR	Fourier Transform Infrared	
GAC	Granular Activated Carbon	
GC/MS	Gas Chromatography-Mass Spectrometry	
HA	Humic Acid	
HPSEC	High Performance Size Exclusion Chromatography	
HS	Humic Substances	
K_a	Langmuir Adsorption Constant	mgL (TOC)
		m^{-1} (UV-vis)
K_d	Distribution coefficient	
K_f	Freundlich Adsorption Capacity Constant	
MW	Molecular Weight	
1/n	Freundlich adsorption intensity parameter	
NMR	Nuclear Magnetic Resonance	
NOM	Natural Organic Matter	

PAC	Powdered Activated Carbon	
q_A	Adsorbed amount per unit weight of adsorbent	$mgL^{-1}g^{-1}$ (TOC) $m^{-1}g^{-1}$ (UV-vis)
q_m	Maximum adsorption	mgg^{-1} (TOC) $m^{-1}g^{-1}$ (UV-vis)
SPE	Solid Phase Extraction	
SOCs	Synthetic Organic Chemicals	
TOC	Total Organic Carbon	mgL^{-1}
UV/Vis	Ultraviolet-Visible	
UF	Ultrafiltration	
UV_{254}	Absorbance at 365 nm	
UV_{280}	Absorbance at 280 nm	
UV_{365}	Absorbance at 254 nm	

1. INTRODUCTION

Humic substances are ubiquitous in the environment. They are found in animals, plants, coals, sediments, soils and water. The ubiquitous presence of humic substances, combined with their ability to provide multiple sites for chemical reaction, makes them relevant to numerous biogeochemical processes such as mineral weathering, nutrient bioavailability, contaminant transport, and affect the rates of geological processes. They are crucial components of the carbon cycle and other life processes. Humic substances have been the subject of numerous scientific studies due to their ability to bind contaminants and therefore strongly affect their environmental behavior.

Humic substances are of amphiphilic nature, they contain both hydrophobic and hydrophilic moieties. Amongst humic substances, humic acids have complex structures and contain a number of biologically active functional groups including carboxylic acid, phenolic hydroxyl, and methoxyl and amine groups. The reactivity of humic substances depends on their functional group chemistry and microstructure.

Chemical composition varies with molecular size and that differences in the chemical composition between size fractions may have significant consequences on the environmental chemistry and geochemistry of humic substances. The differences in the structural characteristics, chemical environments and functional group contents of the humic acid fractions affect the adsorption capability.

Humic substances are responsible for the color in drinking water; they comprise of large complex organic molecules originating from microbial decay of dead organisms. Removal of humic substances has long been of concern in water treatment due to their diverse reactivity and abundance in natural waters. There are several methods to remove the humic acids from water as coagulation, advanced oxidation processes and adsorption.

As a serial study, the adsorption of humic acid and its molecular size fractions onto the bare TiO_2, Fe doped TiO_2 and ascorbic acid modified TiO_2 powders as adsorbents

were studied. The humic acid was fractionated by the ultrafiltration technique to reduce the humic acids chemical heterogeneity. The related data were presented in terms of the UV-vis and TOC properties of humic substances. The molecular and structural characteristics of the humic acid molecule relative to changes during adsorption were monitored by fluorescence spectroscopy (emission and synchronous scan). For comparison purposes, the adsorption data were evaluated in terms of adsorption isotherm models *i.e.* Freundlich model in order to assess the adsorption model parameters.

2. THEORETICAL BACKGROUND

2.1. Natural Organic Matter

The researches has documented that natural organic matter (NOM) contains many organic compounds and composition. This term is used to describe the complex mixture of organic material, such as humic acids, hydrophilic acids, proteins, lipids, amino acids and hydrocarbons, present in all natural water sources. They have different structures, functional group distribution, molecular weights, and composition as well as reactivity. These organic matters are present in all natural waters because of breaking down plant and animal materials. They have essential role in aquatic systems because NOM binds and transports inorganic and organic pollutants in water and promote the formation of harmful by-products during disinfection process and they are used as substrate for undesired heterotrophic growth in water distribution system.

They can be leached from soil, diffused from wetland sediments, and released by plankton and bacteria. Natural organic material adsorbs on natural particles and acts as a particle-stabilizing agent in surface water. It may be associated with toxic metals and synthetic organic chemicals (SOCs) (Snoeyink and Summers, 1999). NOM acts also as important precursor of disinfection by-products (DBPs) and enables the microorganisms to grow in the treatment unit or distribution system (Khan et al., 1998; Siddiqui et al., 1997). Therefore the treatment of water to remove natural organic matter has a crucial importance.

Natural organic matter is a complex mixture of organic compounds, which interact with many inorganic and organic pollutants and may decrease toxicities of these pollutants in water chemistry (Cabaniss and Shuman, 1988; Ma et al., 1999).

To understand the role of NOM including humic substances (HS) in water chemistry, it is often necessary to isolate NOM. Various methods have been used to isolate NOM from natural water. XAD resin method has been reported in many applications for fractionation of NOM and is generally considered as the state-of-art method at present for

such fractionation, though the method at strongly acidic and basic conditions may include certain risks for uncontrolled fractionation or reactions (Leenheer, 1981; Thurman and Malcolm, 1981). After fractionation of NOM by resin adsorption, characterization of NOM is carried out to gather the information on chemical composition by various spectroscopic techniques and on molecular size by high performance size exclusion chromatography (HPSEC). In the use of HPSEC, however, it is not effective for the analyses of small molecular weight compounds including organic carboxylic acids. Spectroscopic techniques such as ultraviolet-visible (UV/Vis), Fourier-transform infrared (FTIR), nuclear magnetic resonance (NMR), and fluorescence have been previously applied for both quantitative and qualitative characterization of NOM (Hautala et al., 2000; Davis et al., 1999; Thomsen et al., 2002; Peuravuori et al., 2002).

2.1.1. Humic Substances

Humic substances are conventionally defined as "a series of relatively high-MW, brown to black colored substances, formed by secondary synthesis reactions" (Stevenson, 1994) or as "a category of naturally occurring, biogenic, heterogeneous organic substances that can generally be characterized as being yellow-to-black in color, of high molecular weight (MW), and refractory" (Aiken et al., 1985).

The humic term is commonly used to refer to three fractions of humic substances: humic acid (HA), fulvic acid (FA), and humin. These fractions are defined operationally in terms of their solubility in aqueous media as a function of pH or in terms of their extractability from soils or sediments as a function of the pH of the extracting medium. Humic acid is the fraction of HS that is not soluble in water under acidic conditions, but becomes soluble (or extractable) at higher pH values. Fulvic acid is the fraction that is soluble in aqueous media at all pH values. Humin represents the fraction that is not soluble in an aqueous medium (or is not extractable with an aqueous medium) at any pH value. Actually, humin consists of an aggregate of humic and nonhumic materials (Rice and MacCarthy, 1990); as such, humin is better described as a humic-containing material rather than as a humic substance.

Table 2.1. Some important functional groups of humic substances

Functional group	**Structure**
Acidic groups	
Carboxyl	R-C=O(-OH)
Enol	R-CH=CH-OH
Phenolic OH	Ar-OH
Quinone	Ar=O
Neutral groups	
Alcoholic OH	R-CH_2-OH
Ether	R-CH_2-O-CH_2-R
Ketone	R-C=O(-R)
Aldehyde	R-C=O(-H)
Ester	R-C=O(-OR)
Basic groups	
Amine	R-CH_2-NH_2
Amide	R-C=O(-NH-R)

R: represents an aliphatic backbone comprising a broad category of straight, branched, saturated or unsaturated carbon compounds

Ar: is an aromatic ring

Despite intensive research on humic substances during the past decades, the chemical nature of humic and fulvic acids is not fully understood. Studies using a variety of spectroscopic techniques have led to major advances in understanding the chemical

structure of humic substances (Stevenson, 1994). As presented in Table 2.1, they are known to contain functional groups *i.e.* C=C, COOH, OH, OCH_3, C=O, NH or NH_2, arrangements such as redox quinone-semiquinone-hydroquinone, charge-transfer planar complexes. Both their dark color and paramagnetism most likely result from the electronic structure of their core; aromatic subunits, an extended (p-electron) system in the semiquinone moieties, and the electron donor-acceptor nature (Suffet and MacCarthy, 1989).

The elemental composition and major types of functional groups of humic and fulvic acids are well established, but the macromolecular structure and chemical heterogeneity of humic substances in relation to molecular size distribution is still controversial (Clapp and Hayes, 1999). The classical view of humic substances states that they are macromolecular, negatively charged, branched polyelectrolyte with mainly carboxylic and phenolic type acidic functional groups (Swift, 1989).

Table 2.2. Elemental composition of humic substances and several plant materials (Kononova, 1966)

Substances	**% dry ash-free basis**			
	C	**H**	**O**	**N**
Fulvic acids	44 – 49	3.5 – 5.0	44 - 49	2.0 – 4.0
Humic acids	52 – 62	3.0 – 5.5	30 - 33	3.5 – 5.0
Proteins	50 – 55	6.5 – 7.3	19 - 24	15.0 – 19.0
Lignin	62 – 69	5.0 – 6.5	26 - 33	-

It is apparent that humic substances consist of a heterogeneous mixture of compounds for which no single structural formula will suffice; however, compositional information can be obtained from elemental and functional group analysis as presented in Table 2.2. Elemental contents of HAs, FAs, and humins from all over the world are remarkably consistent (Rice and MacCarthy, 1991). Of the three humic fractions, humin has received less attention than humic acid and fulvic acid, likely due to its low carbon content. The elemental analysis of humic and fulvic acids from a range of environmental sources show

that the low molecular weight fulvic acids have higher oxygen but lower carbon contents than the high molecular weight humic acids.

Differences between humic acids and fulvic acids can be explained by variations in molecular weight, the number of functional groups (carboxyl, phenolic OH) and the extent of polymerization. Another important difference is that while oxygen in fulvic acids can be accounted for largely in known functional groups (COOH, OH, C=O), a high portion of the oxygen in humic acids seems to occur as a structural components of the molecules.

Table 2.3. Estimated abundance of functional groups (mequiv g^{-1})* in humic and fulvic acids

Functional group	**Humic acid**	**Fulvic acid**
Total acidic groups	5.6-8.9	6.4-14.2
Carboxyl, COOH	1.5-5.7	5.2-11.2
Phenolic, OH	2.1-5.7	0.3-5.7
Alcoholic OH	0.2-4.9	2.6-9.5
Quinoid/keto, C=O	0.1-5.6	0.3-3.1
Methoxy, OCH_3	0.3-0.8	0.3-1.2

*mequiv g^{-1} equivalent to mmol of each group per g of humic substances

Humic acids have lower oxygen but higher carbon contents than fulvic acids. Fulvic acids contain more functional groups of an acidic nature, particularly COOH. Therefore total acidities of fulvic acids are considerably higher than humic acids. The estimated abundances of these groups in humic and fulvic acids are given in Table 2.3. There is an important difference that while the oxygen in fulvic acids can be accounted for largely in known functional groups (COOH, OH, C=O), a high portion of the oxygen in humic acids seems to occur as a structural component of the nucleus.

Characterization with the molecular level of detail available from pyrolysis GC/MS has allowed for the proposal of numerous structural models of humic substances (Schulten and Leinweber, 2000). Humic acids are indeed thought to be complex aromatic macromolecules with amino acids, amino sugars, and peptides, aliphatic compounds involved in linkages between the aromatic groups. Humic substances have an abundance of

oxygen-containing functional groups (carboxyl, phenolic, alcoholic) which dominate their chemical properties. The Figure 2.1 shows hypothetical structure of humic acid which contains free and bound phenolic OH groups, quinone structures, nitrogen and oxygen as bridge units and COOH groups variously placed on aromatic rings.

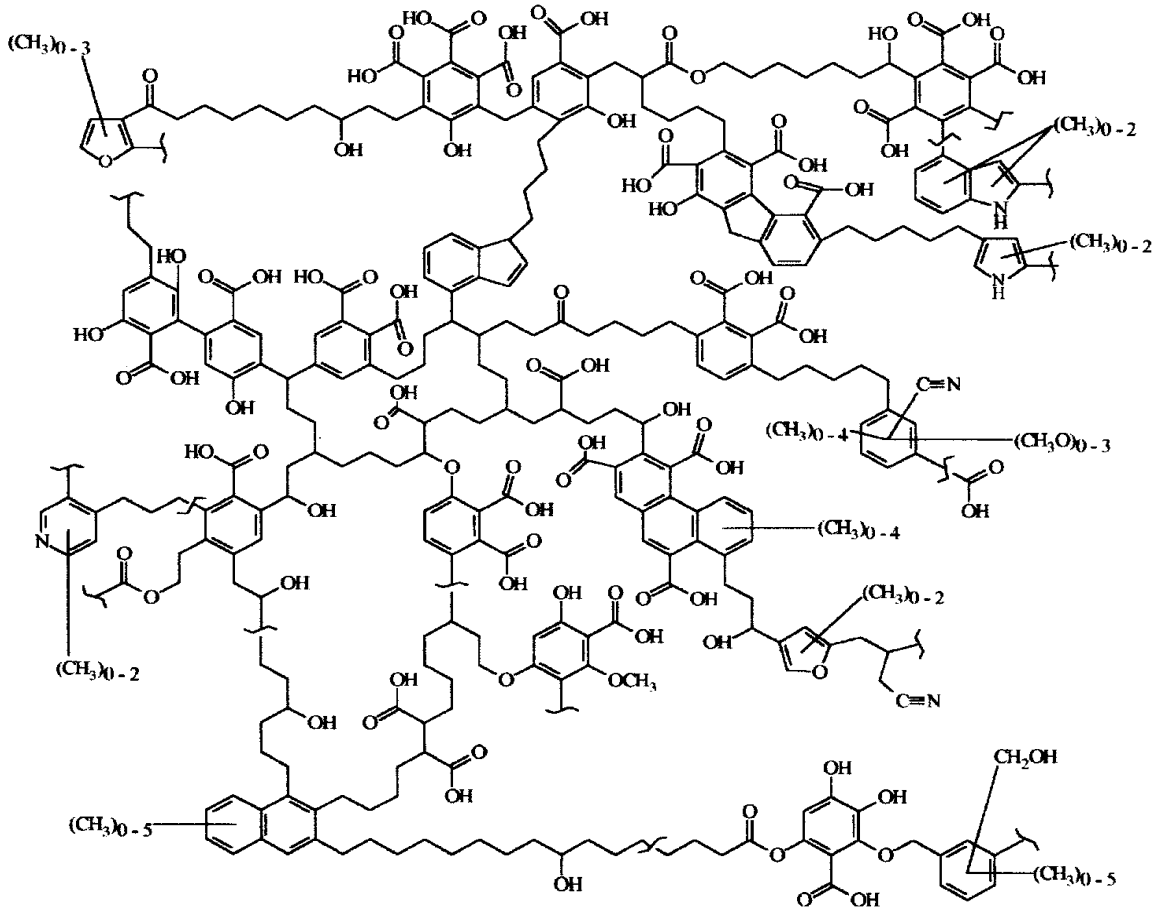

Figure 2.1. State of the art structural concept of a humic acid (Jones and Bryan, 1999)

The hypothetical model structure of fulvic acid (Buffle's model) shown in Figure 2.2, contains both aromatic and aliphatic structures, both extensively substituted with oxygen-containing functional groups. However, the structures of fulvic acid are more aliphatic and less aromatic than humic acids. Fulvic acids contain more functional groups of an acidic nature, particularly COOH. The reason for their high solubility in water at all pH values is mainly due to the presence of carboxylic acid, phenolic and ketonic groups in appreciable amounts.

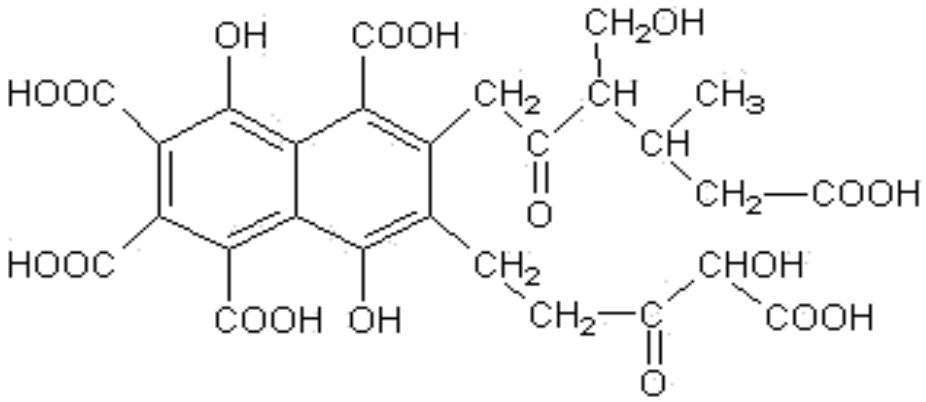

Figure 2.2. Structure of fulvic acid (Buffle et al, 1977)

One-dimensional spectra of humic substances provide information on the relative intensities of the various carbon or nitrogen functional groups, and this information is useful when attempting to derive some structural information. Spectral editing techniques have been utilized in the past to enhance signals from specific groups of functionalized carbons or nitrogens (Wilson, 1987; Preston, 1996).

Natural organic matter, such as humic matter, may arrange in solution to form a supramolecular aggregate composed of hydrophilic and hydrophobic domains which may be contiguous to or contained in each other (Piccolo et al., 2002). A hydrophilic domain is assumed to be more hydrated than the hydrophobic domain and in contact with the external solution, if not totally separated from the aqueous medium by the strictly associated hydrophobic domain (Piccolo et al., 2002).

Micelle formation would require that HS have amphiphilic properties in which the molecules have hydrophobic (nonpolar) and hydrophilic (polar) parts. Charge densities of HS and of the NMR data, which indicate that as much as one carbon in five is present as a carboxyl group, should be considered in the case of some HAs. That phenolic and other weakly acidic functionalities can make significant contributions to charge density, especially at the higher pH values, suggests that it is unlikely that there are extensive hydrophobic stretches in humic molecules, except, perhaps, in the cases of the materials of lowest charge densities that fall in the HA category (Clapp and Hayes, 1999).

HS can be macromolecular, but the extent of their macromolecularity can vary depending, possibly, on the substrate materials, on the extent of the biological degradation and synthesis processes, and on the environments in which they are formed and found (Clapp and Hayes, 1999)

Some researchers have recently proposed an alternative model of humic acids, stating that they are self-associates of small, uniform humic acid molecules which are held together by weak hydrophobic forces (Piccolo et al., 1996; Conte and Piccolo, 1999; Piccolo et al., 1999). Evidence for this view stems primarily from size exclusion chromatography (SEC), in which addition of low molecular weight organic acids leads to drastic decreases in the apparent molecular size (Piccolo et al., 1996; Piccolo et al., 1999). However, the interpretation of such experiments has been questioned because addition of organic acids in SEC may cause experimental artifacts (Perminova, 1999).

A better understanding of the macromolecular structure, molecular size distribution, and chemical heterogeneity in relation to molecular size is a prerequisite for the further development of geochemical models involving humic and fulvic acids. The most valid argument for HA fractionation is that many interactions and processes of HA in the environment can be more or less dependent on their molecular size.

In general, low molecular weight, hydrophilic humic fractions are expected to be more mobile in soils and groundwater than the high molecular weight, hydrophobic humic fractions (Davis and Gloor, 1981). Differences in the chemical composition between size fractions may have a strong influence on the environmental behavior of humic substances (Silva et al., 1981), for instance their binding capability towards pollutants (John, et al., 1988) and their sorption behavior onto mineral surfaces (Tanaka and Senoo, 1995).

Among the fractionation methods available, ultrafiltration (UF) using different suitable membrane filters is a reasonably simple method to differentiate polydisperse mixtures of molecules (Burba et al., 1998, Nifant'eva et al. 1999). It is one of the few separation methods functioning without additional separation media and auxiliary reagents, thus avoiding blank substances as interferents. The simple and reliable scale-up of UF from the micro to the macro dimension in commercial UF units, which allows the rapid

fractionation of relatively large quantities of humic acid, is another relevant advantage of this separation method (Nifant'eva et al. 1999)

The varied structure of humic acids and content of highly diverse functional groups make these substances very important material for many research workplaces. The structure particularly accounts for many very interesting properties of humic acids, e.g. spectral, colloidal, electrochemical, ion-exchangeable, and absorbing ones. Humic acids are capable of absorbing heavy metals by forming complexes with functional groups (COOH, C=O, and -OH) that are bound on the surface of the acids. Utilization of humic acids in the wide spectrum of fields is a subject for further research and development.

2.2. Adsorption

Adsorption, the adhesion of liquids, gases, and dissolved substances to the surface of solids to a surface, is contrasted with absorption, the filling of pores in a solid. It is an important process in transportation of the contaminants and removal of them in environment. In this process molecules or ions present in one phase are called adsorbate condensing and concentrate on the surface of another phase is called adsorbent.

Adsorption can be classified as physical adsorption, chemical adsorption, and exchange adsorption. In the physical adsorption which is relatively nonspecific there are weak forces of attraction or van der Waals' forces between molecules and it is reversible. It is predominant at low temperature, and is characterized by a relatively low energy of adsorption while adsorbed molecule is free to move about over the adsorbent surface. In the chemical adsorption, adsorbed molecules form a layer on the surface. In chemical adsorption, there are much stronger forces between the molecules, so it is rarely reversible. Exchange adsorption refers to electrical attraction between the molecules due to opposite charge on the surface. Chemical adsorption is rarely reversible; hence, in order to remove the adsorbed materials, the adsorbent must be heated to higher temperatures. Electrical attraction between the adsorbate and the surface is classified as exchange adsorption. As a result of electrostatic attraction to sites of opposite charge on the surface, ions of substance concentrate at the surface. Generally, the charge on the ion is the determining factor for

example; trivalent ion is attracted much more strongly toward a site of opposite charge than monovalent ions.

Adsorption is directly related with surface area of the adsorbent, pore size distribution, as well as the characteristic of the adsorbed molecules. Diffusion coefficients, in particular, decrease as molecular size increases, and thus longer times are required to remove the large-molecular-weight humic substances than are needed for the low-molecular-weight phenols, for example. Adsorbent particle size is also important because it determines the time required for transport within the pore to available adsorption sites (Snoeyink and Summers, 1999).

There are other factors that affect the adsorption like pH and temperature. Generally, adsorption is increased at pH ranges where the species have no any charge. Many organics form negative ions at high pH, positive ions at low pH, and neutral species in intermediate pH ranges. Moreover, pH affects the charge on the surface, altering its ability to adsorb materials. Many organic pollutants in water are highly adsorbed by decreasing pH because of neutralization of negative charges at the carbon surface with increasing hydrogen concentration.

When temperature is increased the adsorption extent decreases because adsorption reactions are exothermic. The total amount of heat evolved in the adsorption of a definite quantity of solute on an adsorbent is termed the heat of adsorption, ΔH which is the change in the heat content of the system when adsorption occurs. Heats of gas-phase adsorption generally are several kcal per mole, but because water is desorbed from the surface when adsorption from aqueous solution occurs, heat effects for the latter process are somewhat smaller than those for gas-phase adsorption. (Weber, 1972)

2.2.1. Adsorption Equilibrium

Adsorption of molecules can be represented as a chemical reaction:

$$A + B \leftrightarrow A \cdot B$$

Where A is the adsorbate, B is the adsorbent, and A·B is the adsorbed compound. Adsorbates are held on the surface by various types of chemical forces such as hydrogen

bonds, dipole-dipole interactions, and van der Waals forces (Snoeyink and Summers, 1999). If the reaction is reversible, it is at a critical time that the rate of the forward reaction (adsorption) equals the rate of the reverse reaction (desorption).When this condition exists, equilibrium has been reached and no further change in the concentration of the reactants and products will occur. At this moment, both reactions continue on taking place simultaneously and there is a defined distribution of solute between the solid and the liquid phase. In the adsorption process, this distribution ratio is a measure of the position of equilibrium in the adsorption process; it may be a function of the concentration of the solute, the concentration and nature of competing solutes, the nature of the solution, and so on.

2.2.2. Adsorption Isotherm

The constant-temperature equilibrium relationship between the quantity of adsorbate per unit of adsorbent q_A and its equilibrium solution concentration C_e is called the adsorption isotherm. Adsorption isotherms relate the adsorbate or solute concentration in the bulk liquid to the concentration of the adsorbent on the solid phase at equilibrium. These isotherms are used in the design of adsorption beds and in determining the transport of solutes through them. Several equations or models are available that describe this function (Sontheimer et al., 1988) like Freundlich isotherm, Langmuir isotherm, BET isotherm.

One of the most important characteristics of an adsorbent is the quantity of adsorbate it can accumulate. The constant-temperature equilibrium relationship between the quantity of adsorbate per unit of adsorbent q_A and its equilibrium solution concentration C_e is called the adsorption isotherm (Snoeyink and Summers, 1999). Generally, q_A increases with C but not in direct proportion. The adsorption isotherms are equilibrium equations and apply to conditions resulting after the adsorbate-containing phase has been contact with the adsorbent for sufficient time to reach equilibrium (Sawyer and McCarty, 1978).

Adsorption isotherms for solutes in dilute solutions can be classified according to initial slope (Giles et al., 1960, 1974a, 1974b). Different solutes show different behavior on the adsorbent. (Weber, 1972), so their adsorption isotherms can be termed according to

their shapes resembling the letters, such as “L” type, “S” type, “C” type, etc. (Giles et al., 1960). The four main classes, which are shown in Figure 2.3, are briefly described in Sposito (1989).

The S-curve isotherm is characterized by initially small slope that increases with adsorptive concentration. This indicates that the affinity of the adsorbent for the adsorbate is less than that of the aqueous solution. It may also suggest the presence of cooperative interactions such that increasing surface coverage increases the solute's affinity for the surface. The S-curve isotherm is the result of cooperative interactions among the adsorbed molecules. These interactions cause the adsorbate to become stabilized on a solid surface and, thus produce an enhanced affinity of the surface for the adsorbate as its concentration increases.

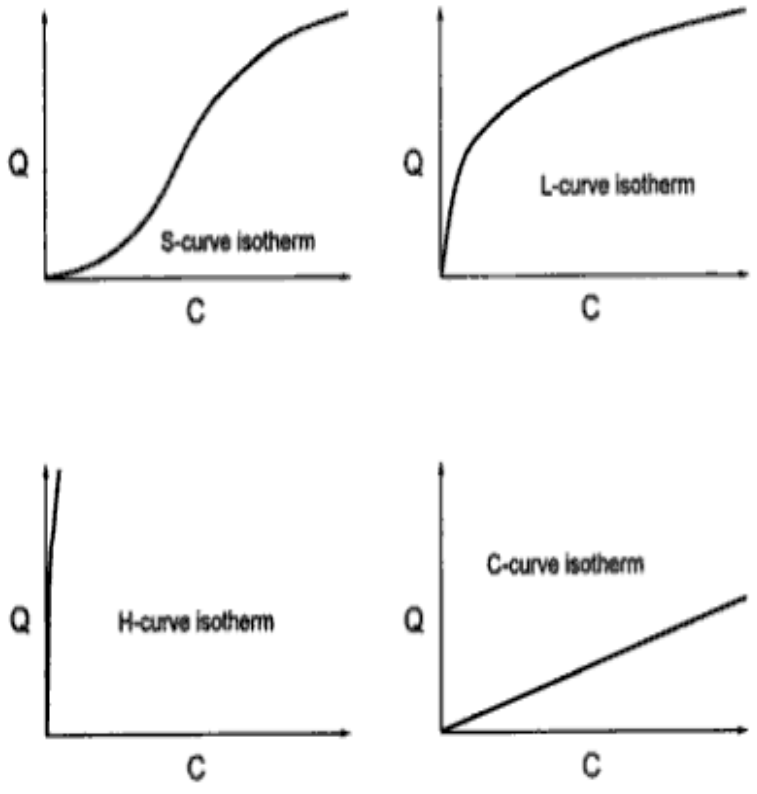

Figure 2.3. The four general categories of adsorption isotherm

L curve isotherm which typically concave to the concentration axis, is generally characterized by an initial slope that does not increase with the concentration of adsorbate in the solution. This type of isotherm is the resultant effect of a high relative affinity of the adsorbent particles for the adsorbate at low concentration. In addition, as the concentration of the adsorbate increases, the amount of the remaining adsorbing surface is decreased.

The C-curve isotherm shows an initial slope that remains independent of adsorptive concentration until the maximum possible adsorption is achieved. This type of isotherm is produced either by a constant partitioning of a substance between the interfacial region and the soil solution or by a proportionate increase in the amount of adsorbing surface as the concentration of an adsorbate increases.

The H-curve isotherm is an extreme version of the L-curve isotherm. It is characterized by a large initial slope suggesting a very high relative affinity of the adsorbent for an adsorbate which is caused either by very specific interactions between the solid phases and the adsorbate (inner-sphere surface complexation) or by significant van der Waals interactions in the adsorption process. It is illustrate that the observed H-curve isotherm is the result of specific adsorption. Large organic molecules and inorganic polymers (e.g., aluminum hydroxyl polymers) provide examples of H-curve isotherms resulting from van der Waals interactions.

2.2.2.1. Linear Model. If the accumulation of solute on the adsorbent is directly proportional to the solution phase concentration, linear model can be used.

Linear model is,

$$C_s = K_d C_e \tag{2.1}$$

Where, K_d represents the distribution coefficient, which can be also named partition coefficient, C_e is the concentration of adsorbate remaining in the solution at equilibrium. And C_s stands for the mass of contaminant adsorbed per unit weight of the adsorbent.

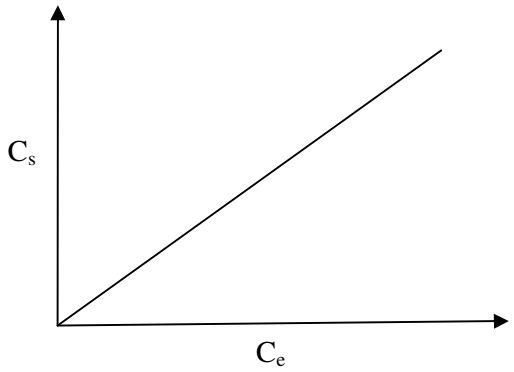

Figure 2.4.Linear adsorption

2.2.2.2. The Langmuir Isotherm. The Langmuir isotherm is based on the assumptions that the sorption for each molecule is independent of surface coverage and adsorbate and solvent molecules compete to adsorb on sites on the surface of the adsorbent. The Langmuir relation assumes that maximum adsorption corresponds to a saturated monolayer of solute molecules on the adsorbent surface, that the energy of adsorption is constant, and that there is no transmigration of adsorbate in the plane of the surface. In other words, adsorption is limited to monolayer coverage. Hence, the quantity adsorbed reaches the maximum quantity adsorbable when all sites are occupied (Weber, 1972).

The Langmuir adsorption isotherm expresses a single layer adsorption and gives a curve that describes the fraction of the surface area of the adsorbent covered with solute, as a function of the concentration of the solute in the contacting liquid phase. The Langmuir isotherm is a curve, convex to the solute concentration axis, and flattens out when the total surface is covered with solute. The isotherm for double layer adsorption is similar to single layer adsorption but the initial convex part of the curve is sharper. The adsorption isotherm only tends to linearity at very low concentrations of solute (at very low surface coverage) and so symmetrical peaks will only be achieved with very small samples.

The Langmuir equation has the form,

$$q_A = \frac{q_m K_a C_e}{1 + K C_e} \qquad (2.2)$$

Here, q_A stands for the mass of the contaminant adsorbed per unit weight of the adsorbent. K_a represents an empirical constant, which is called the binding constant. C_e is the concentration of adsorbate in solution at equilibrium. q_m is the maximum quantity adsorbable when all the adsorption sites are occupied. The experimentally determined values of q_m and K_a often are not constant over the concentration range of interest, possibly because of the heterogeneous nature of the adsorbent surface (a homogeneous surface was assumed in the model development), lateral interactions between adsorbed molecules (all interaction was neglected in the model development), and other factors (Snoeyink and Summers, 1999).

Linear form of the Langmuir equation is obtained by taking the reciprocal of the both side of the equation (2.2) and rearranging it:

$$\frac{1}{q_A} = \frac{1}{q_m} + \frac{1}{K_a q_m C_e} \tag{2.3}$$

The straight line form of the Langmuir isotherm can be obtained by using the linearized model.

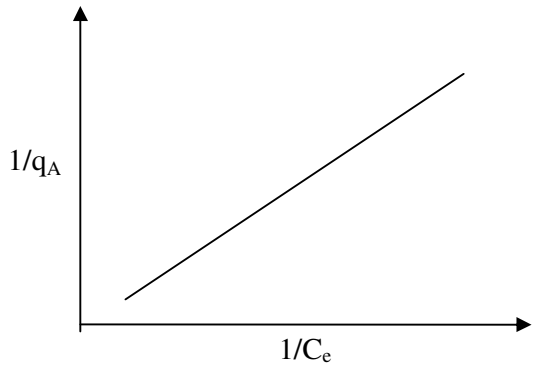

Figure 2.5. The straight line form of the Langmuir Isotherm

2.2.2.3. The Freundlich Isotherm. Freundlich isotherm is a non-linear adsorption equilibrium model that describes the adsorption occurrences on heterogeneous surfaces composed of different adsorption sites with adsorption on each site following Langmuir isotherm. The equation does not imply any particular mechanism of adsorption. It is

purely empirical, and has been found to be most satisfactory in the low concentration range (vanLoon and Duffy, 2000) and it is very useful because it accurately describes much adsorption data.

This equation has the form:

$$q_A = K_f C_e^{1/n} \tag{2.4}$$

Here, C_e (with units of mass/volume, or moles/volume) is the concentration of adsorbate remaining in solution at equilibrium, q_A (with units of mass adsorbate/mass adsorbent, or mole adsorbate/mass adsorbent) stands for the mass of contaminant adsorbed per unit weight of the adsorbent. The terms 1/n is a constant for a given system; 1/n is unitless and it is a function of the strength of adsorption that the rate of the adsorption increase with solute concentration. K_f is also a constant in the Freundlich equation and it is related primarily to the capacity of the adsorbent for the adsorbate. The units of K_f are determined by the units of q_A and C_e.

And the equation (2.4) can be linearized as follows:

$$\log q_A = \log K_f + \log C_e \tag{2.5}$$

The corresponding graph will be:

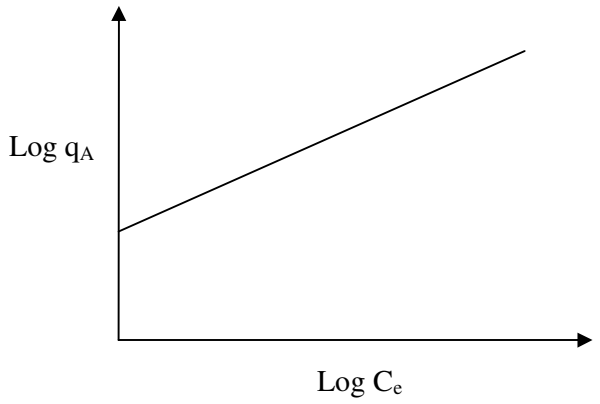

Figure 2.6. Graph of the linearized form of the Freundlich Isotherm

For fixed values of K_f and C_e, the smaller the value of 1/n, the stronger is the adsorption bond. As 1/n becomes very small, the capacity tends to be independent of C_e and the isotherm plot approaches the horizontal level; the value of q_A then is essentially constant, and the isotherm is termed irreversible. If the value of 1/n is large, the adsorption bond is weak, and the value of q_A changes markedly with small changes in C_e (Snoeyink and Summers, 1999). The Freundlich isotherm is known to be operative only within certain concentration limits that adsorbent approaches saturation. At the saturation point, q_A is independent of further increases in C_e, and the Freundlich equation no longer applies.

2.2.2.4. Sorption Efficiency. Percentage of the sorption which is also called sorption efficiency can be used to evaluate the experimental data.

$$\text{Sorbed } \% = \frac{C_s}{C_i} \tag{2.6}$$

Here, C_i is the initial concentration of the material adsorbate, and C_s is the concentration of the sorbed material.

Adsorption plays an important role in the improvement of water quality. Activated carbon, for example, can be used to adsorb specific organic molecules that cause taste and odor, mutagenicity, and toxicity, as well as natural organic matter (NOM) that causes color and that can react with chlorine to form disinfection byproducts (DBPs). NOM is a complex mixture of compounds such as fulvic and humic acids, hydrophilic acids, and carbohydrates. The aluminum hydroxide and ferric hydroxide solids that form during coagulation will also adsorb NOM. Adsorption of NOM on anion exchange resins may reduce their capacity for anions, but ion exchange resins and adsorbent resins are available that can be used for efficient removal of selected organic compounds. Calcium carbonate and magnesium hydroxide solids formed in the lime softening process have some adsorption capacity, and pesticides adsorbed on clay particles can be removed by coagulation and filtration (Snoeyink and Summers, 1999). Several mechanisms are involved in the adsorption of humic substances by clay minerals, the main ones being: van der Waals' forces, bonding by cation bridging, H – bonding, adsorption by association with hydrous oxides, adsorption on interlamellar spaces of clay minerals.

2.3. Titanium Dioxide

Titanium dioxide occurrences in nature are never pure; it is found with contaminant metals such as iron. The oxides can be mined and serve as a source for commercial titanium. The metal can also be mined from other minerals such as ilmenite or leucoxene ores, or one of the purest forms, rutile beach sand. All three of these types are expressed using the same chemical formula (TiO_2); however, their crystal structures are different. Titanium dioxide exists in three forms, rutile (stable phase), anatase (low-temperature phase), brookite (metastable phase). Rutile form which tends to be more stable at high temperature commonly found in igneous rocks and belongs to the tetragonal crystal system. Anatase form also belongs to the tetragonal crystal system but it tends to be more stable at lower temperature. Brookite phase generally found in the minerals and it has a structure belonging to the orthorhombic crystal system. Rutile and anatase forms are more common because they produce easily.

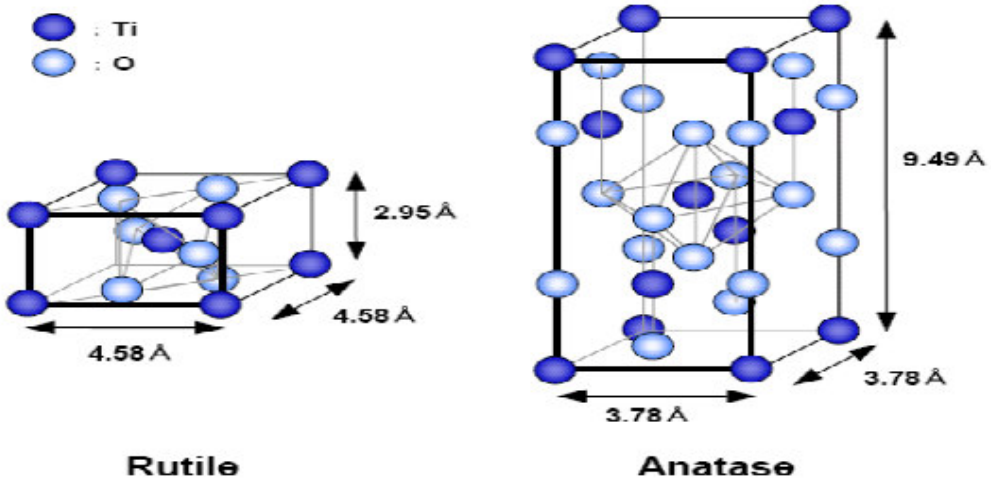

Figure 2.7. Titanium dioxide unit cell

Rutile has a density of 4.2 g mL^{-1} while Anatase has a density of 3.9 g mL^{-1}. This difference is explained by their different crystal structures. The rutile modification is more closely packed than the Anatase crystal, where each metal center occupies the center of an

octahedron of oxygen ligands, each of which is bound to three metals (Balzani and Scandola 1991).

Titanium dioxide (TiO_2), encompassing all its three crystal forms, has wide applications in various fields. One of the most recent applications is as a photocatalyst (Sclafani et al., 1990; Matthews, 1991; Hua et al., 1995; Robertson et al., 1997; Wang and Adesina, 1997; Kosanic′, 1998; Tatsuma et al., 1999). Another promising aspect is as an inorganic ion exchanger and sorbent due to its high chemical stability and high ion exchange capacity, which may find application in solid phase extraction (SPE) (Vassileva et al., 1996).

Titanium dioxide (TiO_2) is a potent photocatalyst that can break down almost any organic compound it touches when exposed to sunlight in the presence of water vapor. TiO_2 is excited due to ultraviolet light with wavelength shorter than 380 nm, and it generates $^{\bullet}OH$ radicals which oxidize organic compounds in water. In recent years, the technique of metal ion- into TiO_2 has been widely studied. Noble metals, e.g. Pt, are most commonly studied (Linsebigler et al., 1995; Sakthivel et al., 2004), and other metals, e.g. Au, Pd, Ru, have been reported to be beneficial for photocatalytic reactions (Sakthivel et al., 2004).

The transitional metal ions, e.g. Fe (Hoffmann et al., 1995), have been used for increasing the photocatalytic activity. Most commercial titanium dioxide products are coated with inorganic (e.g. alumina, zirconia, silica) and organic (e.g. polyols, esters, siloxanes, silanes) compounds to control and improve surface properties. Another purpose of surface modification of TiO_2 is to inhibit recombination of hotogenerated electrons and holes by increasing the charge separation and therefore to enhance the efficiency of the photocatalytic process.

The benefits of surface modification are: (i) inhibiting recombination by increasing the charge separation and therefore the efficiency of the photocatalytic process; (ii) increasing the wavelength response range (i.e. the photocatalyst can be excited in the visible light region); and (iii) changing the selectivity or yield of a particular product (Linsebigler et al., 1995).

Besides its well known photocatalytic activity, titanium dioxide could also be used as a model oxide surface in evaluation the adsorption processes occurring in natural waters. The presence of metal ions and an organic substrate could also serve as the surface modifications that could be attained under conditions prevalent to the natural systems.

Suphandag (1998) studied the adsorption capacity of natural organic matter on semi-conductor powders. The adsorption capacity of humic acid was investigated under different pH conditions onto three different crystal structures of TiO_2 powders that the range changed from 0.1mg mL^{-1} to 1mg mL^{-1}. It was found that the adsorption capacity was higher at lower pH of humic acid solution, regardless of the crystal structures of TiO_2 powders used. Later, Suphandag (2006) examined the adsorption behavior of humic acid on the photocayalyst metal oxide. It was concluded that the adsorption of humic acids onto TiO_2 is affected by buildup of negative surface charge, limited size availability, and factors that control the size of humic acid molecules.

Bas (2001) investigated humic acid and surface interactions for adsorption and desorption at three different pH levels. It was reported that the crystal structures of TiO_2 powders affect the adsorption and desorption behavior of humic acid. Higher adsorption efficiencies were observed for Degussa P-25. Likewise, higher desorption efficiencies were observed for Millenium PC500 within the studied TiO_2 range. Adsorption efficiencies of two commercial humic acids (Aldrich and Roth) were evaluated at different pH and it was concluded that Aldrich humic acid has higher adsorption efficiency due to the differences in their structure and chemical composition.

Uyguner and Bekbolet (2005a) studied the spectral changes of humic acids during oxidation processes and the effects of the molecular size distribution of photocatalytically treated humic acid samples. In order to analyze the spectroscopic characteristics of photocatalytically oxidized humic acid, raw and treated humic acids were ultrafiltered into size fractions using membranes. It was reported that the degradation of the high molecular size fractions of humic acid to lower molecular weight compounds leads to decreasing the TOC value for raw humic acid comparing with that of the corresponding treated humic acid fractions. Since the probable formation of partial oxidation products such as alcohols,

aldehydes, ketones and carboxylic acids, the fluorescence spectra of all the fractions of treated humic acid has lower wavelengths than raw humic acid fractions.

Uyguner and Bekbolet (2004) investigated the effect of the chromium ion concentration on the adsorption of humic acid onto TiO_2. It was concluded that both $Color_{436}$ and UV_{254} was used as parameters in order to evaluate the adsorption effects of humic acid and chromium ions on the titanium dioxide surface. The presence of chromium ions was found to inhibit the adsorption capacity of humic acid onto TiO_2 powder.

Uyguner et al. (2007) reported the ozonation, photocatalysis and sequential oxidation systems followed by adsorption and coagulation characteristic of humic acids. They used two types of activated carbons in adsorption experiments (PAC and GAC) and aluminum sulfate ($Al_2 (SO_4)_3.18H_2O$), and ferric chloride ($FeCl_3 .6H_2O$) in coagulation experiments. It was found that $Color_{436}$ removal efficiencies for untreated, photocatalytically oxidized, ozonated, and sequentially oxidized humic acids increased for increasing PAC doses. $Color_{436}$ removal efficiencies for untreated, sequentially oxidized, photocatalytically oxidized, and ozonated humic acids also increased for GAC. On the other hand, UV_{254} removal efficiencies for untreated, photocatalytically oxidized, ozonated, and sequentially oxidized humic acids decreased for increasing PAC and GAC doses. The adsorption capacities at $Color_{436}$ were higher than for the UV absorbing centers after treatment.

Bekbolet et al. (2002) examined the photocatalytic efficiencies of two commercial TiO_2 powders (Degussa P-25 and Hombikat UV-100) on the decolorisation of humic acids, and adsorption properties of humic acids onto TiO_2 specimens. The photocatalytic degradation efficiencies and adsorption capacities for Degussa P-25 were found to be higher than for Hombikat UV-100. It was concluded that there was certain dependency between the adsorption characteristics and the photocatalytic decolorization rates but no dependency onto the surface area of TiO_2 powders.

Bekbolet et al. (1996) studied the effect of photocatalyzed oxidation on the degradation and decolorization of humic acid. Adsorptive behavior of humic acid was also studied for the photocatalaytically oxidized humic acid. It was reported that with respect to a decrease in the content of organic matter and decolorization an increase in

biodegradability was observed after the photocatalaytic oxidation of humic acid. There was no significant change in adsorptivity but when the irradiation time was increased the adsorption characteristic of humic acid showed a change.

Bekbolet and Ozkosemen (1996) examined the effects of the photocatalyst concentration, pH, and humic acid concentration during photocatalytic degradation of humic acid. The optimum TiO_2 concentration was found as 1.0 mg mL^{-1} since further increase in TiO_2 concentration led to opacity of the solution and acidic medium was found to be more favorable due to positively charged surface characteristic of TiO_2. It was concluded that photocatalaytic oxidation of humic acid by using TiO_2 could be effective pretreatment method to keep the trihalomethane levels below the limit of 100 μgL^{-1}.

Selcuk and Bekbolet (2008) studied the photocatalytic and photoelectrocatalytic treatment methods for removing humic acid under different experimental conditions. Photoelectrocatalytic system was performed for humic acid oxidation in the presence of chloride anion and humic acid to observe the selectivity of the photoelectrocatalytic system. To investigate the inhibitory effect of carbonate species, the system was performed in the presence and absence of carbonate species. It was reported that the attraction of humic acid to the surface of TiO_2 was stronger than that of chloride ions and carbonate ions retarded HA degradation at basic condition.

Uyguner and Bekbolet (2007) examined the impact of aqueous Cr (VI) and Mn (II) species on the photocatalytic oxidation of humic acids as a major component of natural organic matter in aquatic systems. The experiment results were evaluated in terms of Langmuir-Hinshelwood rate with respect to $Color_{436}$ due to the pseudo-first-order rate constant explains the overall removal tendency covering all competitive and consecutive reactions. The presence of these ions affected the adsorptive properties of the photocatalyst and the photocatalytic oxidation rate of humic acids. The impact of manganese ion on the photocatalytic oxidation could be better explained in terms of L-H kinetics where 15% increase was observed with respect to $Color_{436}$ while 54% decrease observed in the presence of chromium.

Uyguner and Bekbolet (2005b) studied the photocatalytic removal of model humic and fulvic acids of different origins (terrestrial and aquatic) by using TiO_2 Degussa P-25 as the photocatalyst. It was reported that there was substantial differences in photocatalytic removal efficiencies of humic and fulvic acids on the basis of their diverse chemical and physical properties such as molecular weight, molecular size, elemental composition and source of origin.

Kerc et al. (2003a) examined the effect of partial oxidation by ozonation on the photocatalytic degradation of humic acids. In order to achieve partially oxidized humic acid samples prior to photocatalytic oxidation, ozonation was applied to humic acid solutions under the specified experimental conditions for an effective $Color_{436}$ and UV_{254} removal. It was concluded that there was no significant correlation between the photocatalytic oxidation rates and the dark adsorption properties of the ozonated as well as untreated humic acid samples.

Kerc et al. (2003b) studied sequential oxidation of humic acids by ozonation and photocatalysis. Titanium dioxide was used as photocatalyst in the photocatalytic oxidation phase. It was concluded that sequential oxidation of humic acids by ozonation and photocatalysis was efficient in both UV absorbing centers and color forming chromophoric moieties removals. The preozonation led to the increasing the photocatalytic degradation rate and the changes in adsorption characteristic due to alterations in humic acid molecular structure with ozonation.

3. MATERIALS AND METHODS

3.1. Materials

All chemicals used in this study are analytical grade.

3.1.1. Humic Acid

The model humic acid used in all experiments was supplied from Aldrich (Aldrich Co. Ltd.,USA). 1000 ppm humic acid solution was prepared by dissolving the humic acid in distilled deionized water and filtering through filter paper. Stock solution of humic acid was stored in amber glass bottles to prevent decomposition due to light. 50 ppm solutions by dilution were prepared before the conducting the experiments from the stock solution. Distilled deionized water that has conductivity less than 10 μS^{-1} was used to prepare these solutions. Humic acid samples were fractionated using ultrafiltration stirred cells into appropriate molecular sizes; 0.45 μm, 100 kDa, and 30 kDa.

3.1.2. Titanium Dioxide

The metal oxide which was used, throughout the experiments was titanium dioxide powder,TiO_2 Degussa P-25, having a BET surface area of 50 ± 15 m^2/g and mainly in anatase crystal form (anatase 70% and rutile 30%),with average particle size of 30 nm.

Modifications in the structure of the titanium dioxide by incorporation of different atoms could extend the utilization of UV-light for the photocatalytic processes. Therefore, the adsorption performances of the metal ion TiO_2, (Fe), and TiO_2 modified with an organic substance (ascorbic acid) samples with TiO_2 Degussa P-25 were studied. AA (ascorbic acid) modified TiO_2 containing 0.05 wt %AA with average particle size of 53 μm and, Fe TiO_2 containing 0.5 wt % with average particle size of 53 μm were used.

Fe doped TiO_2 and ascorbic acid modified TiO_2 photocatalyst samples were prepared by the group of Mert et al. at the research laboratories of Yıldız Technical University. Surface modification was performed by an incipient wet impregnation method. 10 g TiO_2 Degussa P-25 and appropriate amount of ascorbic acid were mixed with definite volumes of doubly distilled water and stirred for 30 minutes. The prepared photocatalyst was washed with water to remove unbound ascorbic acid, heat-treated at 373 K for 24 h to eliminate water, grinded and sifted through a 0.53 μm sieve. The new photocatalyst was characterized by FTIR, XRD, SEM and UV-DRS (Mert et al., 2008). Surface doping was performed by an incipient wet impregnation method. 10 g TiO_2 Degussa P-25 and appropriate amount of Fe^{+3} (0.050 wt %) were mixed with definite volumes of doubly distilled water and stirred for 30 minutes. The prepared photocatalyst was washed with water to remove unbound Fe^{+3}, heat-treated at 373 K for 24 h to eliminate water, grinded and sifted through a 0.53 μm sieve. The new photocatalyst was characterized by FTIR, XRD, SEM and UV-DRS (Yazıcı, 2006)

3.2. Methods

3.2.1. Laboratory Equipment

Bardelin Sonerex RK 100 Sonication: The homogeneous suspension was provided by sonication of slurry for two minutes.

Glassware: Various types and sizes of glassware were utilized during the experiments. Each of them was first rinsed with tap water and then washed with deionized water to remove especially TiO_2. They were dried in the oven at 110 ^oC before being used.

Hettich EBA 8S Centrifuge: It was used for the removal of TiO_2. The suspensions were centrifuged for 10 minutes.

Memmert Water Bath Shaker Model WB/OB 7-45: It was used for continuous mixing of the humic acid for 24 hours.

Memmert Oven: It was used to dry glassware.

Perkin Elmer Lamda 35 UV-vis Double Beam Spectrophotometer: UV-Visible absorption spectra of humic acid solutions were recorded employing Hellma cuvettes of 1.0 cm optical path length.

Sartorius Balance: It was used for weighing measured TiO_2 loadings.

Sterile Millex-HA Millipore Filter: The 0.45 μm diameter Millipore filters were used for the removal of TiO_2 from the suspension.

Syringe: Syringes were used to filter the suspensions.

WTW series pH 720: It was used to measure pH values of humic acid solutions.

3.2.2. Experimental Procedure

3.2.2.1. Batch adsorption experiments. A series of batch adsorption experiments were conducted to determine the effects of molecular size dependent fractions of humic acid solution on surface modified TiO_2 surfaces. Batch adsorption experiments were held using 100 mL Erlenmeyer flasks. Each flask was filled with 50 mL humic acid solution. Increased amounts of surface modified TiO_2 were added to each Erlenmeyer flask starting from 0.1 mg mL^{-1} to 1.0 mg mL^{-1}. One extra flask was filled with only 50 ppm humic acid solution for comparative purpose. Each sample was sonicated before being inserted to the shaker for evenly distribution of TiO_2 in the slurry. The samples were then immersed the water-bath which is equipped with shaking device and the appliance was set to room temperature. The flasks were kept shaking for 24 hours. The samples then centrifuged for 10 minutes in 5000 cycles min^{-1}.The supernatant then filtered by the 0.45 μm Millipore 49,filter.

Adsorption experiments with metal ion TiO_2, (Fe), and TiO_2 modified with an organic substance (ascorbic acid) samples with TiO_2 Degussa P-25 were studied in same procedure.

3.2.2.2. Molecular Size Fractionation via Ultrafiltration. Humic acid solutions were fractionated using a 10 mL Amicon Model 8010 ultrafiltration stirred cells into appropriate molecular sizes; 100 kDa, 30 kDa, and were subjected batch adsorption experiments using TiO_2 as the adsorbent. Initially, the samples were filtered through 0.45 µm (approximately 450 kDa) Millipore cellulose acetate membrane filters. Then, filtration was repeated in a series mode using Millipore YM series cellulose membranes. The cell was run on a magnetic stirrer with 50mL samples. A nitrogen gas tube equipped with a pressure control valve was attached to the stirred reactor to provide the operating pressure inside the cell. A schematic diagram of stirred cell system was presented in Figure 3.1.

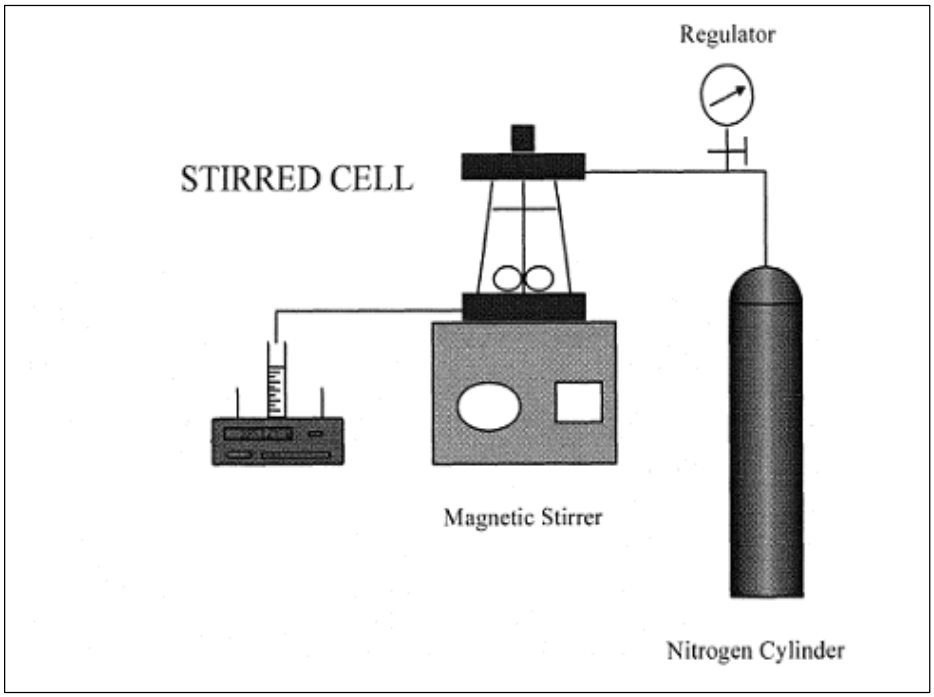

Figure 3.1.Schematic diagram of stirred cell system

Millipore YM series cellulose membrane filters with 25 mm diameter and with nominal molecular weight cutoffs 100 kDa, 30 kDa, with a sequence of decreasing pore size were used within the stirred cell. The specifications of the membranes as explained by the manufacturer are tabulated in Table 3.1.

Table.3.1. Specifications of the cellulose membranes used in ultrafiltration

Membrane type	Nominal molecular weight cutoff (kDa)	Operating pressure ($kgcm^{-2}$)
YM 100	100	1.0
YM 30	30	3.5

At the beginning of each run the membranes were kept in deionized water for 15 minutes and then the cell was run on a magnetic stirrer with 50mL deinoized water. After use, YM membranes were washed with 0.1 M NaOH solution and kept in deionized water for 15 minutes for storage. Millipore YM series cellulose membranes were stored in 10% ethanol/water solution and preserved in refrigerator. Fractionated humic acid solutions were stored in amber glass bottles.

3.2.3. Analytical Methods

3.2.3.1. Total Organic Carbon (TOC) Analysis. Total organic carbon (TOC, mg L-1) measurements of humic substances were performed on a Shimadzu TOC V wp Total Organic Carbon Analyzer. Calibration of the instrument was done using potassium hydrogen phthalate in the concentration range of 5-25 mg L-1.

3.2.3.2. UV-vis Measurements. UV-vis absorption spectra were recorded on a Perkin Elmer Lamda 35 UV-vis double beam spectrophotometer employing Hellma quartz cuvettes of 1.0 cm optical path length. Humic acid samples were characterized by UV/vis spectra. Absorbance values at 436 nm (Color436), 365 nm (UV365), 280 nm (UV280), and 254 nm (UV254) were recorded.

3.2.3.3. Fluorescence Measurements. Fluorescence spectra in the emission and synchronous scan modes were recorded on a Perkin Elmer LS 55 Luminescence Spectrometer equipped with a 150W Xenon arc lamp and a red sensitive photomultiplier tube. A 1-cm path length quartz cell was used. Both the excitation and the emission slits of the instrument were 10 nm. A scan speed of 400 nm min^{-1} was used with a slit width opening of 10 nm. Synchronous scan spectra were recorded in the excitation wavelength

range of 200-600 nm excitation wavelength range using the bandwidth of $\Delta\lambda$=18 nm between the excitation and emission monochromators (Senesi, 1990). The scan speed was 400 nm min^{-1}. The emission spectra were scanned over the range of 360-600 nm at a constant excitation wavelength of 350 nm (Senesi, 1990, Hautala et al., 2000). Since all of the spectra were recorded on the same instrument using the same experimental parameters, a comparative discussion of the spectra is acceptable although, no corrections for fluctuation of instrumental factors and for scattering effects (e.g. primary and secondary inner filter effects) were applied to the data (Senesi, 1990, Peuravuori et al., 2002).

4. RESULTS AND DISCUSSIONS

In this study, adsorption experiments were carried out in order to examine the effect of molecular size fractionation on the sorption properties of humic acid onto metal ion TiO_2 (Fe), and TiO_2 modified with an organic substance (ascorbic acid) samples in comparison to TiO_2 Degussa P-25.

The adsorption experiments were conducted with various molecular size fractions of, namely 0.45 μm, 100 kDa, and 30 kDa of 50 mg L^{-1} humic acid solution. Bare TiO_2 in the range of 0.1-1.0 mg mL^{-1}, Fe and ascorbic acid modified TiO_2 in the range of 0.2-1.0 mg mL^{-1} were used as adsorbents. The adsorption experiments were conducted at natural pH that the values were changed between 6.6 and 7.1 under all experimental conditions.

Raw humic acid and humic acid molecular size fractions were characterized in relation to their UV-vis parameters and TOC (Table 1).

Table 4.1. Characterization of humic acid and molecular size of fractions

Humic Acid	Raw	0.45 μm	100 kDa	30 kDa
$Color_{436}$, m^{-1}	25.3	18.4	10.4	4.30
UV_{365}, m^{-1}	49.1	38.5	21.7	8.50
UV_{280}, m^{-1}	105.8	94.8	51.5	22.5
UV_{254}, m^{-1}	121.8	105.5	60.6	27.7
TOC, mg L^{-1}	17.2	14.3	7.14	3.21

The batch adsorption experiments were conducted according to the methods outlined in the Materials and Methods section. The results were evaluated according to the methodology outlined in Section 2.2. The selected parameters are $Color_{436}$, UV_{254}, and TOC. The adsorption isotherms of these parameters are presented in the following sections whereas the adsorption isotherms of UV_{365} and UV_{280} are presented in Appendix A-B and

C. The Freundlich adsorption model parameters, of all of these parameters were tabulated in respective tables.

For comparison purposes, adsorption isotherms, q_A versus C_e graphs were plotted for each system comprised of humic acids and fractionated humic acid and bare TiO_2 as well as the modified TiO_2 surfaces. A set of points showing a linear trend with a slope of 1/n and an intercept equal to the value of log K_f is found by applying logarithmic form of Freundlich equation to the experimental readings. The adsorption capacity, K_f, and adsorption strength, 1/n, for humic acid-Degussa P-25 TiO_2 system were listed in tables.

4.1. Adsorption Studies of TiO_2-Degussa P-25

4.1.1. Raw Humic Acid Adsorption onto Degussa P-25 TiO_2

In order to evaluate the effect of molecular size on adsorption properties of humic acid, preliminary experiments were carried out with raw humic acid. The adsorption isotherms for $Color_{436}$, UV_{254} and TOC changes of humic acids were given in the Figure 4.1, Figure 4.2, and Figure 4.3, respectively.

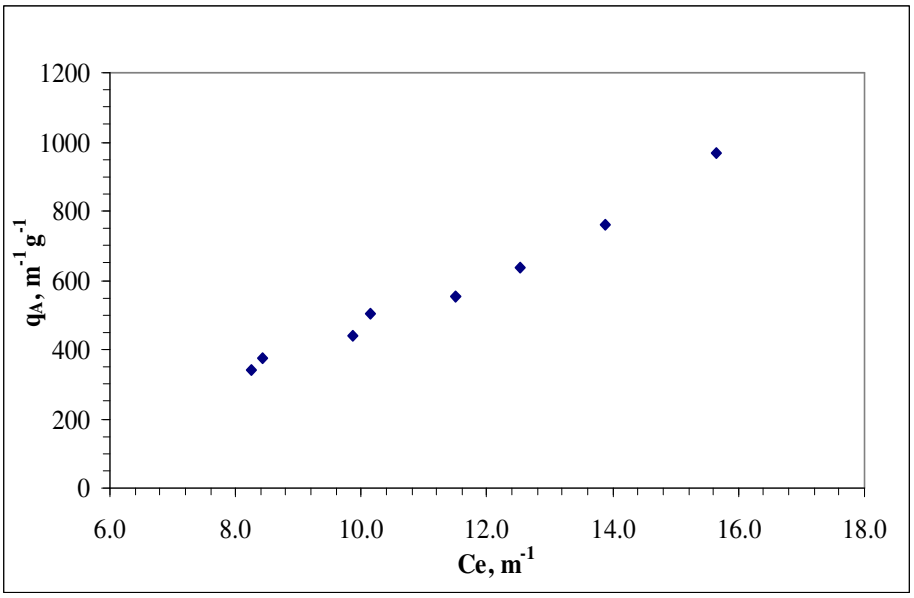

Figure 4.1. $Color_{436}$ adsorption isotherm of humic acid on Degussa P-25

Figure 4.1 indicated that C_e values varied between 8.24-15.6 m^{-1} for $Color_{436}$ depending on the amount of TiO_2 present in solution. The values of q_A calculated to be in the range of 341– 966 m^{-1} g^{-1} for the corresponding C_e values.

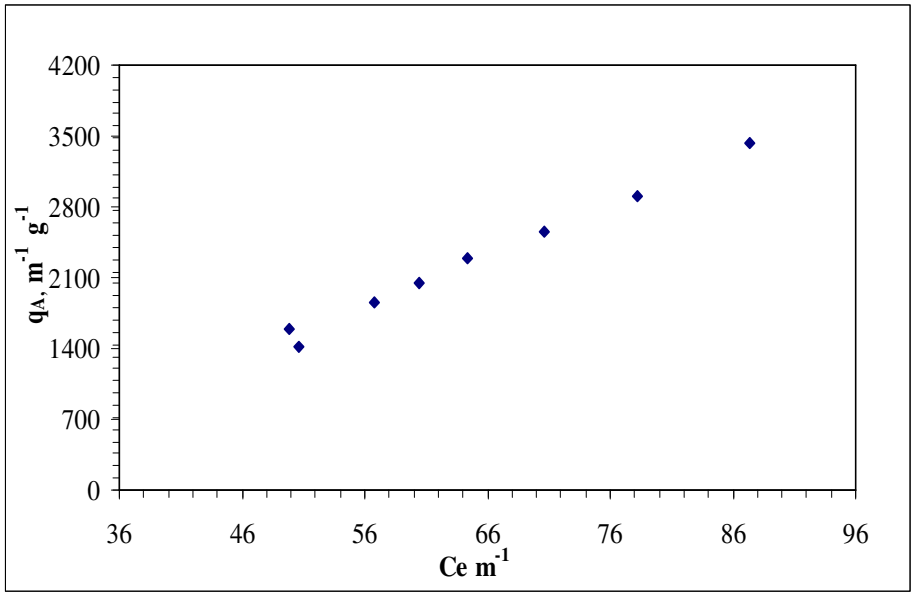

Figure 4.2. UV_{254} adsorption isotherm of humic acid on Degussa P-25

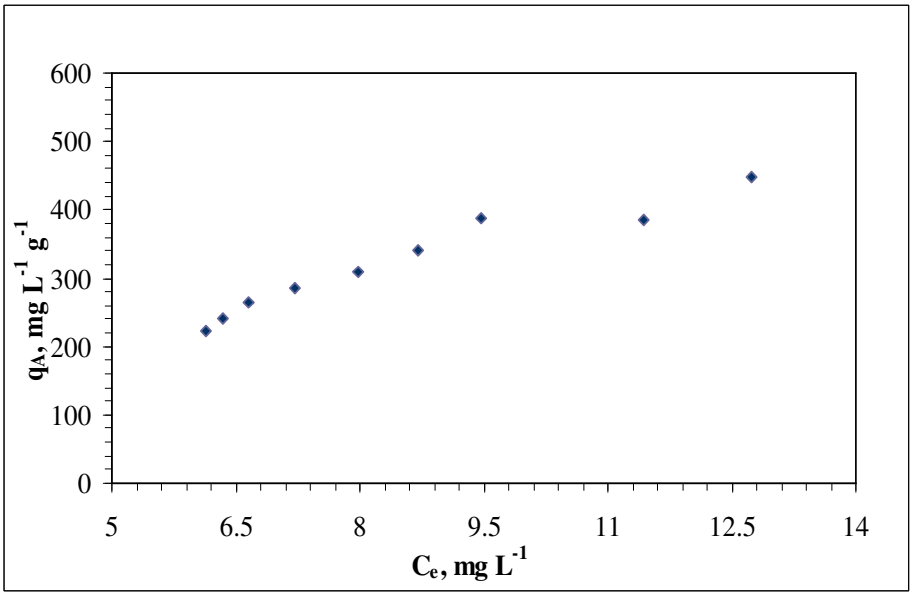

Figure 4.3. TOC adsorption isotherm of humic acid on Degussa P-25

As could be seen in Figure 4.2, C_e values varied between 49.8–87.4 m^{-1} for $UV_{254.}$ The values of q_A calculated to be in the range of 1422–3438 m^{-1} g^{-1} for the corresponding C_e values. Figure 4.3 represented that the values of C_e varied from 6.1 to 12.7 mg L^{-1} for TOC. The calculated q_A values varied in between 221– 447 mg $L^{-1}g^{-1}$.

As can be seen from Figure 4.1, Figure 4.2 and Figure 4.3 above, the adsorption isotherms showed similar trend both in terms of $Color_{436}$ and UV_{254} parameters. This exhibited trend would have agreed well with the linear pattern. ΔC_e and Δq_A values for raw humic acid were 7.36 m^{-1} and 625 m^{-1} g^{-1} respectively at $Color_{436}$. ΔC_e and Δq_A for UV_{254} were 37.6 m^{-1} and 2016 m^{-1} g^{-1}, respectively. TOC isotherm for humic acid gave a ΔC_e of 6.6 mg L^{-1} where Δq_A was 226 mg L^{-1} g^{-1}. The value of q_A changed markedly with small changes in C_e.

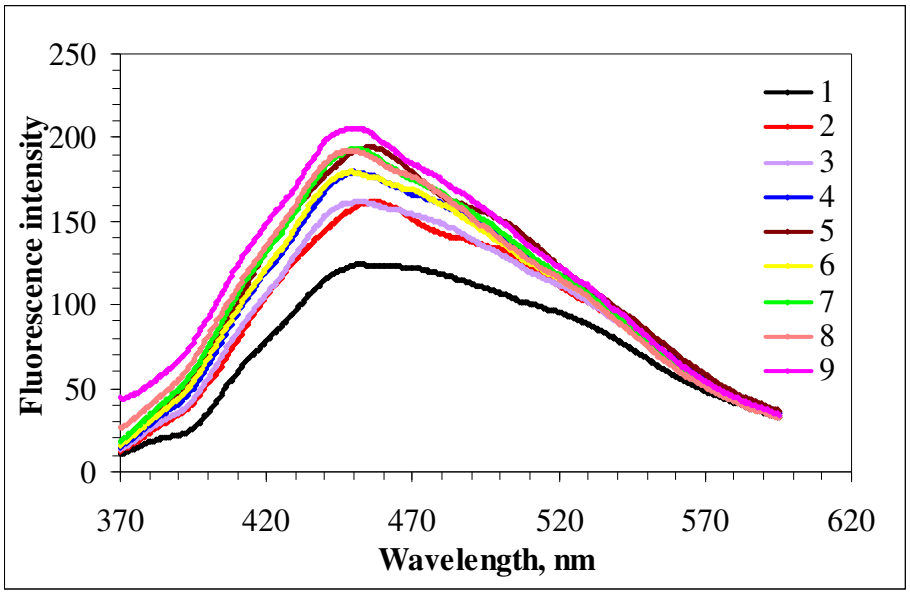

Figure 4.4. Emissions scan spectra of humic acid onto Degussa P-25
Where numbers represent, 1: Raw AHA, 2: 0.2 mg mL^{-1} TiO_2, 3: 0.3 mg mL^{-1} TiO_2, 4: 0.4 mg mL^{-1} TiO_2, 5: 0.5 mg mL^{-1} TiO_2, 6: 0.6 mg mL^{-1} TiO_2, 7: 0.7 mg mL^{-1} TiO_2, 8: 0.9 mg mL^{-1} TiO_2, 9: 1.0 mg mL^{-1} TiO_2

Followed by adsorption experiments, the effect of TiO_2 concentration (0.1 mg mL^{-1} to 1.0 mg mL^{-1} TiO_2) on the fluorescence spectra of humic acid has been studied. The

emission and synchronous scan fluorescence spectra of raw humic acid were illustrated in Figure 4.4 and Figure 4.5. The concentration change of TiO_2 for the samples were symbolized with increasing numbers in the figures that one represented the 50 mg L^{-1} humic acid solution, respectively.

As seen in Figure 4.4, a continuously increasing trend in fluorescence intensity at λ_{max}=450 nm was observed with respect to increasing TiO_2 dose for raw as well as the lower molecular weight fractions of humic acid.

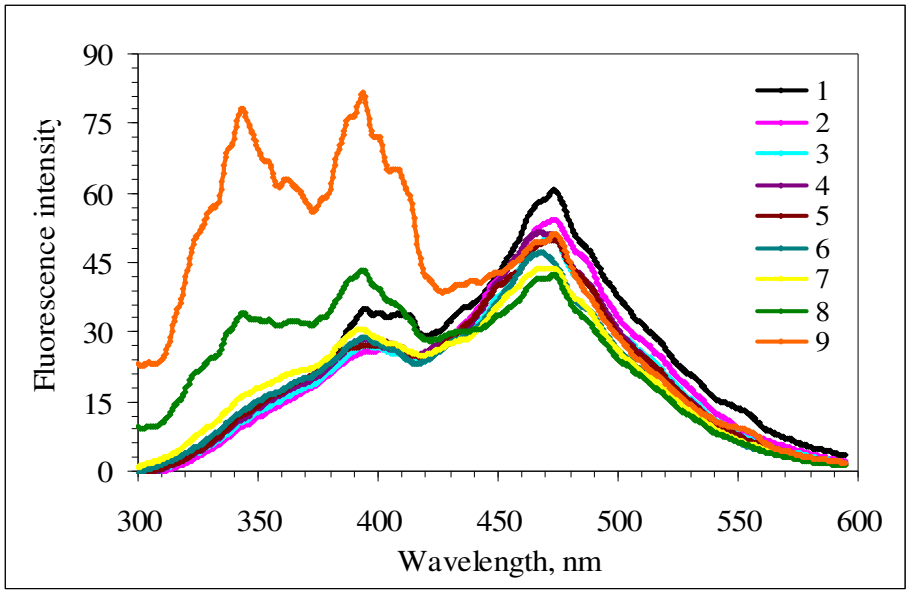

Figure 4.5. Synchronous scan spectra of humic acid onto Degussa P-25
Where numbers represent, 1: Raw AHA, 2: 0.2 mg mL^{-1} TiO_2, 3: 0.3 mg mL^{-1} TiO_2, 4: 0.4 mg mL^{-1} TiO_2, 5: 0.5 mg mL^{-1} TiO_2, 6: 0.6 mg mL^{-1} TiO_2, 7: 0.7 mg mL^{-1} TiO_2, 8: 0.9 mg mL^{-1} TiO_2, 9: 1.0 mg mL^{-1} TiO_2

Adsorption dependent λ_{max} (470 nm) fluorescence intensity displayed a decreasing trend with respect to increased TiO_2 dose except 1.0 mg mL^{-1} dose of TiO_2. On the other hand, double peaks observed at approximately 345 nm and 355 nm appeared in the presence of higher doses of TiO_2.

In order to evaluate the experimental results, the data were fitted to the Freundlich Model. The adsorption capacity, K_f, and adsorption strength, 1/n, for humic acid-Degussa P-25 TiO_2 system were listed in Table 4.2 ($R^2 \geq 0.64$)

Table 4.2. Freundlich coefficients of humic acid- Degussa P-25 TiO_2

	K_f	1/n
$Color_{436}$, m^{-1}	13.81	0.986
UV_{365}, m^{-1}	10.04	1.47
UV_{280}, m^{-1}	3.733	1.56
UV_{254}, m^{-1}	4.758	1.48
TOC, mg L^{-1}	48.06	0.885

According to Table 4.2, adsorption capacity constants for $Color_{436}$ and UV_{365} were found to be very close to each other when adsorption capacity constants for UV absorbing centers (UV_{280}, and UV_{254}) were approximately equal to each other. 1/n values for UV_{365}, UV_{280} and UV_{254} were found to be higher than one, it indicated that the adsorption bond was weak, and the value of q_A changed markedly with small changes in C_e. They express strong favorable adsorption intensity and concentration dependency. On the other hand, 1/n values for $Color_{436}$ were found to be almost equal to one representing a linear trend.

4.1.2. 0.45 μm Fractionated Humic Acid Adsorption onto Degussa P-25 TiO_2

In order to investigate the adsorption phenomena in 0.45 μm size fraction of humic acid solution, batch adsorption experiments were carried out with bare TiO_2. The adsorption isotherms for $Color_{436}$, UV_{254} and TOC changes of humic acids were given in the Figure 4.6, Figure 4.7, and Figure 4.8, respectively.

Figure 4.6 indicated that C_e values varied between 4.2–14.5 m^{-1} for $Color_{436}$ depending on the amount of TiO_2 present in solution. The values of q_A calculated to be in the range of 280 – 774 m^{-1} g^{-1} for the corresponding C_e values. As could be seen in Figure 4.7, C_e values varied between 29.2–84.5 m^{-1} for UV_{254}. The values of q_A calculated to be in the range of 1477–4210 m^{-1} g^{-1} for the corresponding C_e values.

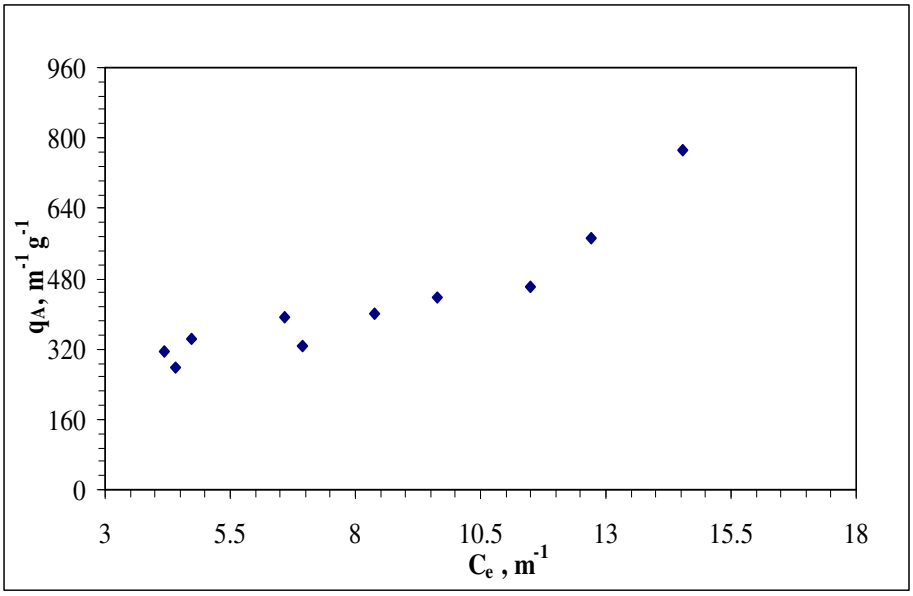

Figure 4.6. $Color_{436}$ adsorption isotherm of 0.45 µm humic acid on Degussa P-25

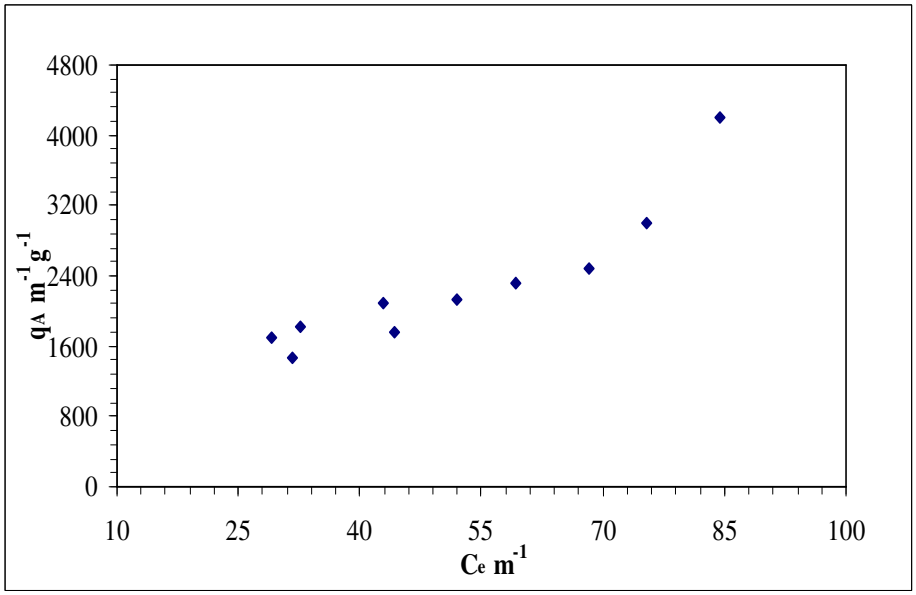

Figure 4.7. UV_{254} Adsorption Isotherm of 0.45 µm humic acid on Degussa P-25

Figure 4.8 represented that the values of C_e varied from 3.79 to 10.3 mg L^{-1} for TOC. The calculated q_A values varied in between 183– 800 mg L^{-1} g^{-1}.

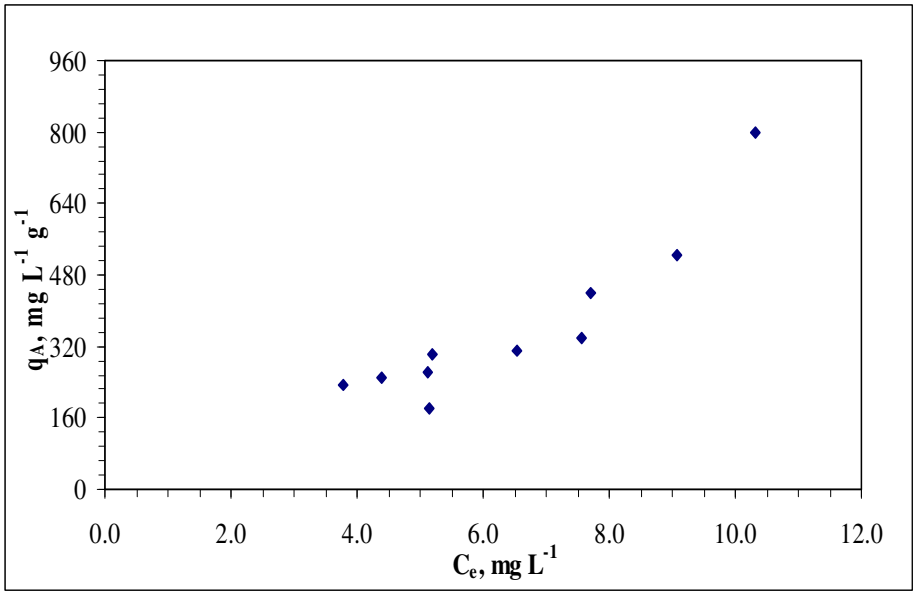

Figure 4.8. TOC adsorption isotherm of 0.45 μm humic acid on Degussa P-25

It could clearly be seen from figures that the TOC isotherm showed similar pattern with $Color_{436}$ and UV_{254} isotherms. The $Color_{436}$ isotherm for 0.45 μm filtered humic acid, (Figure 4.6) was distributed in a narrow C_e range (ΔC_e =10.3 m^{-1}), where Δq_A was 494 m^{-1} g^{-1}. The isotherm (Figure 4.7) gave 2733 m^{-1} g^{-1} for Δq_A and 55.3 m^{-1} for ΔC_e at UV_{254}. Δq_A and ΔC_e for TOC isotherm (Figure 4.8) were 617 mg $L^{-1}g^{-1}$ and 6.51 mg L^{-1} respectively. This exhibited trend would have agreed well with the C-curve type isotherm that an initial slope remains independent of adsorptive concentration until the maximum possible adsorption is achieved.

The emission and synchronous scan fluorescence spectra of 0.45 μm filtered humic acid were illustrated in Figure 4.9 and Figure 4.10. As it was seen in the Figure 4.9, a continuously increasing trend in FI at λ_{max}=450 nm was observed with respect to increasing TiO_2 dose for raw as well as the lower molecular weight fractions of humic acid. In the synchronous scan spectra of 0.45 μm filtered humic acid (Figure 4.10), a decreasing trend was observed in the fluorescence intensity (λ_{max}=470 nm) with respect to TiO_2 dose.

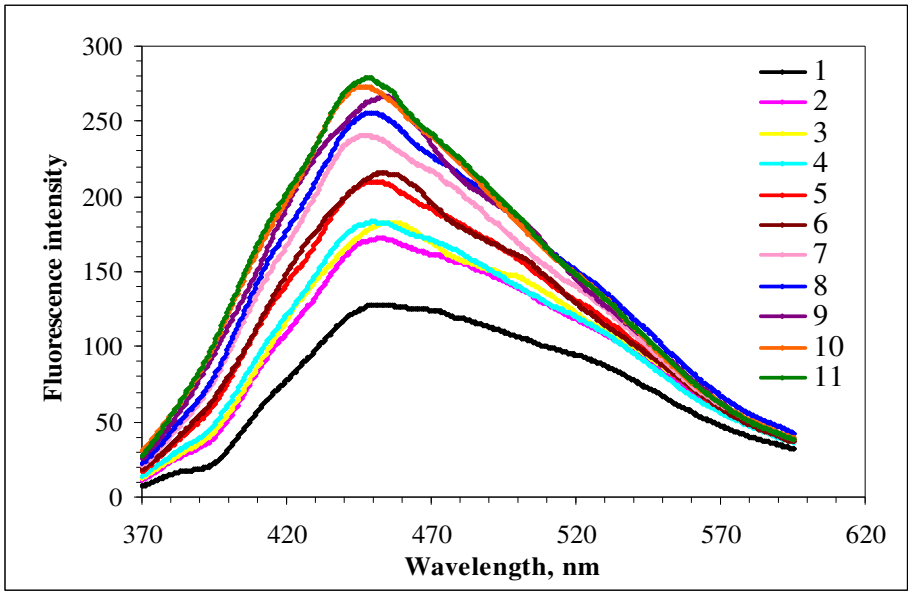

Figure 4.9. Emissions scan spectra of 0.45 µm humic acid onto Degussa P-25

Where numbers represent, 1: 0.45µm fractionated AHA, 2: 0.1 mg mL^{-1} TiO_2, 3: 0.2 mg mL^{-1} TiO_2, 4: 0.3 mg mL^{-1} TiO_2, 5: 0.4 mg mL^{-1} TiO_2, 6: 0.5 mg mL^{-1} TiO_2, 7: 0.6 mg mL^{-1} TiO_2, 8: 0.7 mg mL^{-1} TiO_2, 9: 0.8 mg mL^{-1} TiO_2, 10: 0.9 mg mL^{-1} TiO_2, and 11: 1.0 mg mL^{-1} TiO_2

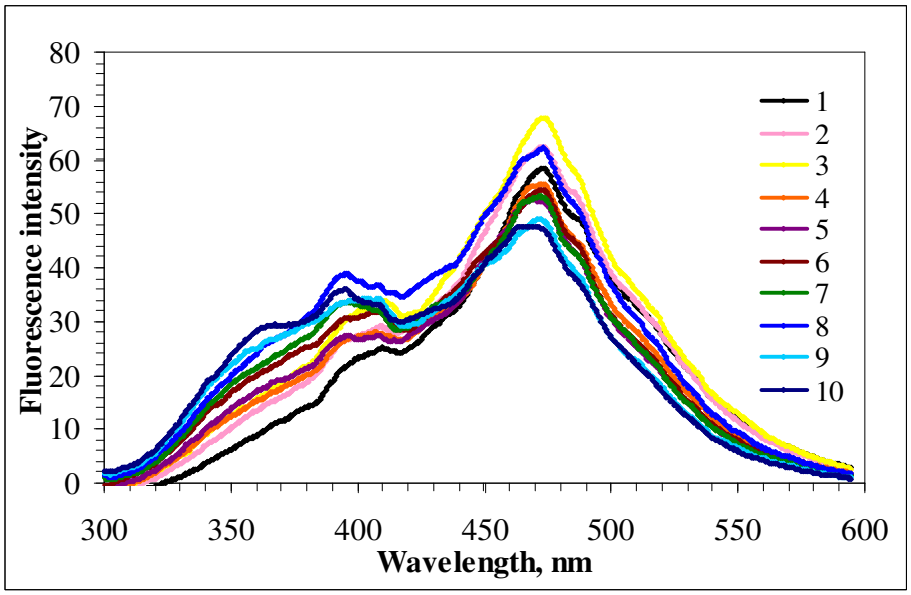

Figure 4.10. Synchronous scan spectra of 0.45 µm humic acid onto Degussa P-25

Where numbers represent, 1: 0.45μm fractionated AHA, 2: 0.1 mg mL^{-1} TiO_2, 3: 0.2 mg mL^{-1} TiO_2, 4: 0.3 mg mL^{-1} TiO_2, 5: 0.4 mg mL^{-1} TiO_2, 6: 0.5 mg mL^{-1} TiO_2, 7: 0.6 mg mL^{-1} TiO_2, 8: 0.7 mg mL^{-1} TiO_2, 9: 0.8 mg mL^{-1} TiO_2, 10: 0.9 mg mL^{-1} TiO_2, and 11: 1.0 mg mL^{-1} TiO_2

The application of the Freundlich model revealed adsorption capacity, K_f, and adsorption strength, 1/n, for 0.45 μm filtered humic acid-Degussa P-25 TiO_2 system were as listed in Table 4.3.

Table 4.3. Freundlich coefficients of 0.45 μm molecular size fraction of humic acid-Degussa P-25 TiO_2

	K_f	1/n
$Color_{436}$, m^{-1}	118.3	0.612
UV_{365}, m^{-1}	138.5	0.642
UV_{280}, m^{-1}	93.70	0.837
UV_{254}, m^{-1}	124.0	0.738
TOC, mg L^{-1}	39.12	1.17

According to Table 4.3, adsorption capacities of 0.45 μm molecular size fraction of humic acid were found to be higher than the adsorption capacities of raw humic acid for each parameter. On the other hand, adsorption intensities for each UV-vis parameter were found to be lower than one, it indicated that the adsorption bond was strong; the capacity tended to be independent of C_e and the isotherm plot approaches the horizontal level. q_A is essentially constant, and the isotherm is termed irreversible (Letterman at al., 1999). They expressed unfavorable adsorption. However, K_f value for TOC was 39.12 and 1/n value was 1.17.

4.1.3. 100 kDa Fractionated Humic Acid Adsorption onto Degussa P-25 TiO_2

In order to evaluate the molecular size effect on adsorption properties of humic acid, experiments were carried out with 100 kDa molecular size fraction of humic acid. The

Freundlich adsorption isotherms for $Color_{436}$, UV_{254} and TOC changes of humic acids were given in the Figure 4.11, Figure 4.12 and Figure 4.13, respectively.

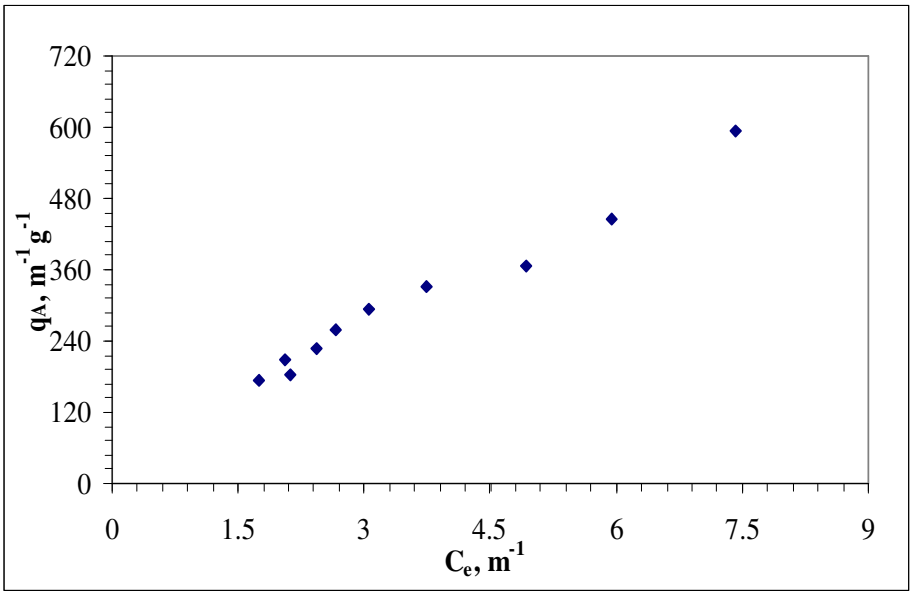

Figure 4.11. $Color_{436}$ adsorption isotherm of 100 kDa humic acid on Degussa P-25

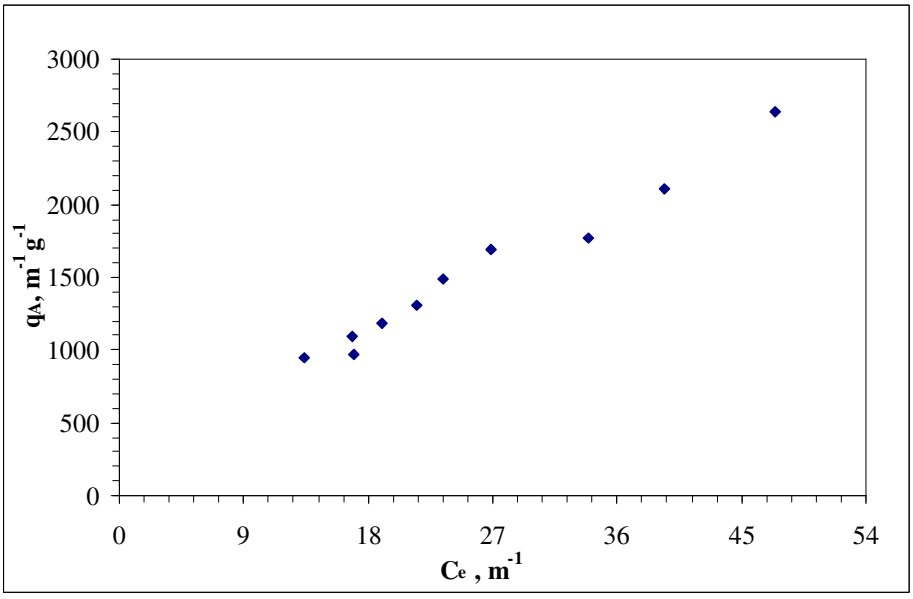

Figure 4.12. UV_{254} adsorption isotherm of 100 kDa humic acid on Degussa P-25

Figure 4.11 indicated that C_e values varied between 1.75–7.43 m^{-1} for $Color_{436}$ depending on the amount of TiO_2 present in solution. The values of q_A calculated to be in the range of 173–594 m^{-1} g^{-1} for the corresponding C_e values.

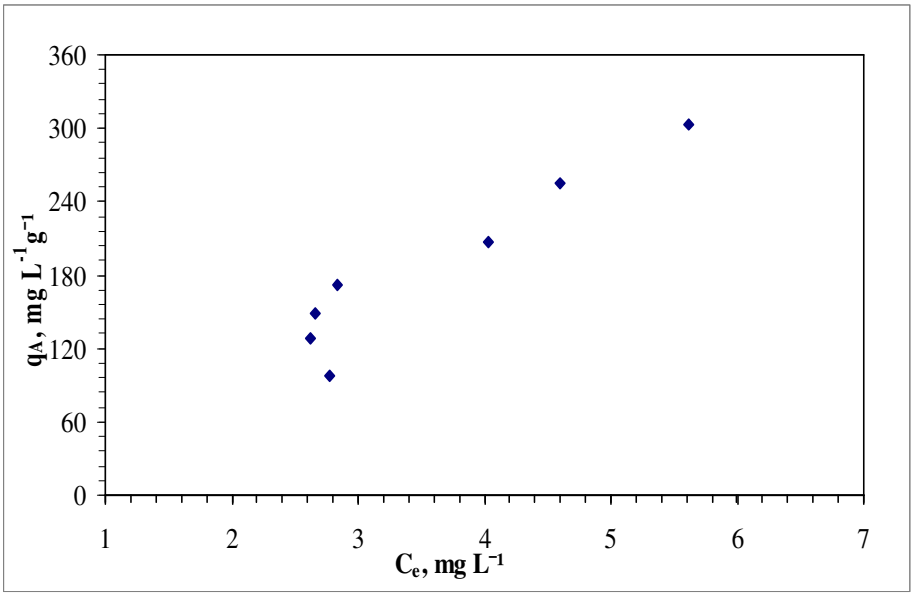

Figure 4.13. TOC adsorption isotherm of 100 kDa humic acid on Degussa P-25

As seen in Figure 4.12, C_e values varied between 13.4–47.4 m^{-1} for $UV_{254.}$ The corresponding values of q_A calculated to be in the range of 945–2642 m^{-1} g^{-1} for the corresponding C_e values.

Figure 4.13 represented that the values of C_e varied from 2.63 to 5.62 mg L^{-1} for TOC. The calculated q_A values varied in between 97.1–304 mg $L^{-1}g^{-1}$.

As isotherm for $Color_{436}$ followed the same pattern with UV_{254}, for the 100 kDa filtered humic acid, Δq_A and ΔC_e for $Color_{436}$ were 421m^{-1} g^{-1} and 5.68 m^{-1} respectively. The isotherm gave 1697 m^{-1} g^{-1} for Δq_A and 34 m^{-1} for ΔC_e at UV_{254}. TOC isotherm for humic acid gave a ΔC_e of 2.99 mg L^{-1} where Δq_A was 206.9 mg $L^{-1}g^{-1}$. The isotherms showed linear pattern.

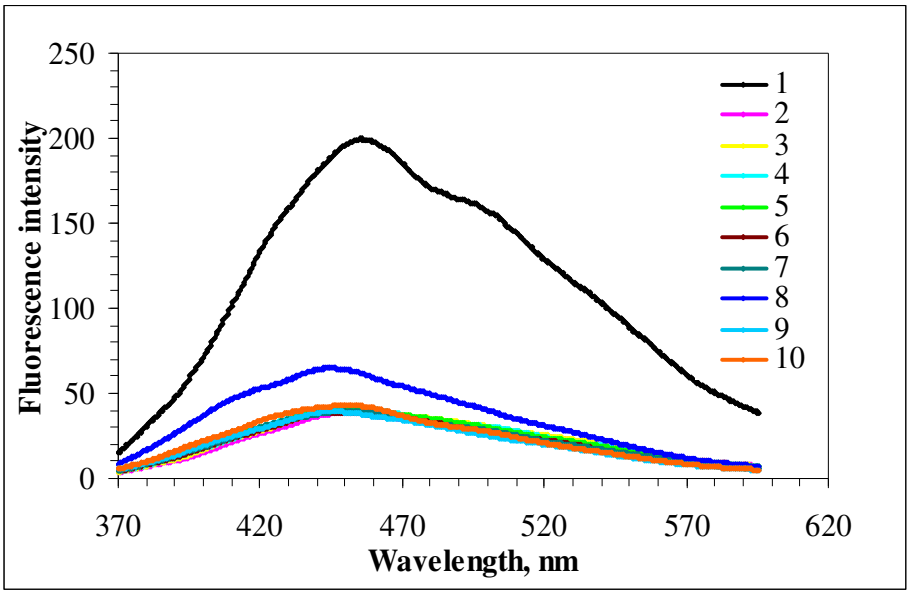

Figure 4.14. Emissions scan spectra of 100 kDa humic acid onto Degussa P-25
Where numbers represent, 1: 100 kDa AHA, 2: 0.1 mg mL^{-1} TiO_2, 3: 0.2 mg mL^{-1} TiO_2, 4: 0.3 mg mL^{-1} TiO_2, 5: 0.4 mg mL^{-1} TiO_2, 6: 0.5 mg mL^{-1} TiO_2, 7: 0.6 mg mL^{-1} TiO_2, 8: 0.8 mg mL^{-1} TiO_2, 9: 0.9 mg mL^{-1} TiO_2, 10: 1.0 mg mL^{-1} TiO_2

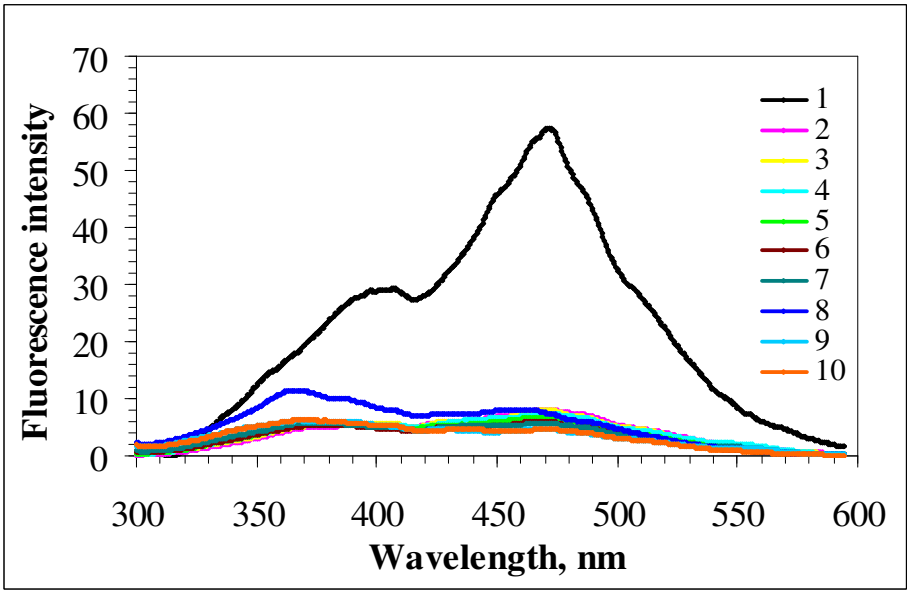

Figure 4.15. Synchronous scan spectra of 100 kDa humic acid onto Degussa P-25

Where numbers represent, 1: 100 kDa AHA, 2: 0.1 mg mL^{-1} TiO_2, 3: 0.2 mg mL^{-1} TiO_2, 4: 0.3 mg mL^{-1} TiO_2, 5: 0.4 mg mL^{-1} TiO_2, 6: 0.5 mg mL^{-1} TiO_2, 7: 0.6 mg mL^{-1} TiO_2, 8: 0.8 mg mL^{-1} TiO_2, 9: 0.9 mg mL^{-1} TiO_2, 10: 1.0 mg mL^{-1} TiO_2

As it was seen in the Figure 4.14, a decreasing trend in FI at λ_{max}=450 nm was observed with respect to increasing TiO_2 dose for raw as well as the lower molecular weight fractions of humic acid. 100 kDa fraction of humic acid (Figure 4.15) displayed a remarkable FI at λ_{max}=470 nm whereas higher doses of TiO_2 significantly removed the FI.

Table 4.4. Freundlich coefficients of 100 kDa molecular size fraction of humic acid-Degussa P-25 TiO_2

	K_f	1/n
$Color_{436}$, m^{-1}	111.2	0.806
UV_{365}, m^{-1}	114.8	0.791
UV_{280}, m^{-1}	110.5	0.802
UV_{254}, m^{-1}	106.7	0.820
TOC, mg L^{-1}	42.18	1.15

The Freundlich adsorption model parameters as the adsorption capacity, K_f, and adsorption strength, 1/n, for 100 kDa filtered humic acid-Degussa P-25 TiO_2 system were listed in Table 4.4.

According to Table 4.4, adsorption capacity constants for both the UV absorbing centers and the color forming chromophoric groups were found to be very close to each other. 1/n values were found to be lower than one, it indicated that the adsorption bond was strong; the capacity tended to be independent of C_e. They expressed unfavorable adsorption. K_f value was determined as 42.18 g^{-1} for TOC and 1/n value was found to be 1.15.

4.1.4. 30 kDa Fractionated Humic Acid Adsorption onto Degussa P-25 TiO_2

In order to examine the molecular size effect on the adsorption behavior of humic acid, the batch adsorption experiments were also carried out with 30 kDa molecular size fractionated humic acid. The adsorption isotherms of $Color_{436}$, UV_{254} and TOC were shown in Figures 4.16, Figures 4.17 and Figures 4.18, respectively.

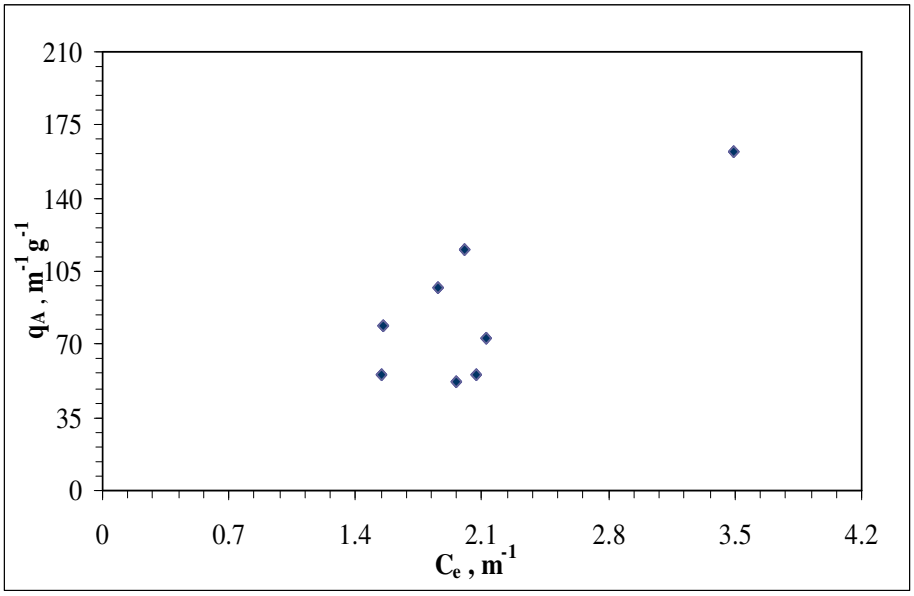

Figure 4.16. $Color_{436}$ adsorption isotherm of 30 kDa humic acid on Degussa P-25

Figure 4.16 indicated that C_e values varied between 1.5 – 3.5 m^{-1} for $Color_{436}$ depending on the amount of TiO_2 present in solution. The values of q_A calculated to be in the range of 52 – 162 m^{-1} g^{-1} for the corresponding C_e values.

As it could be seen in Figure 4.17, C_e values varied between 11.3–23.6 m^{-1} for $UV_{254.}$ The values of q_A calculated to be in the range of 321–812 $m^{-1}g^{-1}$ for the corresponding C_e values.

Figure 4.18 showed that the values of C_e varied from 1.60 to 2.50 mg L^{-1} for TOC. The calculated q_A values varied in between 35.4– 142 mg $L^{-1}g^{-1}$.

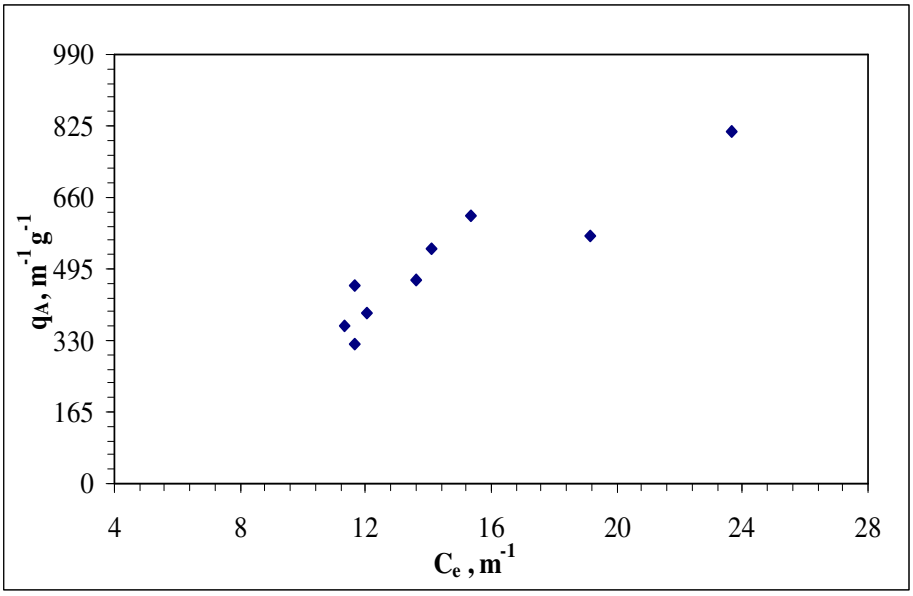

Figure 4.17. UV_{254} adsorption isotherm of 30 kDa humic acid on Degussa P-25

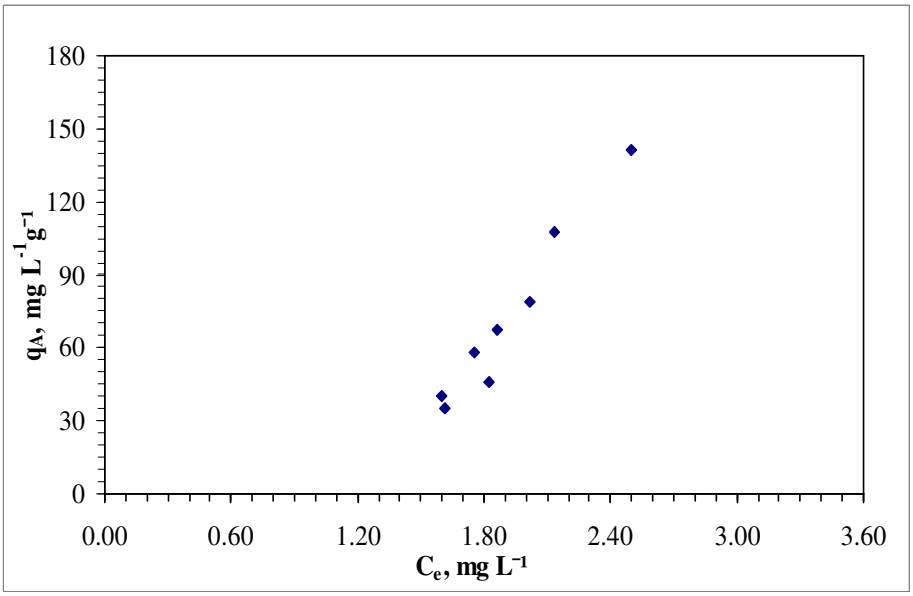

Figure 4.18. TOC adsorption isotherm of 30 kDa humic acid on Degussa P-25

ΔC_e and Δq_A values for 30 kDa filtered humic acid were 1.95 m^{-1} and 110 m^{-1} g^{-1} respectively at $Color_{436}$. The isotherm for $Color_{436}$ was more like a cluster of data points with a narrow ΔCe values. ΔC_e and Δq_A for UV_{365} were 4.2 m^{-1} and 106 m^{-1} g^{-1}

respectively. It indicated that there was no exact adsorption profile depending on the TiO_2 amounts. Hence the adsorption data for color forming groups did not fit to Freundlich isotherm for 30 kDa molecular size fraction of humic acid. ΔC_e and Δq_A for UV_{254} were 12.3 m^{-1} and 491 m^{-1} g^{-1}, respectively. Molecular size fractionation of humic acid resulted in steep curves with high Δq_A of 106 mg $L^{-1}g^{-1}$ in a short Ce range of 0.90 mg L^{-1} for TOC isotherm.

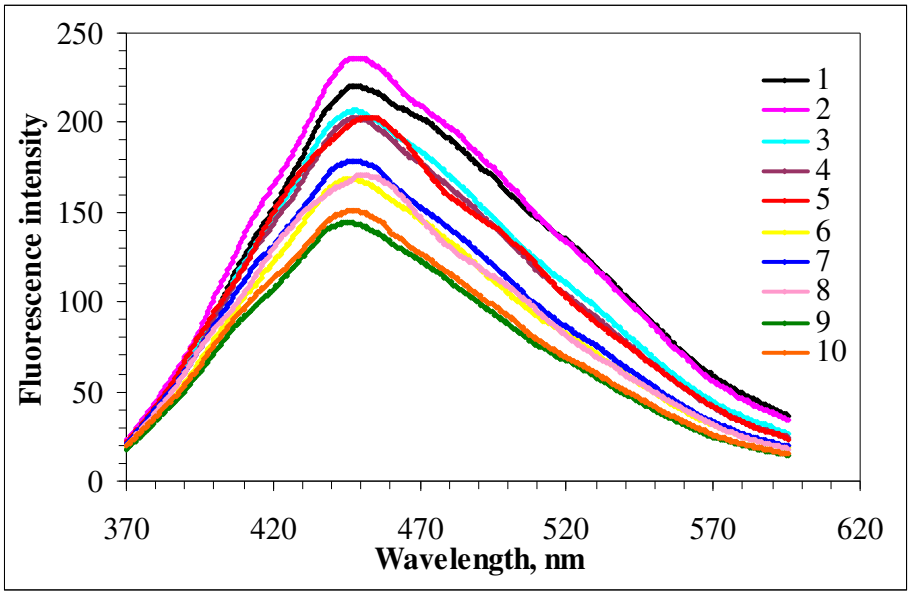

Figure 4.19. Emissions scan spectra of 30 kDa humic acid onto Degussa P-25
Where numbers represent, 1: 100 kDa AHA, 2: 0.1 mg mL^{-1} TiO_2, 3: 0.3 mg mL^{-1} TiO_2, 4: 0.4 mg mL^{-1} TiO_2, 5: 0.5 mg mL^{-1} TiO_2, 6: 0.6 mg mL^{-1} TiO_2, 7: 0.7 mg mL^{-1} TiO_2, 8: 0.8 mg mL^{-1} TiO_2, 9: 0.9 mg mL^{-1} TiO_2, 10: 1.0 mg mL^{-1} TiO_2

As it was seen in the Figure 4.19, a decreasing trend in FI at λ_{max}=450 nm was observed with respect to increasing TiO_2 dose for raw as well as the lower molecular weight fractions of humic acid. As it could be seen in the Figure 4.20, dose dependent continuous decreasing trend was observed at both of the λ_{max} values as 395 nm and 470 nm for 30 kDa fraction of humic acid.

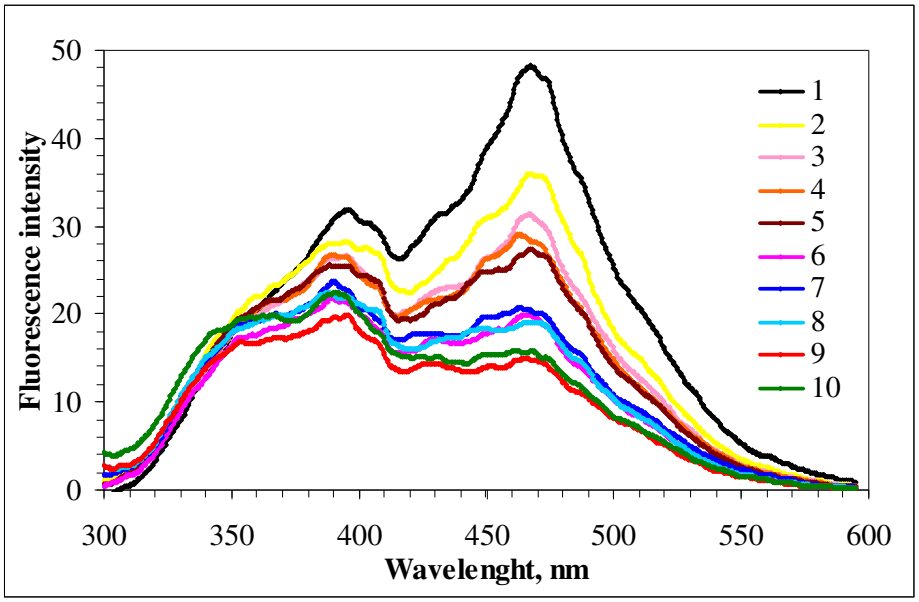

Figure 4.20. Synchronous scan spectra of 30 kDa humic acid onto Degussa P-25
Where numbers represent, 1: 100 kDa AHA, 2: 0.2 mg mL^{-1} TiO_2, 3: 0.3 mg mL^{-1} TiO_2, 4: 0.4 mg mL^{-1} TiO_2, 5: 0.5 mg mL^{-1} TiO_2, 6: 0.6 mg mL^{-1} TiO_2, 7: 0.7 mg mL^{-1} TiO_2, 8: 0.8 mg mL^{-1} TiO_2, 9: 0.9 mg mL^{-1} TiO_2, 10: 1.0 mg mL^{-1} TiO_2

For comparison purposes maximum fluorescence emission scan intensity values were displayed for all of the humic acid fractions as well as raw humic acid (Figure 4.21). Maximum emission scan FI values displayed a range of 124-205 for raw AHA, 127-275 for 0.45 µm AHA, 39-199 for 100 kDa and 144-206 for 30 kDa. A no consistent change was observed for raw humic acid and an increasing trend was obtained for 0.45 µm humic acid fraction for all of the TiO_2 doses after respective adsorption equilibrium. For lower molecular weight fraction as 30 kDa a general decreasing trend was attained for all of the adsorbent doses, and a sharp decreasing trend was observed for 100 kDa fraction of humic acid. The highest FI values recorded were 206 for raw humic acid for TiO_2 dose of 1.0 mg mL^{-1}, 279 for 0.45 µm AHA for TiO_2 dose of 1.0 mg mL^{-1}, for 100 kDa fraction 199 for raw humic acid and for 30 kDa fraction 236 for 0.1 mg mL^{-1}.

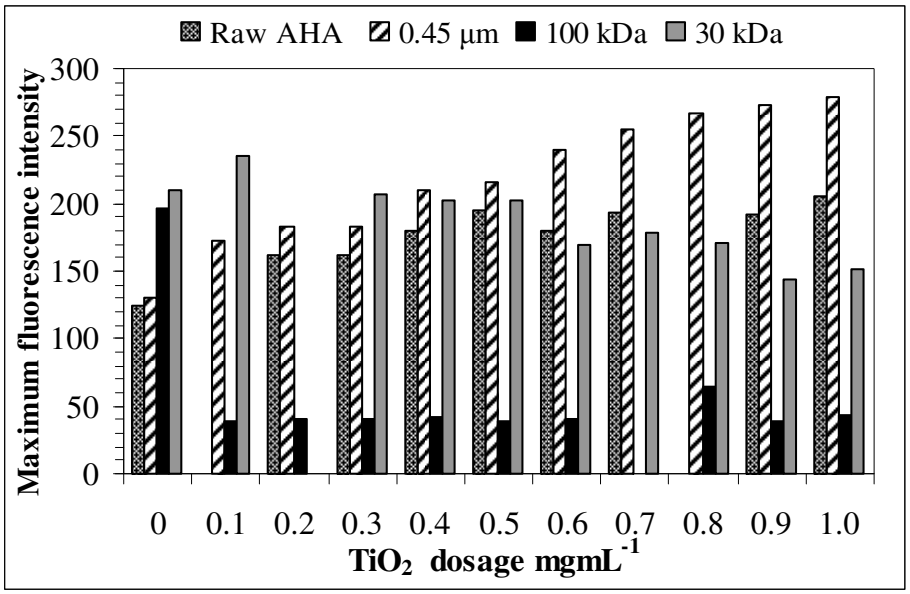

Figure 4.21. Maximum fluorescence intensity of humic acid-bare TiO_2 emission scan

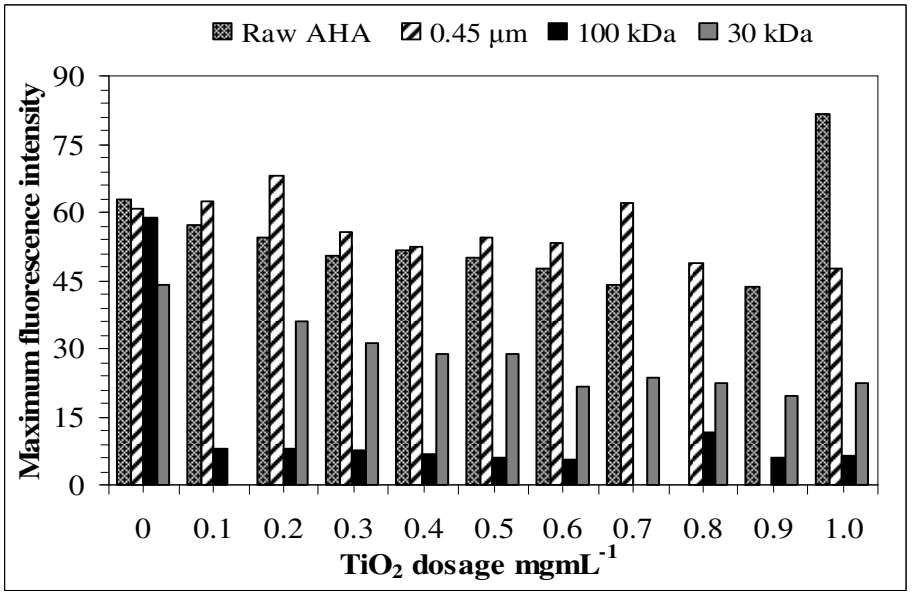

Figure 4.22. Maximum fluorescence intensity of humic acid bare TiO_2 synchronous scan

A similar approach was also presented for synchronous scan spectra maximum intensity values (Figure 4.22). Maximum synchronous scan FI values displayed a range of 43-81 for raw AHA, 47-67 for 0.45 µm AHA, 5.7-57 for 100 kDa and 19-48 for 30 kDa.

The highest FI was recorded for 81 for raw AHA for TiO_2 dose of 1.0 mg mL^{-1}. However a slight decreasing trend was attained for raw humic acid displaying a different behavior for 1.0 mg mL^{-1} TiO_2. An inconsistent trend was obtained for 0.45 μm humic acid fraction and 30 kDa humic acid fraction a decreasing trend was observed. On the other hand, 100 kDa fraction displayed a sharp decrease in FI values.

The Freundlich coefficients for 30 kDa molecular size fraction of humic acid are listed in Table 4.5.

Table 4.5. Freundlich coefficients of 30 kDa molecular size fraction of humic acid-Degussa P-25 TiO_2

	K_f	1/n
UV_{280}, m^{-1}	50.84	0.826
UV_{254}, m^{-1}	32.59	1.02
TOC, mg L^{-1}	8.954	3.10

According to Table 4.5, adsorption capacities, K_f, of UV_{254} and TOC for 30 kDa filtered humic acid were found to be 32.59 and 8.954, respectively. Moreover, the adsorption intensity, 1/n were 1.02 and 3.10, respectively. These values indicated the strong concentration dependency and favorable adsorption intensity because 1/n values were found to be higher than one.

4.2. Adsorption Studies of Fe Doped TiO_2

4.2.1. Raw Humic Acid Adsorption onto Fe Doped TiO_2

In order to evaluate the molecular size effect on adsorption properties of humic acid onto Fe doped TiO_2, experiments were carried out with raw humic acid. The adsorption isotherms for $Color_{436}$, UV_{254} and TOC changes of humic acids were given in the Figure 4.23, Figure 4.24, and Figure 4.25, respectively.

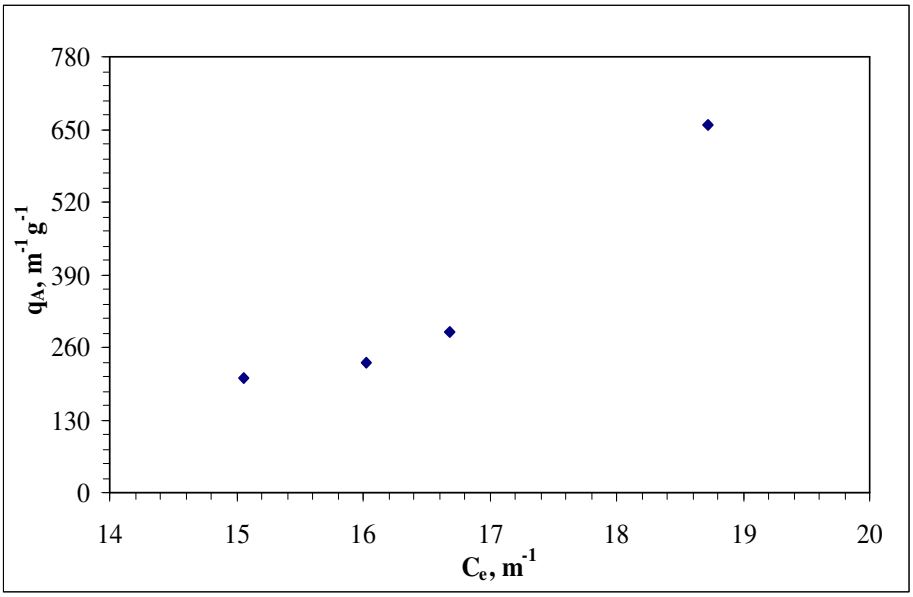

Figure 4.23. $Color_{436}$ adsorption isotherm of humic acid onto Fe doped TiO_2

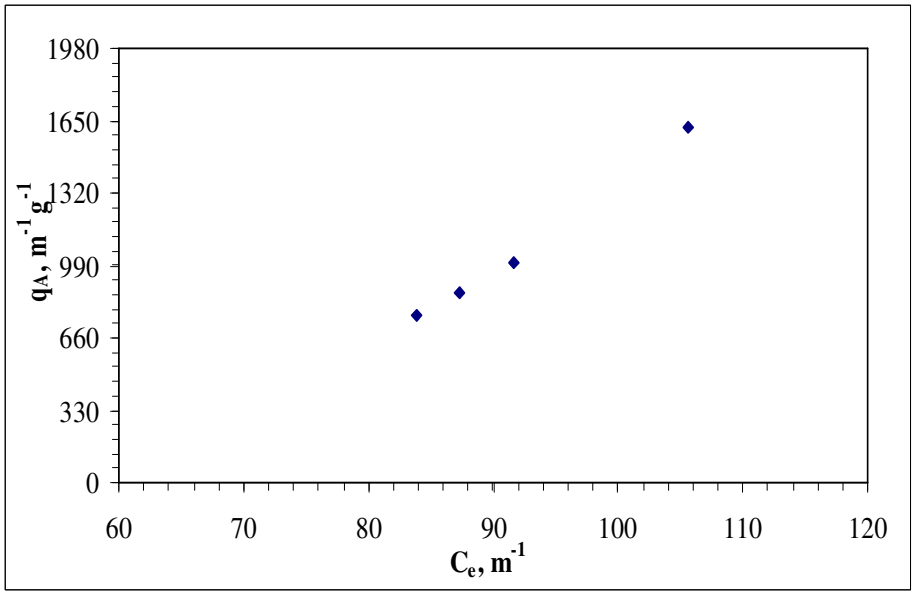

Figure 4.24. UV_{254} adsorption isotherm of humic acid onto Fe doped TiO_2

Figure 4.23 indicated that C_e values varied between 15.1–18.7 m^{-1} for $Color_{436}$ depending on the amount of TiO_2 present in solution. The values of q_A calculated to be in the range of 205 – 658 m^{-1} g^{-1} for the corresponding C_e values.

As it seen in Figure 4.24, C_e values varied between 83.8–105.6 m^{-1} for $UV_{254.}$ The values of q_A calculated to be in the range of 759–1618 m^{-1} g^{-1} for the corresponding C_e values.

Figure 4.25 represented that the values of C_e varied from 12.6 to 16.7 mg L^{-1} for TOC. The calculated q_A values varied in between 148–322 mg $L^{-1}g^{-1}$.

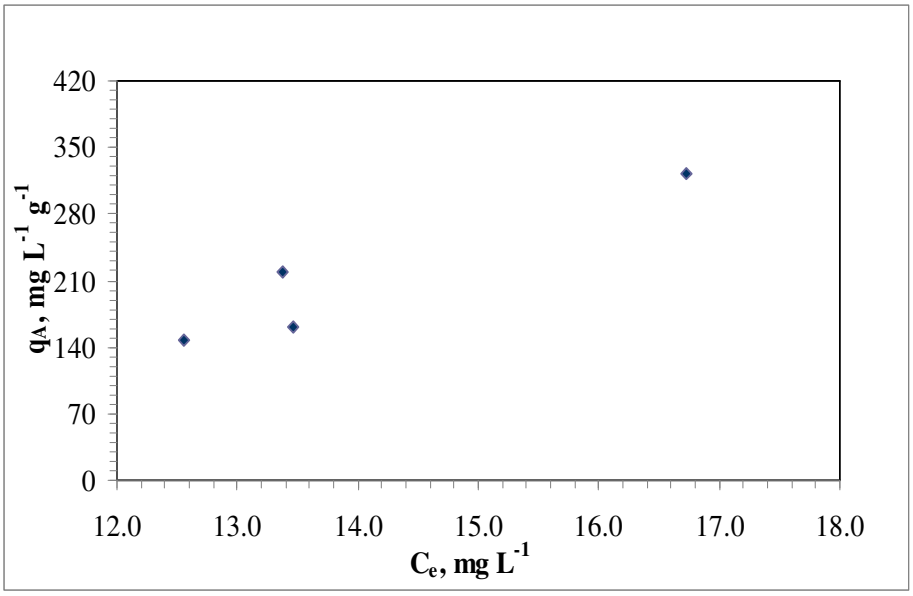

Figure 4.25. TOC adsorption isotherm of humic acid onto Fe doped TiO_2

As can be seen from Figure 4.23, Figure 4.24 and Figure 4.25 above, the adsorption isotherms showed similar trend both in terms of TOC and UV_{254} parameters. This exhibited trend would have agreed well with the linear type isotherm. Δq_A values for raw humic acid were 3.6m^{-1} and 453 m^{-1} g^{-1} respectively at $Color_{436}$. ΔC_e and Δq_A for UV_{254} were 21.8 m^{-1} and 859 m^{-1} g^{-1}, respectively. TOC isotherm for humic acid gave a ΔC_e of 4.1 mg L^{-1} where Δq_A was 174 mg $L^{-1}g^{-1}$. The exhibited trend would have agreed well with the C-curve type isotherm for $Color_{436}$ because the adsorptive can penetrate into the interlayer region, thereby creating new adsorbing surface for itself (Sposito, 1989) and initial slope was independent of adsorptive concentration.

The effect of concentration on the fluorescence spectra of Fe-modified TiO_2 has been studied in starting from 0.2 mg mL^{-1} and increasing with 0.2 mg for each sample up to 1.0 mg mL^{-1} concentration range. Both the emission and synchronous scan fluorescence spectra of raw humic acid onto Fe-modified TiO_2 were illustrated in Figure 4.26 and Figure 4.27. The concentration change of TiO_2 for the samples were symbolized with increasing numbers in the figures that one represented the 50 mg L^{-1} humic acid solution, respectively.

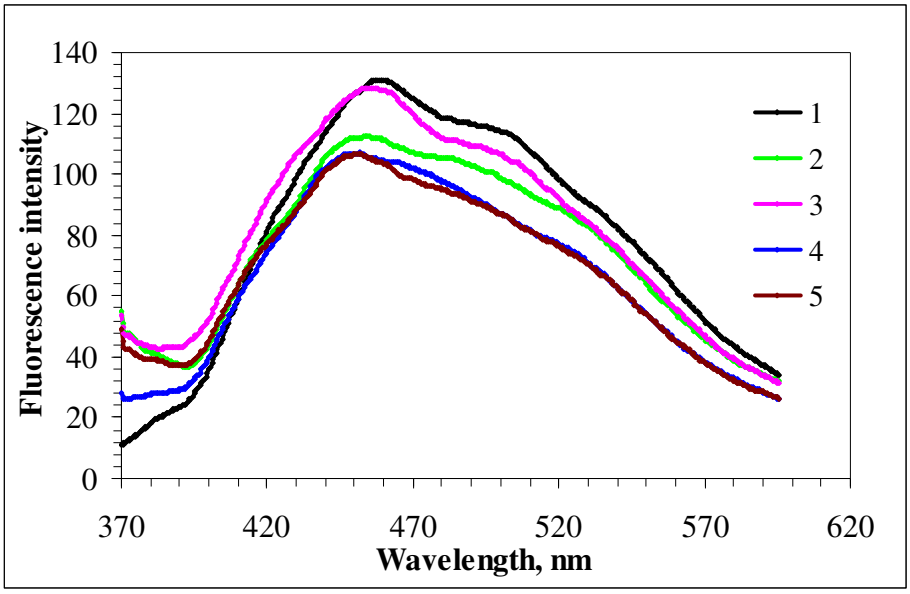

Figure 4.26**.** Emission scan spectra of humic acid onto Fe doped TiO_2.
Where numbers represent, 1: Raw AHA, 2: 0.4 mg mL^{-1} TiO_2, 3: 0.6 mg mL^{-1} TiO_2, 4: 0.8 mg mL^{-1} TiO_2, 5: 1.0 mg mL^{-1} TiO_2

Emission scan spectra recorded for raw humic acid and its lower molecular weight fractions displayed a decreasing trend in FI at λ_{max} 470 nm with respect to increasing Fe doped TiO_2. Remarkably noticeable FI values at all of the λ_{max} values at 345, 370 and 395 nm for lower doses of TiO_2 considering the higher dose of 1.0 mg mL^{-1} TiO_2 no distinct FI could be recorded for all of the λ_{max} values.

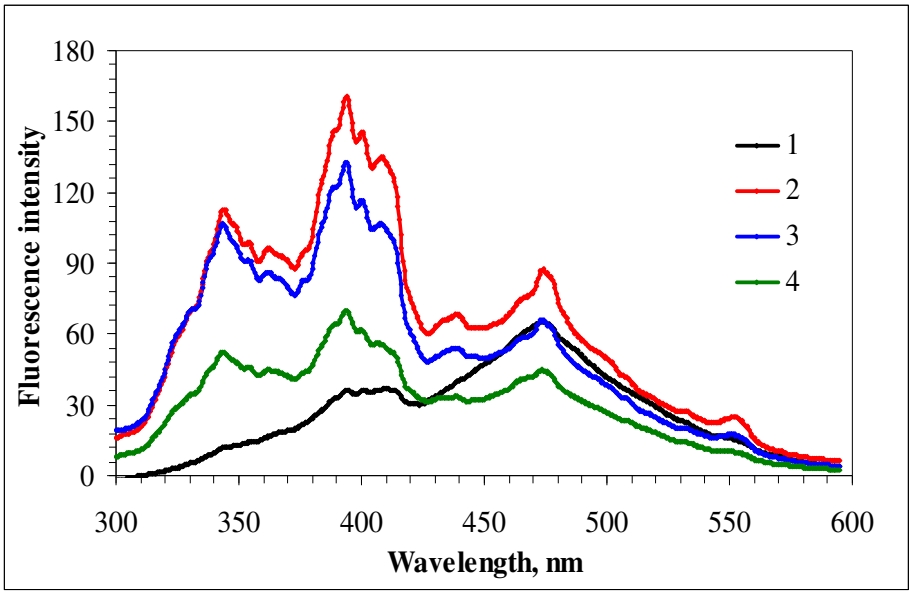

Figure 4.27. Synchronous scan spectra of humic acid onto Fe doped TiO_2.
Where numbers represent, 1: Raw AHA, 2: 0.4 mg mL^{-1} TiO_2, 3: 0.6 mg mL^{-1} TiO_2, 4: 1.0 mg mL^{-1} TiO_2

The adsorption capacity, K_f, and adsorption intensity, 1/n, for humic acid- Fe doped TiO_2 system were listed in Table 4.6.

Table 4.6. Freundlich coefficients of humic acid- Fe doped TiO_2

	K_f	1/n
$Color_{436}$, m^{-1}	4.775E-05	5.58
UV_{365}, m^{-1}	4.090E-05	4.62
UV_{280}, m^{-1}	3.717E-04	3.35
UV_{254}, m^{-1}	3.681E-04	3.28
TOC, mg L^{-1}	0.2193	2.59

The adsorption effects of humic acid on the Fe doped titanium dioxide surface were interpreted with the Freundlich adsorption model, which depends on a heterogeneous surface with a continuous distribution of adsorption sites. According to Table 4.6, adsorption capacity constants for $Color_{436}$ and UV_{365} were found to be very close to each

other when adsorption capacity constants for UV absorbing centers (UV_{280}, and UV_{254}) are approximately equal to each other. 1/n values for $Color_{436}$, UV_{365}, UV_{280} and UV_{254} are found to be between 1 and 10 represent beneficial adsorption, it indicated weak adsorption bond, and the value of q_A changed markedly with small changes in C_e. The values of 1/n, which was related to the distribution of bonded ions on the adsorbent surface indicated that adsorption of raw humic acid onto the Fe- TiO_2 was favorable.

4.2.2. 0.45 µm Fractionated Humic Acid Adsorption onto Fe Doped TiO_2

In order to investigate the adsorption phenomena in 0.45 µm size fraction of humic acid solution onto Fe doped TiO_2, batch adsorption experiments were carried out with Fe doped TiO_2. The adsorption isotherms for $Color_{436}$, UV_{254} and TOC changes of humic acids were given in the Figure 4.28, Figure 4.29, and Figure 4.30 respectively.

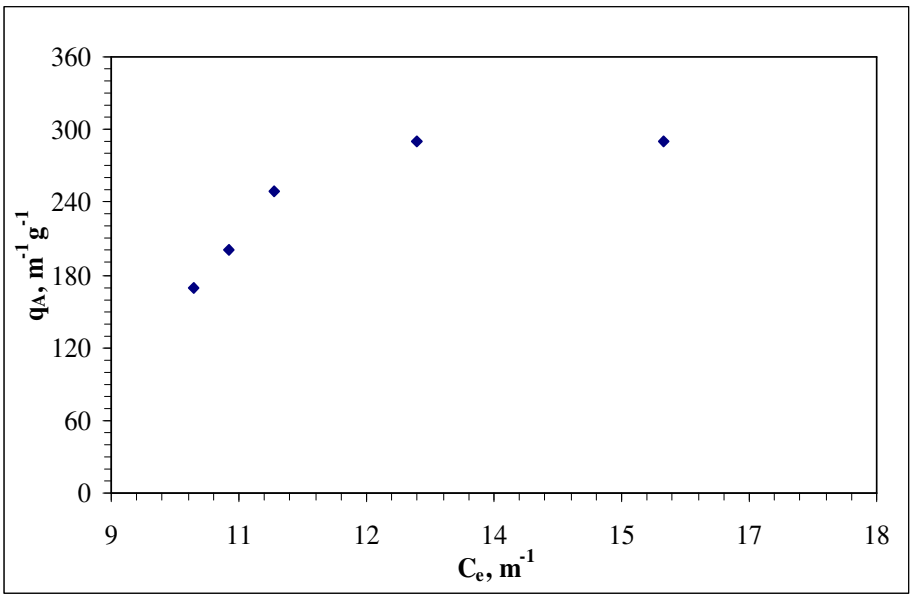

Figure 4.28. $Color_{436}$ adsorption isotherm of 0.45 µm humic acid onto Fe doped TiO_2

Figure 4.28 indicated that C_e values varied between 10.0–15.5 m^{-1} for $Color_{436}$ depending on the amount of TiO_2 present in solution. The values of q_A calculated to be in the range of 169–291 m^{-1} g^{-1} for the corresponding C_e values.

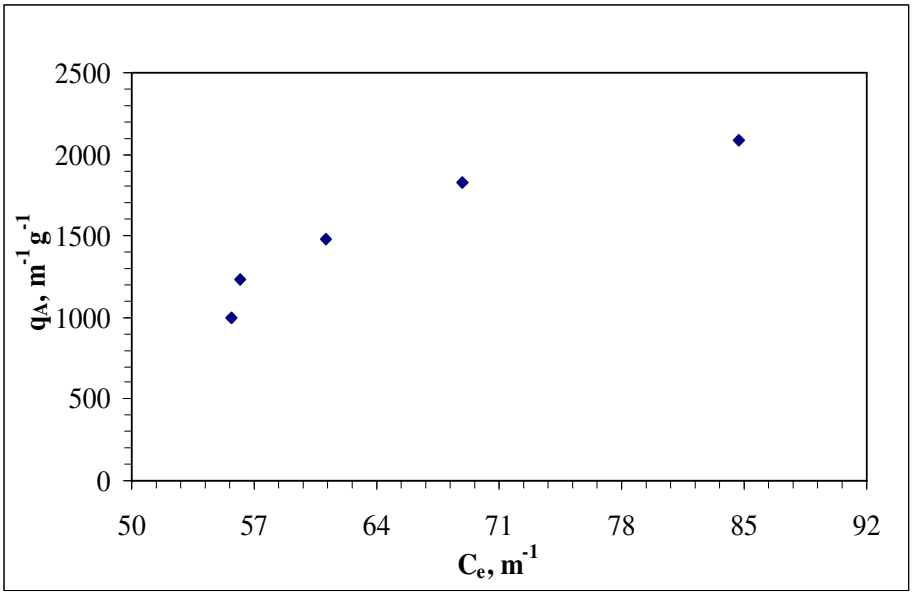

Figure 4.29. UV_{254} adsorption isotherm of 0.45 μm humic acid onto Fe doped TiO_2

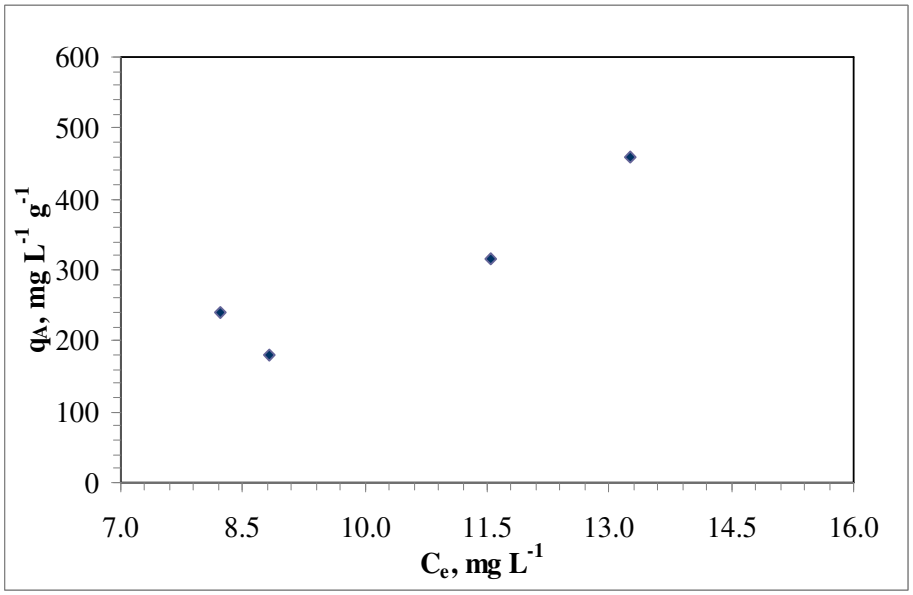

Figure 4.30. TOC adsorption isotherm of 0.45 μm humic acid onto Fe doped TiO_2

As it was seen in Figure 4.29, C_e values varied between 37.0–52.7 m^{-1} for UV_{254}. The values of q_A calculated to be in the range of 472–793 m^{-1} g^{-1} for the corresponding C_e values.

Figure 4.30 represented that the values of C_e varied from 8.22 to 13.3 mg L^{-1} for TOC. The calculated q_A values varied in between 180– 459 mg L^{-1} g^{-1}.

It could clearly be seen from figures that the $Color_{436}$ isotherm showed similar pattern with UV_{254} isotherm. The $Color_{436}$ isotherm for 0.45 µm filtered humic acid was distributed in a narrow C_e range (ΔC_e =5.5 m^{-1}), where Δq_A was 122 m^{-1} g^{-1}. The isotherm gave 321 m^{-1} g^{-1} for Δq_A and 15.7 m^{-1} for ΔC_e at UV_{254}. Δq_A and ΔC_e for TOC isotherm were 279 mg L^{-1} g^{-1} and 5.08 mg L^{-1} respectively.

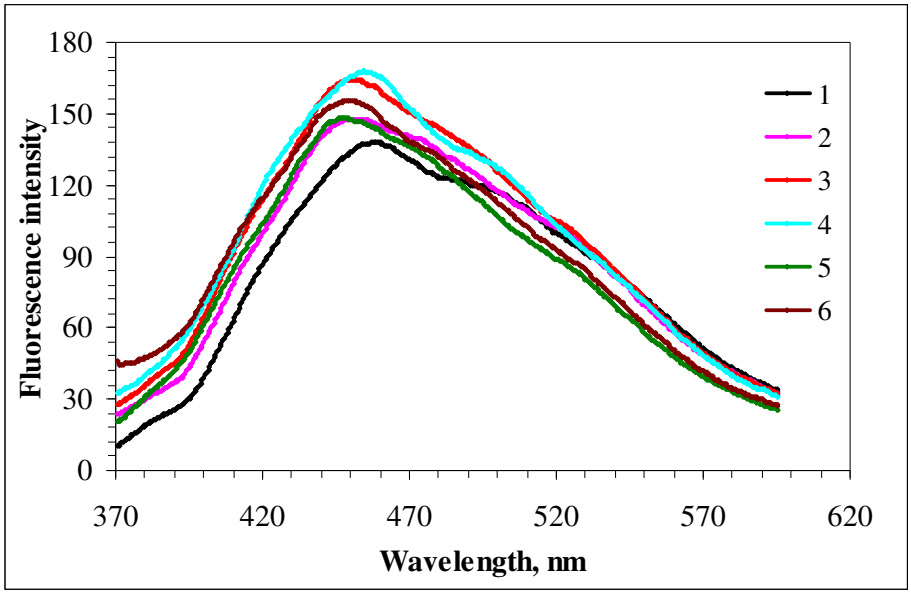

Figure 4.31.Emission scan spectra of 0.45 µm humic acid onto Fe doped TiO_2
Where numbers represent, 1: 0.45 µm fractionated AHA, 2: 0.2 mg mL^{-1} TiO_2, 3: 0.4 mg mL^{-1} TiO_2, 4: 0.6 mg mL^{-1} TiO_2, 5: 0.8 mg mL^{-1} TiO_2, 6: 1.0 mg mL^{-1} TiO_2

Emission scan spectra (Figure 4.31) recorded for 0.45 µm displayed a nonconsistent trend in FI at λ_{max} 470 nm with respect to increasing Fe doped TiO_2. In the synchronous spectra of 0.45 µm fraction of humic acid (Figure 4.32), a decreasing trend was recorded with raw humic acid at λ_{max} 470 nm with respect to increasing Fe doped TiO_2.

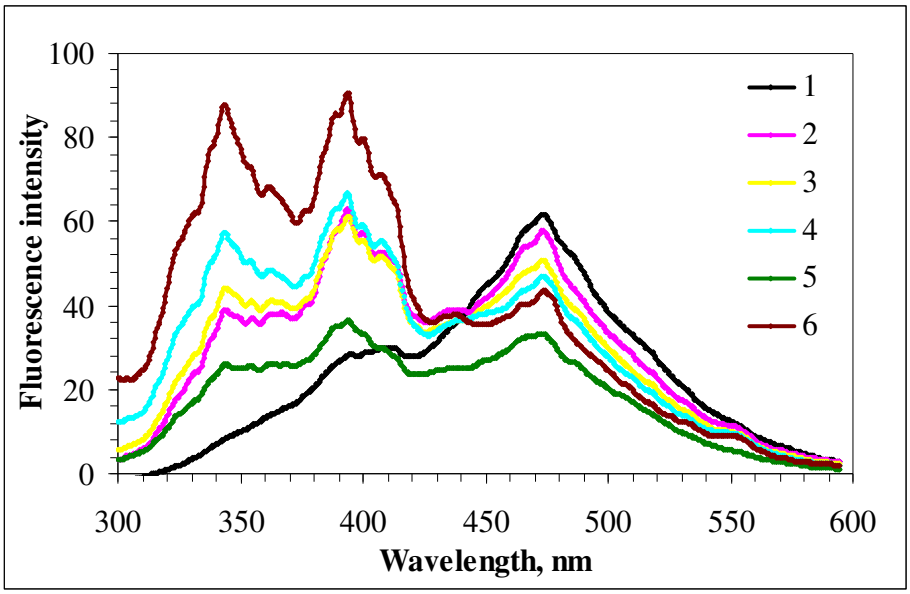

Figure 4.32.Synchronous spectra of 0.45 µm humic acid onto Fe doped TiO_2
Where numbers represent, 1: 0.45 µm fractionated AHA, 2: 0.2 mg mL^{-1} TiO_2, 3: 0.4 mg mL^{-1} TiO_2, 4: 0.6 mg mL^{-1} TiO_2, 5: 0.8 mg mL^{-1} TiO_2, 6: 1.0 mg mL^{-1} TiO_2

Freundlich adsorption model displayed adsorption capacity, K_f, and adsorption strength, 1/n, for 0.45 µm filtered humic acid-Degussa Fe doped TiO_2 system that were listed in Table 4.7.

Table 4.7. Freundlich coefficients of 0.45 µm molecular size fraction of humic acid- Fe doped TiO_2

	K_f	1/n
$Color_{436}$, m^{-1}	15.45	1.11
UV_{365}, m^{-1}	11.84	1.18
UV_{280}, m^{-1}	2.883	1.56
UV_{254}, m^{-1}	2.211	1.56
TOC, mg L^{-1}	7.032	1.58

According to Table 4.7, adsorption capacities of 0.45 μm molecular size fraction of humic acid onto Fe doped TiO_2 were found to be higher than the adsorption capacities of raw humic acid for each parameter. Moreover, adsorption intensities for each parameter were found to be higher than one, it indicates that the adsorption bond was weak; the capacity tended to be dependent of C_e.

4.2.3. 100 kDa Fractionated Humic Acid Adsorption onto Fe Doped TiO_2

In order to evaluate the molecular size effect on the adsorption properties of humic acid onto the modified TiO_2 surfaces (Fe), experiments were carried out with 100 kDa molecular size fraction of humic acid. The Freundlich adsorption isotherms for $Color_{436}$, UV_{254} and TOC changes of humic acids were given in the Figure 4.33, Figure 4.34 and Figure 4.35, respectively.

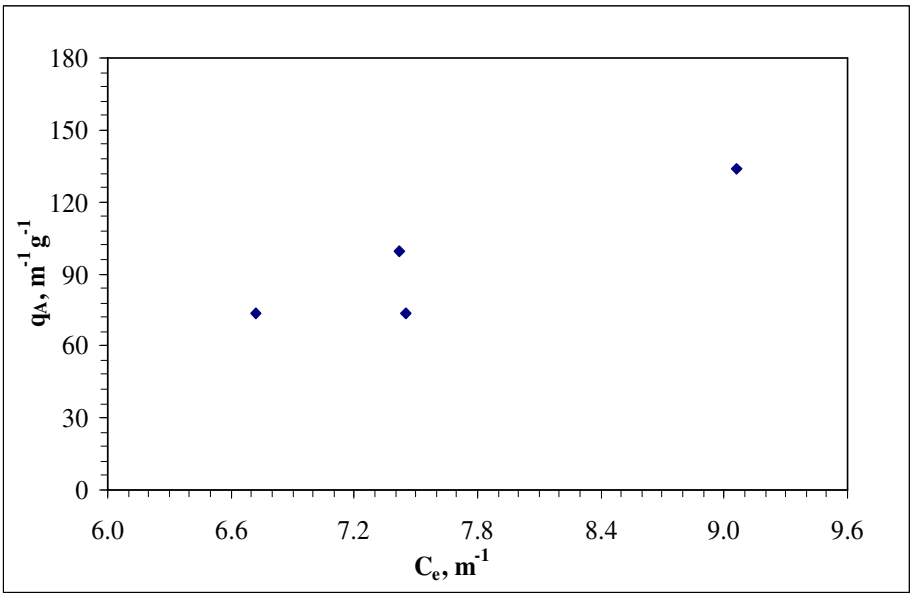

Figure 4.33. $Color_{436}$ adsorption isotherm of 100 kDa humic acid onto Fe doped TiO_2

Figure 4.33 indicated that C_e values varied between 6.72–9.06 m^{-1} for $Color_{436}$ depending on the amount of TiO_2 present in solution. The values of q_A calculated to be in the range of 74–134 m^{-1} g^{-1} for the corresponding C_e values.

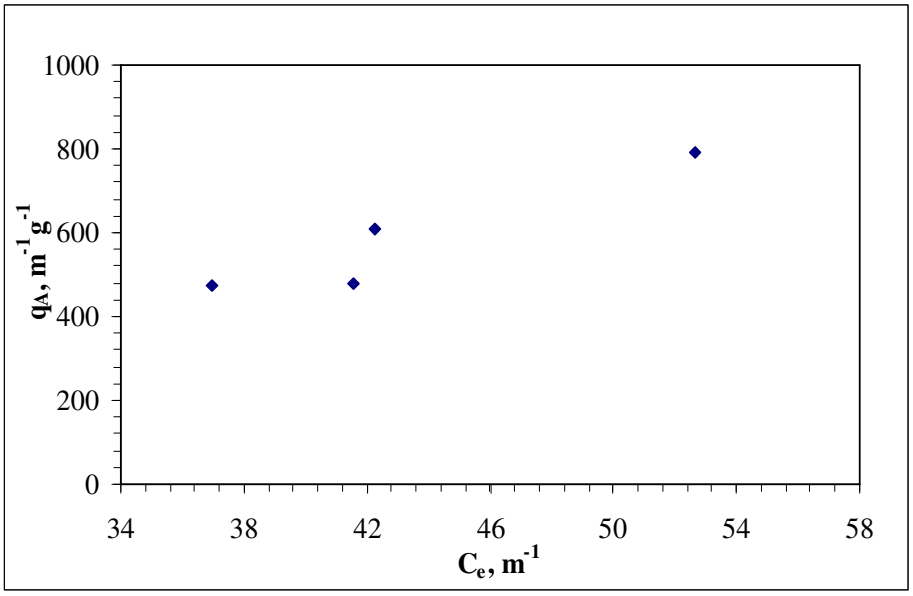

Figure 4.34. UV_{254} adsorption isotherm of 100 kDa humic acid onto Fe doped TiO_2

As it was seen in Figure 4.34, C_e values varied between 37.0–52.7 m^{-1} for UV_{254}. The values of q_A calculated to be in the range of 472–793 m^{-1} g^{-1} for the corresponding C_e values.

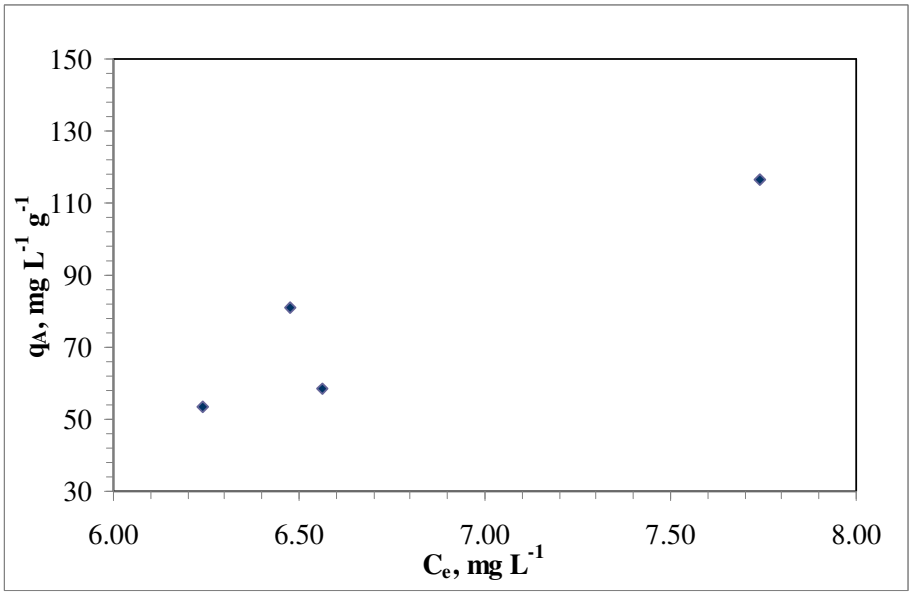

Figure 4.35. TOC adsorption isotherm of 100 kDa humic acid onto Fe doped TiO_2

Figure 4.35 represented that the values of C_e varied from 6.24 to 7.74 mg L^{-1} for TOC. The calculated q_A values varied in between 53–117 mg $L^{-1}g^{-1}$.

As isotherm for $Color_{436}$ showed same pattern with UV_{254}. For the 100 kDa filtered humic acid- Fe doped TiO_2, Δq_A and ΔC_e for $Color_{436}$ were 60 m^{-1} g^{-1} and 2.34 m^{-1} respectively. The isotherm gave 321 m^{-1} g^{-1} for Δq_A and 15.7 m^{-1} for ΔC_e at UV_{254}. TOC isotherm for humic acid gave a ΔC_e of 1.50 mg L^{-1} where Δq_A was 64.0 mg $L^{-1}g^{-1}$. The isotherms showed C-curve type isotherm.

Emission scan spectra recorded for 100 kDa fraction of humic acid displayed a decreasing trend in FI at λ_{max} 470 nm with respect to increasing Fe doped TiO_2. Lower molecular weight fraction of humic acid displayed completely different patterns. 100 kDa fraction retained λ_{max} at 470 nm whereas significant decreasing trend was recorded for lower λ_{max} values for 30 kDa fraction.

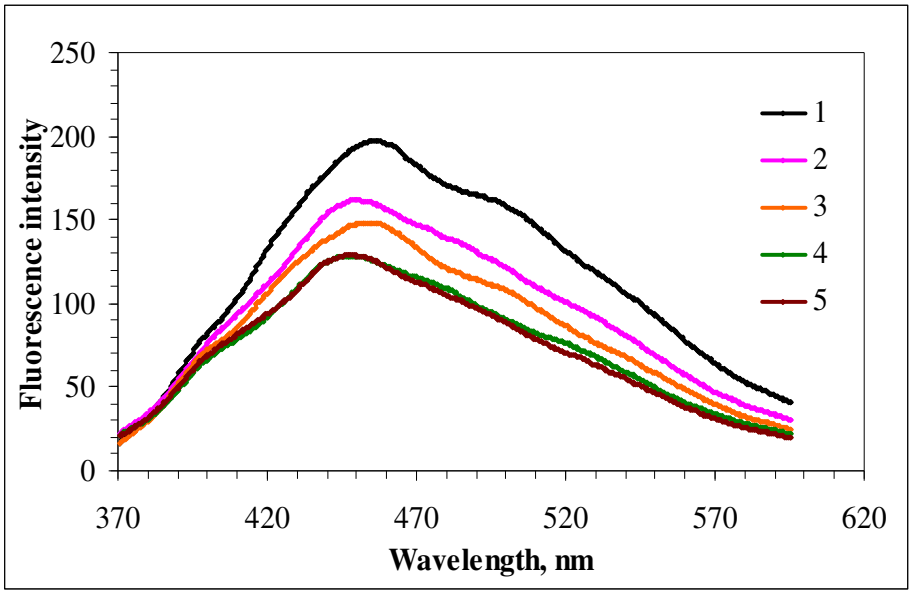

Figure 4.36. Emission scan spectra of 100 kDa humic acid onto Fe doped TiO_2
Where numbers represent, 1: 100 kDa AHA, 2: 0.4 mg mL^{-1} TiO_2, 3: 0.6 mg mL^{-1} TiO_2, 4: 0.8 mg mL^{-1} TiO_2, 5: 1.0 mg mL^{-1} TiO_2

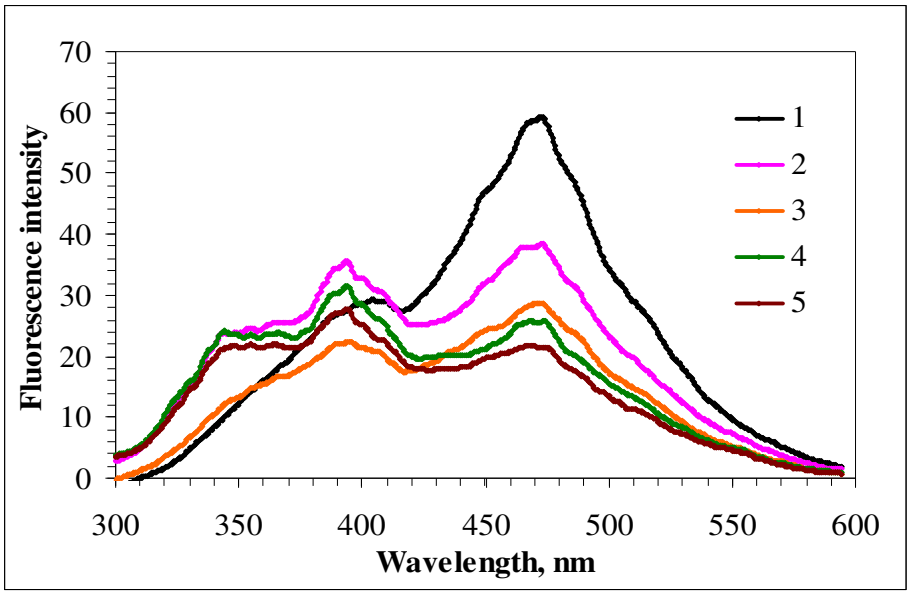

Figure 4.37. Synchronous scan spectra of 100 kDa humic acid onto Fe doped TiO_2
Where numbers represent, 1: 100 kDa AHA, 2: 0.4 mg mL^{-1} TiO_2, 3: 0.6 mg mL^{-1} TiO_2, 4: 0.8 mg mL^{-1} TiO_2, 5: 1.0 mg mL^{-1} TiO_2

The adsorption capacity, K_f, and adsorption strength, 1/n, for 100 kDa filtered humic acid-Fe doped TiO_2 system were listed in Table 4.8.

Table 4.8. Freundlich coefficients of 100 kDa molecular size fraction of humic acid- Fe doped TiO_2

	K_f	1/n
$Color_{436}$, m^{-1}	1.449	2.05
UV_{365}, m^{-1}	1.573	1.77
UV_{280}, m^{-1}	1.759	1.56
UV_{254}, m^{-1}	1.788	1.54
TOC, mg L^{-1}	0.1356	3.30

According to Table 4.8, adsorption capacity constants for both the UV absorbing centers and the color forming groups were found to be very close to each other. 1/n values

were found to be higher than one, it indicated that the adsorption bond was weak; the capacity tended to be dependent of C_e. They expressed favorable adsorption.

4.2.4. 30 kDa Fractionated Humic Acid Adsorption onto Fe Doped TiO_2

In order to examine the molecular size effect on the adsorption behavior of humic acid onto Fe doped TiO_2, the batch adsorption experiments were also carried out with 30 kDa molecular size fractionated humic acid. The adsorption isotherms of $Color_{436}$, UV_{254} and TOC were shown in Figures 4.38, Figures 4.39 and Figures 4.40, respectively.

Figure 4.38 indicated that C_e values varied between 2.76–3.68 m^{-1} for $Color_{436}$ depending on the amount of TiO_2 present in solution. The values of q_A calculated to be in the range of 30.8–62.0 m^{-1} g^{-1} for the corresponding C_e values.

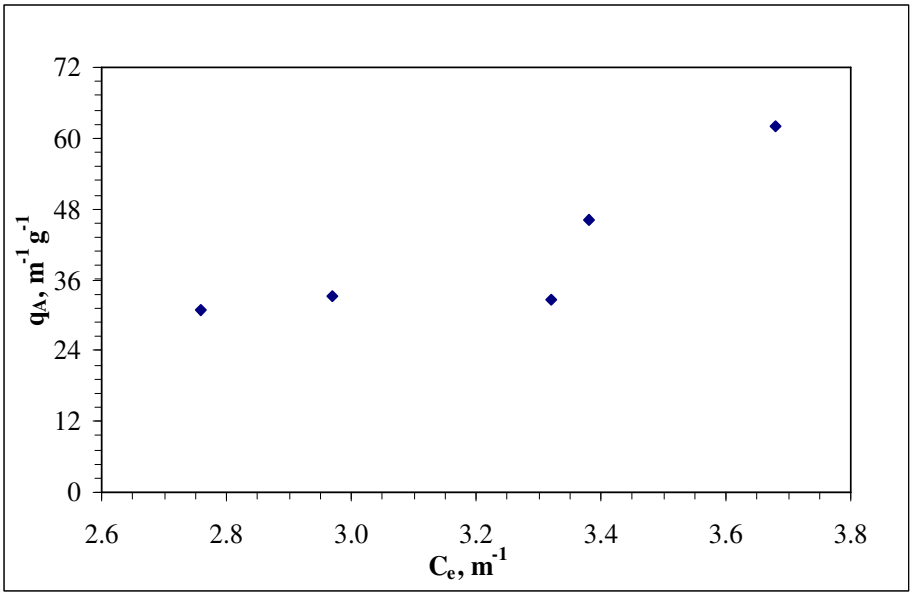

Figure 4.38. $Color_{436}$ adsorption isotherm of 30 kDa humic acid onto Fe doped TiO_2

As seen in Figure 4.39, C_e values varied between 14.4–22.5 m^{-1} for $UV_{254.}$ The values of q_A calculated to be in the range of 265–520 m^{-1} g^{-1} for the corresponding C_e values.

Figure 4.40 showed that the values of C_e varied from 2.47 to 2.73 mg L^{-1} for TOC. The calculated q_A values varied in between 42.0–181 mg $L^{-1}g^{-1}$.

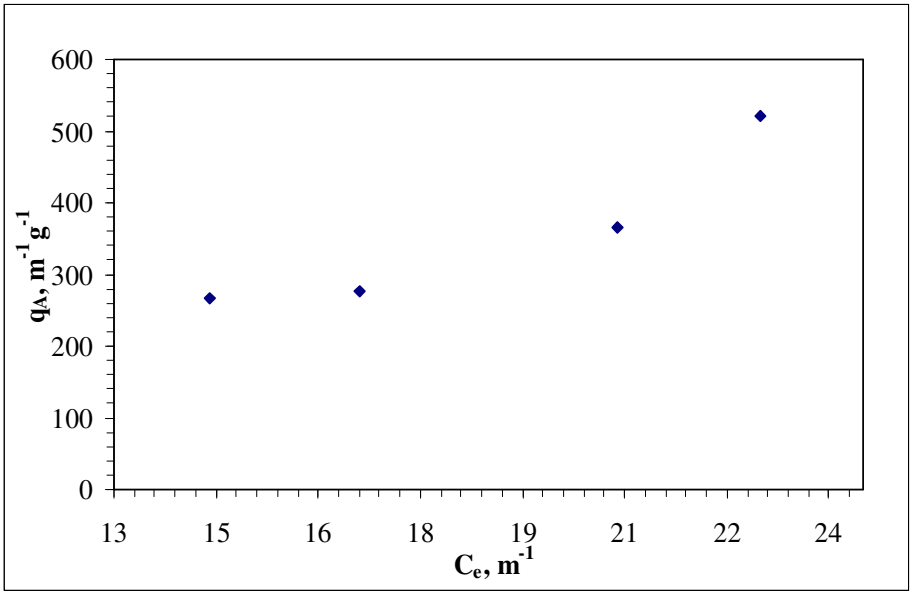

Figure 4.39. UV_{254} adsorption isotherm of 30 kDa humic acid onto Fe doped TiO_2

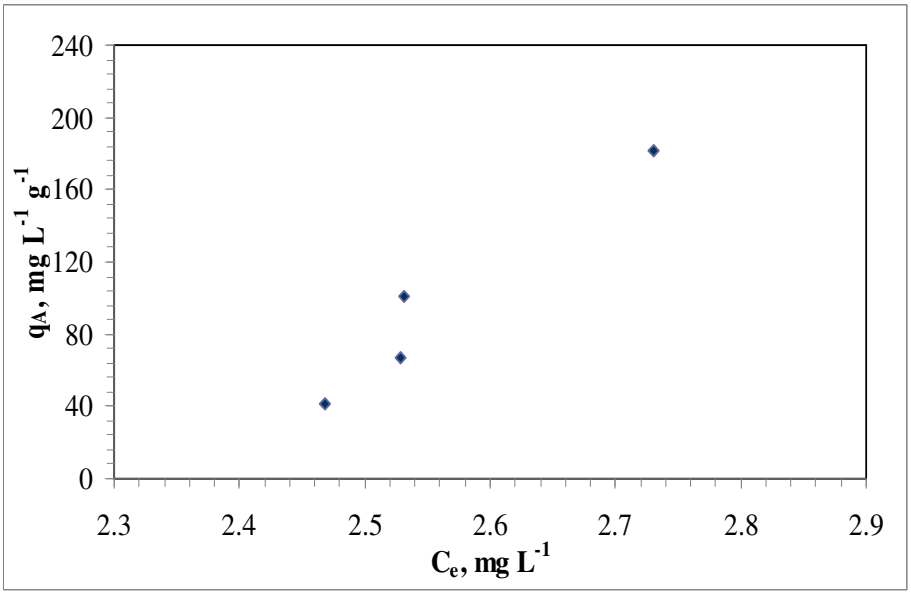

Figure 4.40. TOC adsorption isotherm of 30 kDa humic acid onto Fe doped TiO_2

ΔC_e and Δq_A values for 30 kDa filtered humic acid were 0.92 m^{-1} and 31.2 $m^{-1}g^{-1}$ respectively at $Color_{436}$. ΔC_e and Δq_A for UV_{254} were 8.1 m^{-1} and 255 m^{-1} g^{-1}, respectively. Molecular size fractionation of humic acid resulted in steep curves with high Δq_A of 139 mg L^{-1} g^{-1} in a short C_e range of 0.26 mg L^{-1} for TOC isotherm. The shape of isotherms for color forming groups and UV centers showed same pattern with the smaller ΔC_e when compared to isotherm of TOC.

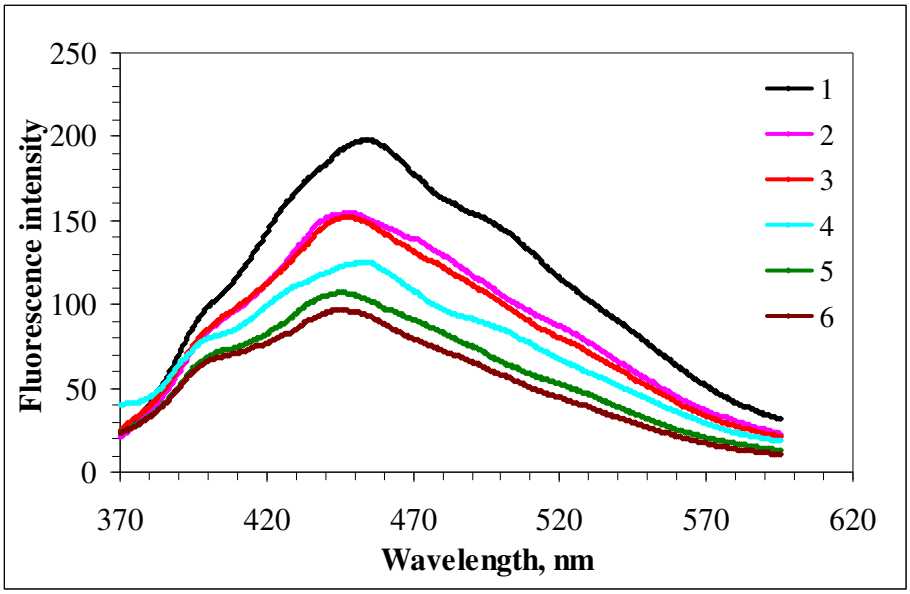

Figure 4.41. Emission scan spectra of 30 kDa humic acid onto Fe doped TiO_2
Where numbers represent, 1: 30 kDa AHA, 2: 0.2 mg mL^{-1} TiO_2, 3: 0.4 mg mL^{-1} TiO_2, 4: 0.6 mg mL^{-1} TiO_2, 5: 0.8 mg mL^{-1} TiO_2, 6: 1.0 mg mL^{-1} TiO_2

Emission scan spectra recorded for 30 kDa fraction of humic acid displayed a continuously decreasing trend in FI at λ_{max} 470 nm with respect to increasing Fe doped TiO_2. Lower molecular weight fraction of humic acid displayed completely different patterns. In the synchronous scan spectra, 100 kDa fraction retained λ_{max} at 470 nm whereas significant decreasing trend was recorded for lower λ_{max} values for 30 kDa fraction.

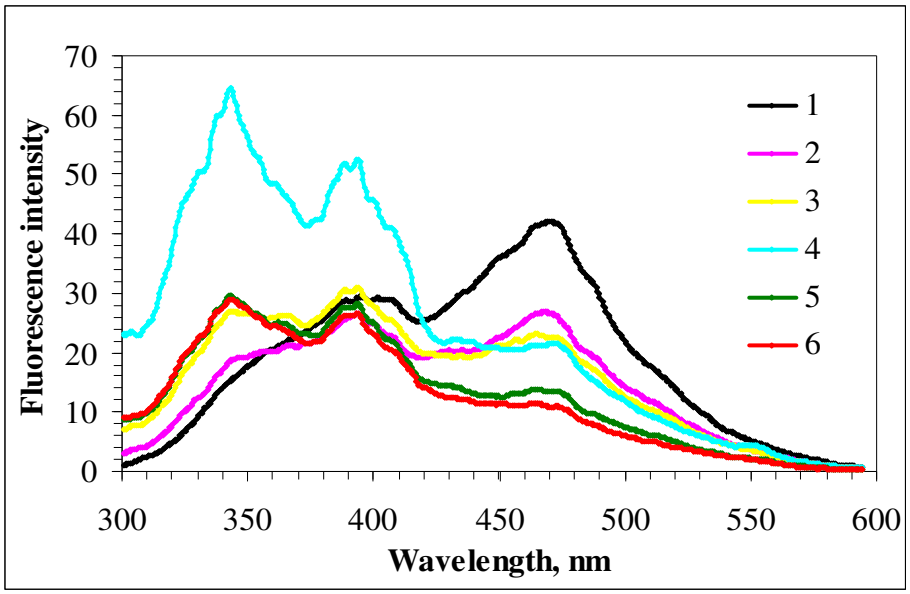

Figure 4.42. Synchronous scan spectra of 30 kDa humic acid onto Fe doped TiO_2

Where numbers represent, 1: 30 kDa AHA, 2: 0.2 mg mL^{-1} TiO_2, 3: 0.4 mg mL^{-1} TiO_2, 4: 0.6 mg mL^{-1} TiO_2, 5: 0.8 mg mL^{-1} TiO_2, 6: 1.0 mg mL^{-1} TiO_2

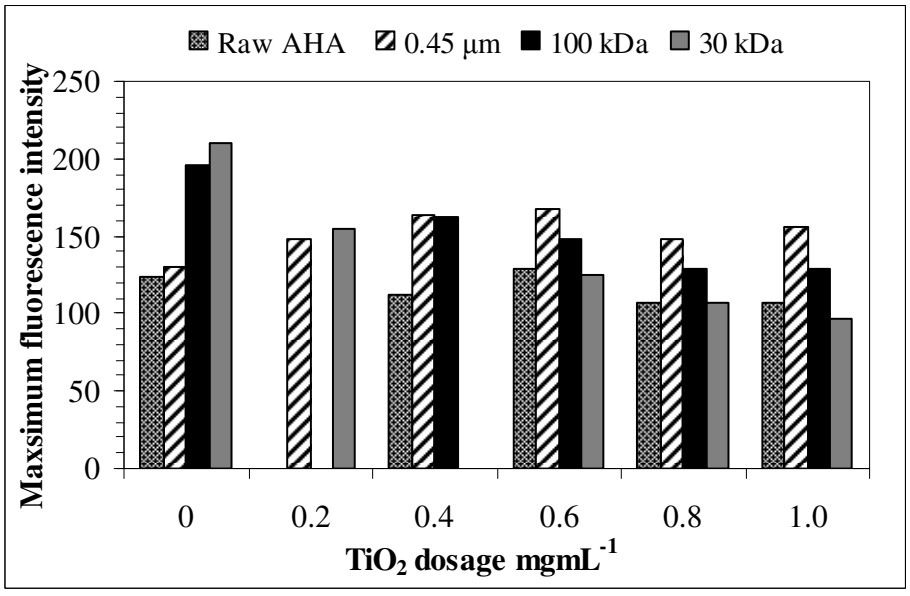

Figure 4.43. Maximum fluorescence intensity of humic acid- Fe doped TiO_2 emission scan

For comparison purposes maximum fluorescence emission scan intensity values were displayed for all of the humic acid fractions as well as raw humic acid (Figure 4.43). Maximum emission scan FI values displayed a range of 124-131 for raw AHA, 138-167 for 0.45 μm AHA, 128-197 for 100 kDa and 96-198 for 30 kDa. A slightly decreasing trend was observed for raw humic acid fraction as well as for 100 kDa and 30 kDa fractions. However inconsistent trends in FI values were recorded for 0.45 μm fraction of humic acid after respective adsorption equilibrium. The highest FI values recorded were 198 for 100 kDa and 30 kDa fractions of raw humic acid.

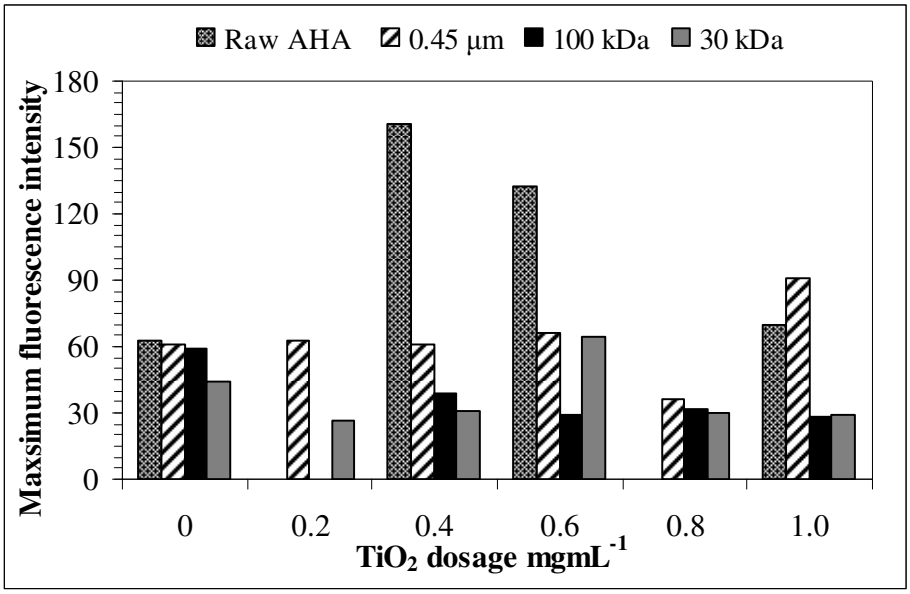

Figure 4.44. Maximum fluorescence intensity of humic acid- Fe doped TiO_2 synchronous scan.

A different trend was presented for synchronous scan spectra maximum intensity values (Figure 4.44). Maximum synchronous scan FI values displayed a range of 65-160 for raw AHA, 36-90 for 0.45 μm AHA, 28-59 for 100 kDa and 26-64 for 30 kDa. The highest FI was recorded for 160 for raw AHA for TiO_2 dose of 0.4 mg mL^{-1}. However a slight decreasing trend was attained for 100 kDa molecular weight fraction of raw humic acid.

Table 4.9. Freundlich coefficients of 30 kDa molecular size fraction of humic acid- Fe doped TiO_2

	K_f	1/n
$Color_{436}$, m^{-1}	2.963	2.22
UV_{365}, m^{-1}	11.47	1.03
UV_{280}, m^{-1}	9.045	1.22
UV_{254}, m^{-1}	5.252	1.44
TOC, mg L^{-1}	3.367E-04	13.2

The Freundlich coefficients for 30 kDa molecular size fraction of humic acid are listed in table 4.9. According to Table 4.9, adsorption capacities, K_f, of $Color_{436}$, UV_{254} and TOC for 30 kDa filtered humic acid–Fe doped TiO_2 were found to be 2.96, 5.25 and 3.37E-04, respectively. The adsorption capacity for UV absorbing centers was higher than color forming groups. Moreover, considering 1/n values were merely the empirical linearization constants of the curvilinear plots covering the concentration effects of the adsorption process (Bekbolet at al., 2002), the adsorption intensity, 1/n are 2.22, 1.44 and 13.2, respectively. These values indicated the strong concentration dependency and favorable adsorption intensity because 1/n values were found to be higher than one.

4.3. Adsorption Studies of Ascorbic Acid Modified TiO_2

4.3.1. Raw Humic Acid Adsorption onto Ascorbic Acid Modified TiO_2

In order to evaluate the molecular size effect on the adsorption properties of humic acid onto ascorbic acid modified TiO_2, preliminary experiments were carried out with raw humic acid. The adsorption isotherms for $Color_{436}$, UV_{254} and TOC changes of humic acids were given in the Figure 4.45, Figure 4.46, and Figure 4.47, respectively.

Figure 4.45 indicates that C_e values varied between 12.7–13.9 m^{-1} for $Color_{436}$ depending on the amount of TiO_2 present in solution. The values of q_A calculated to be in the range of 314–1144 m^{-1} g^{-1} for the corresponding C_e values.

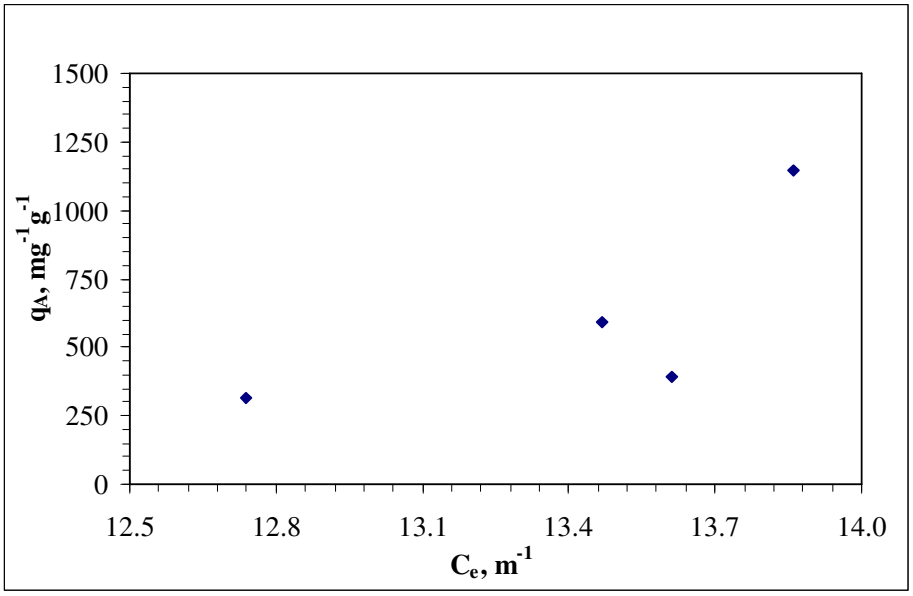

Figure 4.45. $Color_{436}$ adsorption isotherm of humic acid onto ascorbic acid modified TiO_2

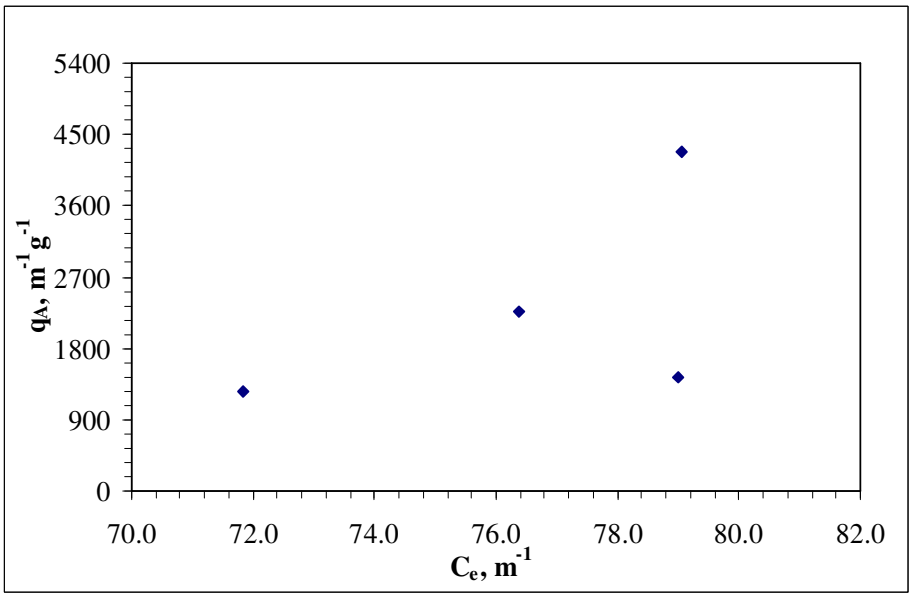

Figure 4.46. UV_{254} adsorption isotherm of humic acid onto ascorbic acid modified TiO_2

As it could be seen in Figure 4.46, C_e values varied between 71.8–79.1 m^{-1} for $UV_{254.}$ The values of q_A calculated to be in the range of 1249–4273 m^{-1} g^{-1} for the corresponding C_e values.

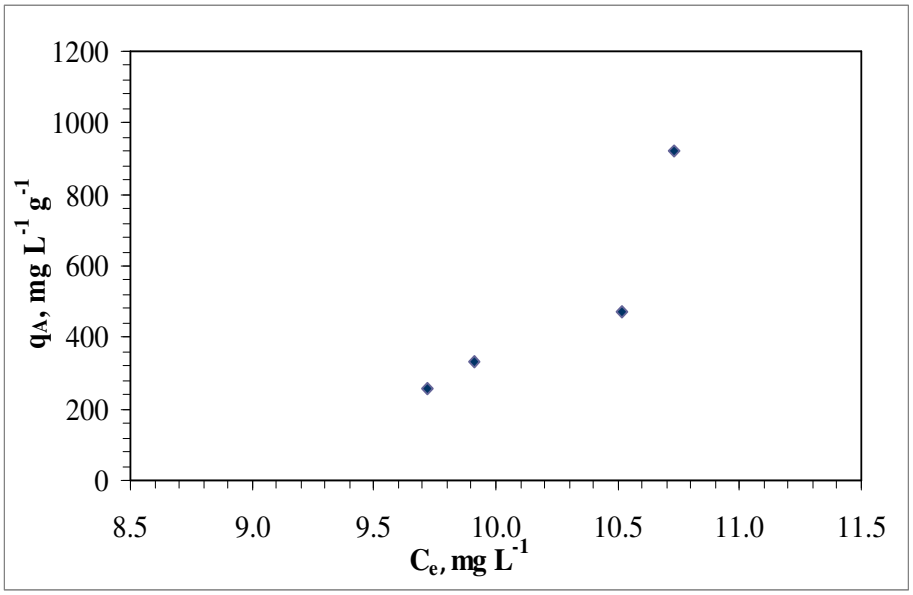

Figure 4.47. TOC adsorption isotherm of humic acid onto ascorbic acid modified TiO_2

Figure 4.47 represented that the values of C_e varied from 9.72 to 10.7 mg L^{-1} for TOC. The calculated q_A values varied in between 256– 921 mg $L^{-1}g^{-1}$.

UV_{365} and UV_{280} adsorption isotherms were given in Appendix C. Figure C-1 showed that the value of C_e varied from 33.6– 46.5 m^{-1} for UV_{365} depending on the amount of TiO_2. The calculated q_A values varied in between 283-2052 m^{-1} g^{-1} for the corresponding C_e values. Figure C-2 shows that the value of C_e varied from 62.1–67.9 m^{-1} for UV_{280} depending on the amount of TiO_2. The calculated q_A values varied in between 1093-3795 $m^{-1}g^{-1}$ for the corresponding C_e values.

As can be seen from Figure 4.45 and Figure 4.46 above, the adsorption isotherms showed similar trend both in terms of $Color_{436}$ and UV_{254} parameters. ΔC_e and Δq_A values for raw humic acid-ascorbic acid modified TiO_2 were 1.20 m^{-1} and 830 m^{-1} g^{-1} respectively at $Color_{436}$. ΔC_e and Δq_A for UV_{254} were 7.3 m^{-1} and 3024 m^{-1} g^{-1}, respectively. The isotherm for UV_{365} gave a ΔC_e of 12.9 m^{-1} and for UV_{280} it was 5.7 m^{-1}; where Δq_A's were 1769 m^{-1} g^{-1} and 2702 m^{-1} g^{-1} respectively. In general, isotherms showed wide span of q_A range with the smaller ΔC_e. TOC isotherm for humic acid-ascorbic acid modified TiO_2

gave a ΔC_e of 0.98 mg L^{-1} where Δq_A was 665 mg $L^{-1}g^{-1}$. The isotherm for TOC showed a C-curve type isotherm. The value of q_A changes markedly with small changes in C_e.

The effect of concentration on the fluorescence spectra of ascorbic acid modified TiO_2 has been studied in starting from 0.2 mg mL^{-1} and increasing with 0.2 mg for each sample up to 1.0 mg mL^{-1} concentration range. Both the emission and synchronous scan fluorescence spectra of raw humic acid onto ascorbic acid modified TiO_2 were illustrated in Figure 4.48 and Figure 4.49. The concentration change of TiO_2 for the samples were symbolized with increasing numbers in the figures that one represented the 50 mg L^{-1} humic acid solution, respectively.

Adsorption of humic acid onto ascorbic acid modified TiO_2 could also be followed by decreasing FI values at λ_{max}=450 nm for all of the humic acid fractions as well as the raw humic acid. In the synchronous scan spectra of raw humic acid, significantly higher FI values were recorded at λ_{max} 395 and 470 nm for higher doses of ascorbic acid modified TiO_2.

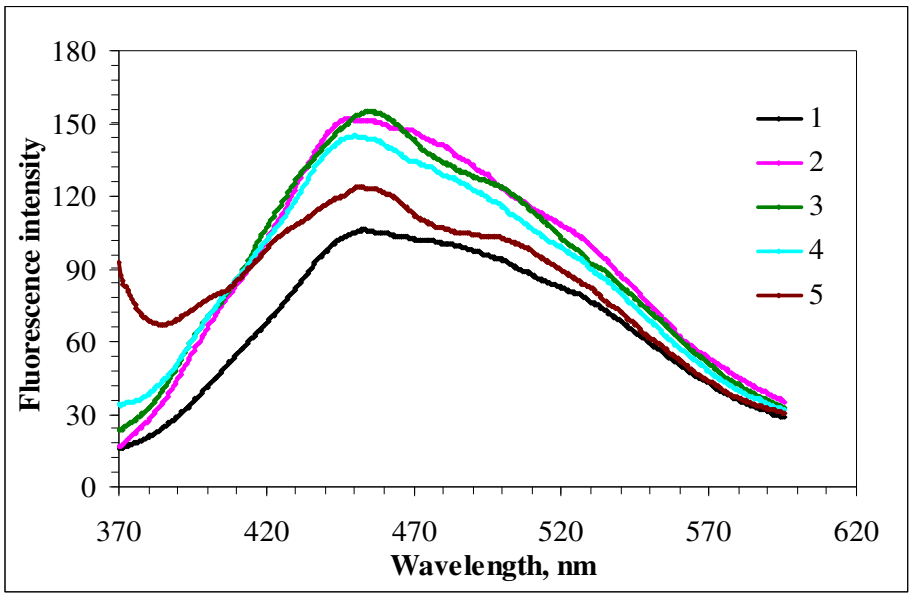

Figure 4.48. Emission scan spectra of humic acid onto ascorbic acid modified TiO_2
Where numbers represent, 1: Raw AHA, 2: 0.2 mg mL^{-1} TiO_2, 3: 0.4 mg mL^{-1} TiO_2, 4: 0.6 mg mL^{-1} TiO_2, 5: 1.0 mg mL^{-1} TiO_2

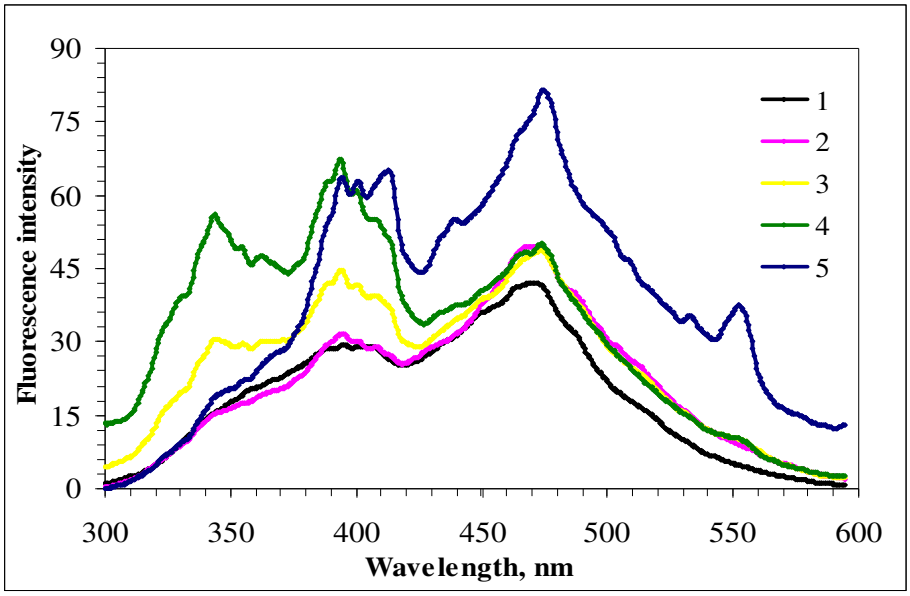

Figure 4.49. Synchronous scan spectra of humic acid onto ascorbic acid modified TiO_2 Where numbers represent, 1: Raw AHA, 2: 0.2 mg mL^{-1} TiO_2, 3: 0.4 mg mL^{-1} TiO_2, 4: 0.6 mg mL^{-1} TiO_2, 5: 1.0 mg mL^{-1} TiO_2

In order to evaluate experimental results, data were fitted to the Freundlich Model for TOC values. The adsorption capacity, K_f, and adsorption strength, 1/n, for humic acid-ascorbic acid modified TiO_2 system were 3.373E-09 and 11.0, respectively. According to the values, adsorption capacity constant for TOC was found to be low whereas 1/n value for TOC was found to be higher than one; it indicated that the adsorption bond was weak.

4.3.2. 0.45 µm Fractionated Humic Acid Adsorption onto Ascorbic Acid Modified TiO_2

In order to investigate the adsorption phenomena in 0.45 µm size fraction of humic acid solution, batch adsorption experiments were carried out with ascorbic acid modified TiO_2. The adsorption isotherms for $Color_{436}$, UV_{254} and TOC changes of humic acids were given in the Figure 4.50, Figure 4.51, and Figure 4.52, respectively.

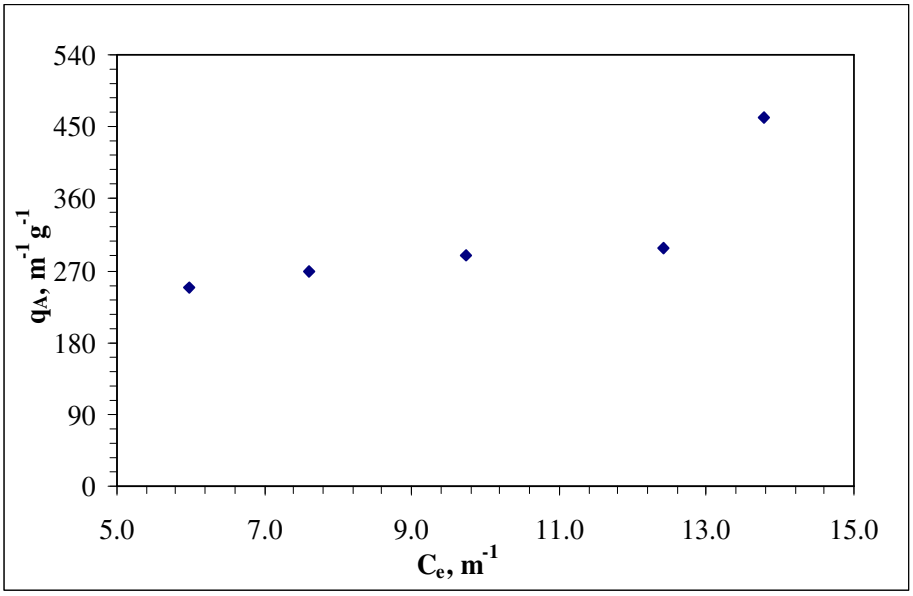

Figure 4.50. $Color_{436}$ adsorption isotherm of 0.45 µm humic acid onto ascorbic acid modified TiO_2

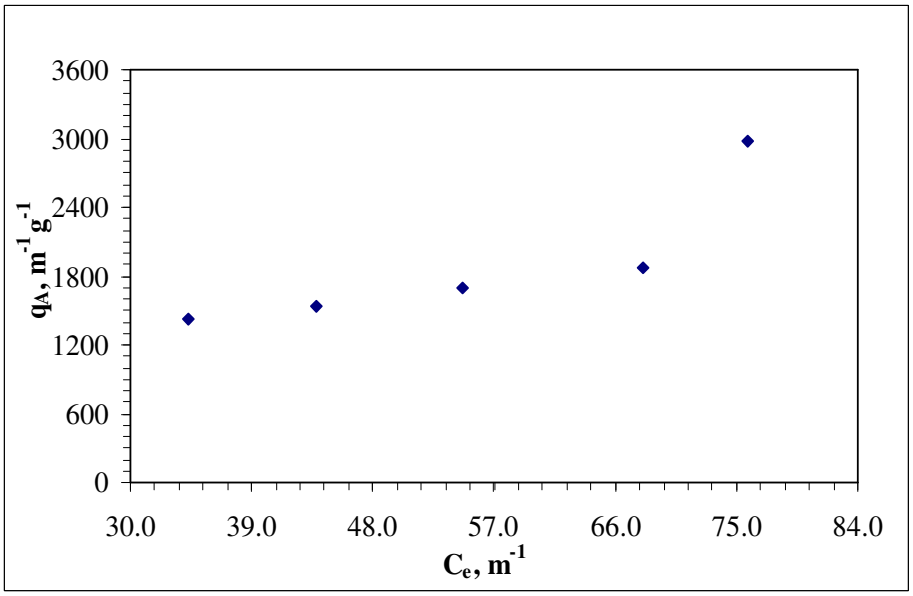

Figure 4.51. UV_{254} adsorption isotherm of 0.45 µm humic acid onto ascorbic acid modified TiO_2

Figure 4.50 represented that the values of C_e varied from 5.99 to 13.8 m^{-1} for $Color_{436}$. The calculated q_A values varied in between 248– 461 m^{-1} g^{-1}.

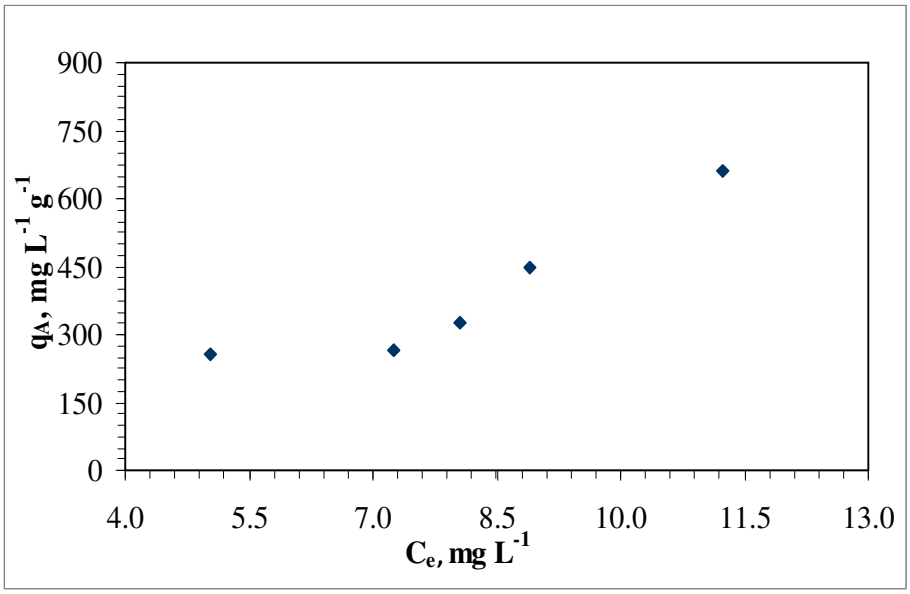

Figure 4.52. TOC adsorption isotherm of 0.45 μm humic acid onto ascorbic acid modified TiO_2

As it is seen in Figure 4.51, C_e values varied between 34.3–75.8 m^{-1} for $UV_{254.}$ The values of q_A calculated to be in the range of 1425–2972 m^{-1} g^{-1} for the corresponding C_e values.

Figure 4.52 indicated that C_e values varied between 5.03–11.2 mg L^{-1} for TOC depending on the amount of TiO_2 present in solution. The values of q_A calculated to be in the range of 256–662 mg $L^{-1}g^{-1}$ for the corresponding C_e values.

It can clearly be seen from figures that the TOC isotherm showed similar pattern with $Color_{436}$ and UV_{254} isotherms. The $Color_{436}$ isotherm for 0.45 μm filtered humic acid, (Figure 4.50) was distributed in a narrow C_e range (ΔC_e =7.81 m^{-1}), where Δq_A was 213 m^{-1} g^{-1}. The isotherm (Figure 4.51) gave 1547 m^{-1} g^{-1} for Δq_A and 41.5 m^{-1} for ΔC_e at UV_{254}. Δq_A and ΔC_e for TOC isotherm (Figure 4.52) were 406 mg $L^{-1}g^{-1}$ and 6.17 mg L^{-1} respectively. The isotherms exhibited C-curve type isotherm.

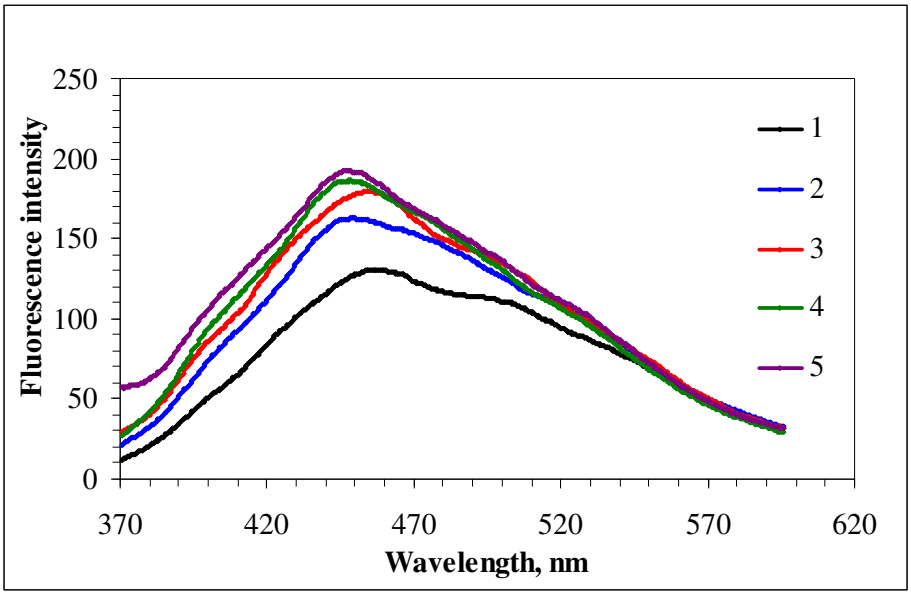

Figure 4.53. Emission scan spectra of 0.45 µm humic acid onto ascorbic acid modified TiO_2

Where numbers represent, 1: 0.45 µm fractionated AHA, 2: 0.2 mg mL^{-1} TiO_2, 3: 0.4 mg mL^{-1} TiO_2, 4: 0.8 mg mL^{-1} TiO_2, 5: 1.0 mg mL^{-1} TiO_2

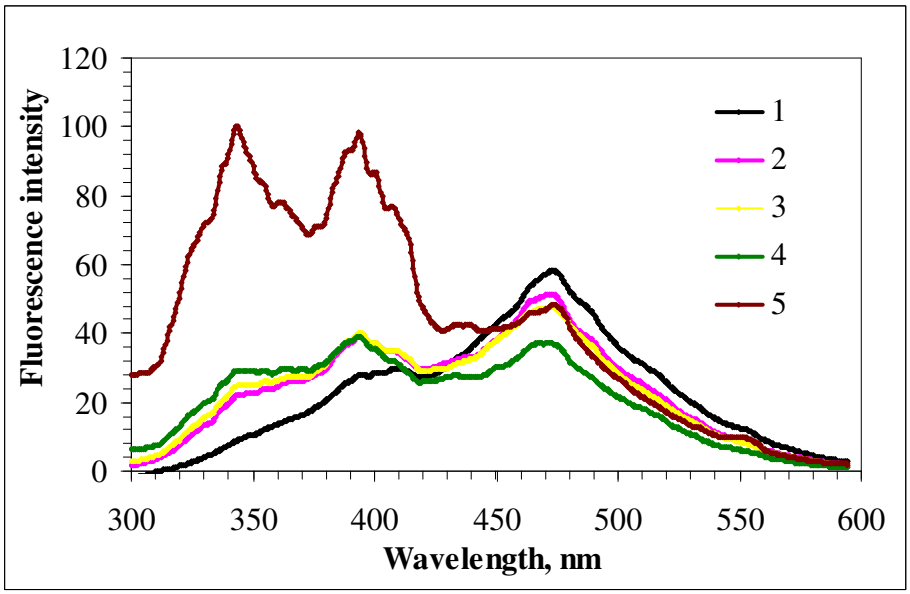

Figure 4.54. Synchronous scan spectra of 0.45 µm humic acid onto ascorbic acid modified TiO_2

Where numbers represent, 1: 0.45 μm fractionated AHA, 2: 0.2 mg mL^{-1} TiO_2, 3: 0.4 mg mL^{-1} TiO_2, 4: 0.8 mg mL^{-1} TiO_2, 5: 1.0 mg mL^{-1} TiO_2

Adsorption of 0.45 μm fraction of humic acid onto ascorbic acid modified TiO_2 could also be followed by increasing FI values at λ_{max}=450 nm for all of the humic acid fractions as well as the raw humic acid by increasing TiO_2 doses in emission scan spectra. As it seen in Figure 4.54, a different trend was observed for 0.45 μm fraction of humic acid and a distinct decreasing trend was recorded at λ_{max} 470 nm.

The adsorption capacity, K_f, and adsorption strength, 1/n, for 0.45 μm filtered humic acid-ascorbic acid modified TiO_2 system were listed in Table 4.10.

Table 4.10. Freundlich coefficients of 0.45 μm molecular size fraction of humic acid-ascorbic acid modified TiO_2

	K_f	1/n
$Color_{436}$, m^{-1}	84.91	0.570
UV_{365}, m^{-1}	104.4	0.632
UV_{280}, m^{-1}	70.04	0.844
UV_{254}, m^{-1}	89.06	0.762
TOC, mg L^{-1}	31.15	1.20

According to Table 4.10, adsorption capacities of 0.45 μm molecular size fraction of humic acid were found to be close to each other for color moieties groups and UV absorbing centers. Adsorption intensities for each parameter were found to be lower than one and 1/n values for UV centers were found to be higher than color forming groups. It indicated that the adsorption bond was strong; the capacity tended to be independent of C_e. On the other hand, 1/n value for TOC found to be higher than one.

4.3.3. 100 kDa Fractionated Humic Acid Adsorption onto Ascorbic Acid Modified TiO_2

In order to evaluate the molecular size effect on the adsorption properties of humic acid, experiments were carried out with 100 kDa molecular size fraction of humic acid onto ascorbic acid modified TiO_2. The Freundlich adsorption isotherms for $Color_{436}$, UV_{254} and TOC changes of humic acids were given in the Figure 4.55, Figure 4.56 and Figure 4.57, respectively.

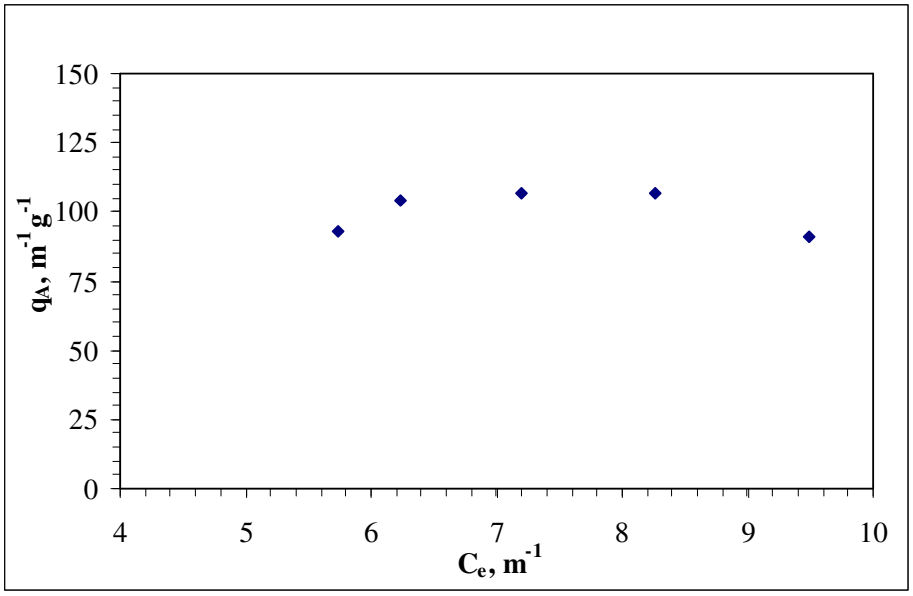

Figure 4.55. $Color_{436}$ adsorption isotherm of 100 kDa humic acid onto ascorbic acid modified TiO_2

Figure 4.55 represented that the values of C_e varied from 5.74 to 9.49 m^{-1} for $Color_{436}$. The calculated q_A values varied in between 91–107 m^{-1} g^{-1}.

As it could be seen in Figure 4.56, C_e values varied between 32.4–53.1 m^{-1} for UV_{254}. The values of q_A calculated to be in the range of 565–753 m^{-1} g^{-1} for the corresponding C_e values.

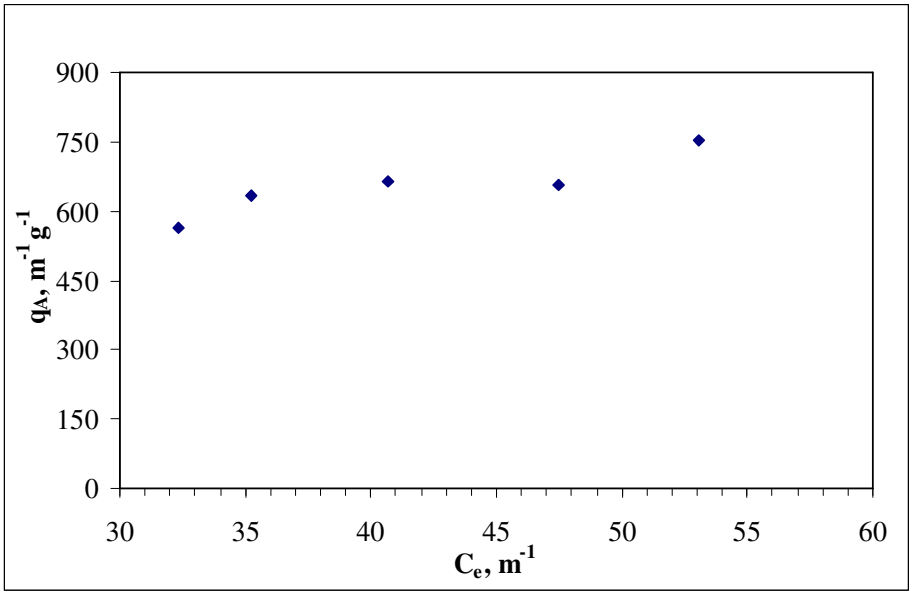

Figure 4.56. UV_{254} Adsorption isotherm of 100 kDa humic acid onto ascorbic acid modified TiO_2

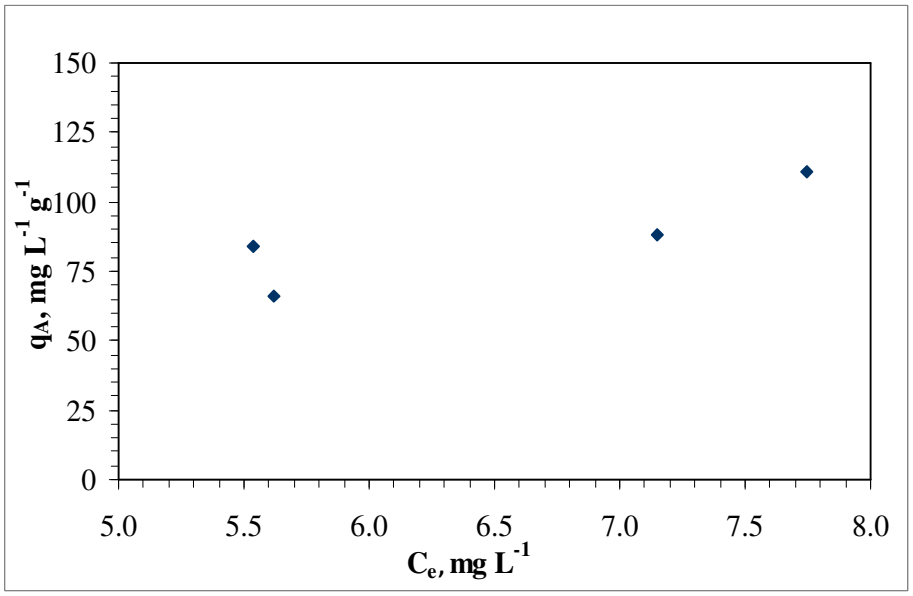

Figure 4.57. TOC adsorption isotherm of 100 kDa humic acid onto ascorbic acid modified TiO_2

Figure 4.57 indicated that C_e values varied between 5.54-7.74 mg L^{-1} for TOC depending on the amount of TiO_2 present in solution. The values of q_A calculated to be in the range of 66-111 mg $L^{-1}g^{-1}$ for the corresponding C_e values.

As isotherm for TOC showed same pattern with UV_{254}. For the 100 kDa filtered humic acid onto ascorbic acid modified TiO_2, Δq_A and ΔC_e for $Color_{436}$ were 16 m^{-1} g^{-1} and 3.75 m^{-1} respectively. The isotherm gave 188 m^{-1} g^{-1} for Δq_A and 20.7 m^{-1} for ΔC_e at UV_{254}. TOC isotherm for humic acid gave a ΔC_e of 2.20 mg L^{-1} where Δq_A was 45 mg $L^{-1}g^{-1}$. The isotherms exhibited linear adsorption isotherm for TOC and UV_{254}. On the other hand, the isotherm for $Color_{436}$ was more like a cluster of data points with a narrow Δq_A values. Amount of humic acid adsorbed onto ascorbic acid modified TiO_2 was not change with the concentration dependency for 100 kDa filtered humic acid. Hence the adsorption data for color forming groups did not fit to Freundlich isotherm for 100 kDa molecular size fraction of humic acid.

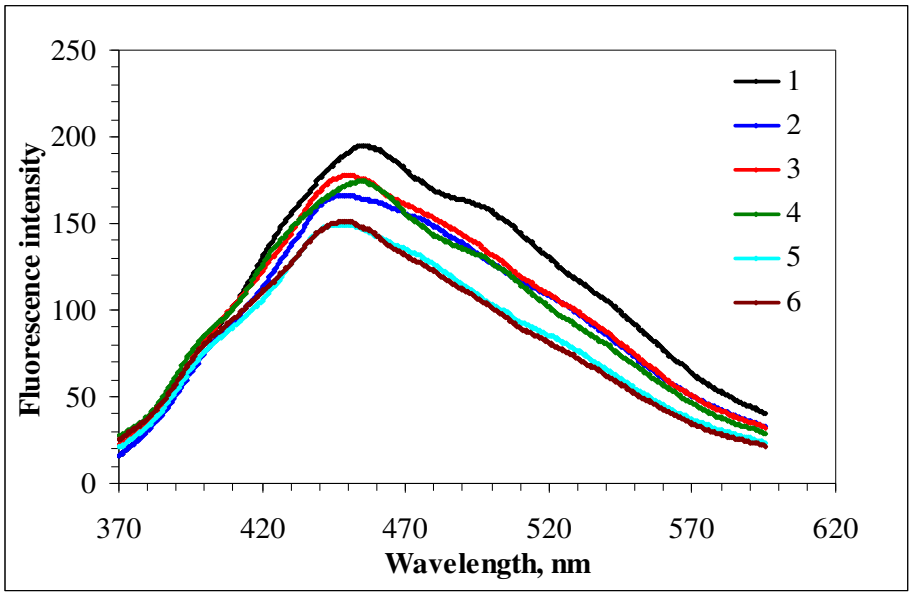

Figure 4.58. Emission scan spectra of 100 kDa humic acid onto ascorbic acid modified TiO_2.

Where numbers represent, 1: 100 kDa AHA, 2: 0.2 mg mL^{-1} TiO_2, 3: 0.4 mg mL^{-1} TiO_2, 4: 0.6 mg mL^{-1} TiO_2, 5: 0.8 mg mL^{-1} TiO_2, 6: 1.0 mg mL^{-1} TiO_2

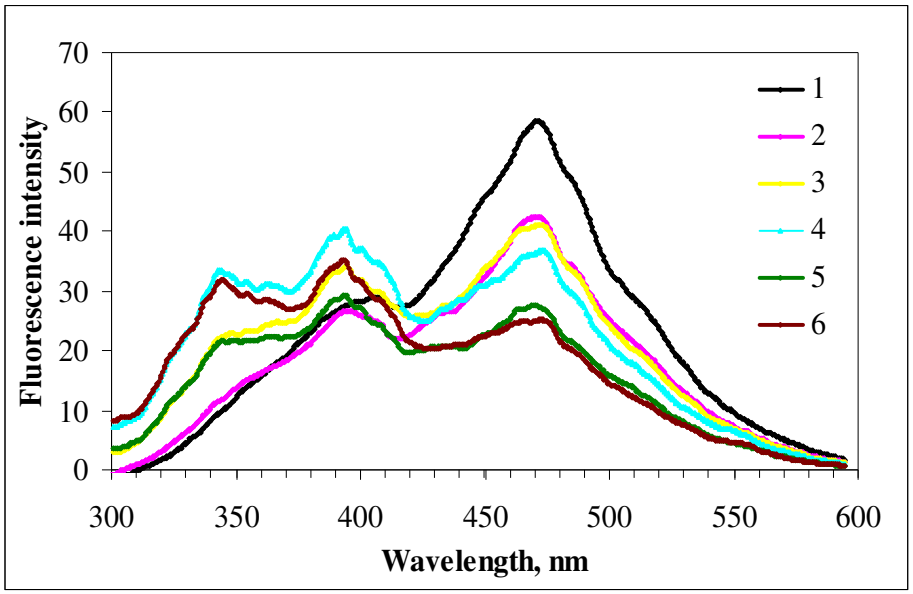

Figure 4.59. Synchronous scan spectra of 100 kDa humic acid onto ascorbic acid modified TiO_2.
Where numbers represent, 1: 100 kDa AHA, 2: 0.2 mg mL^{-1} TiO_2, 3: 0.4 mg mL^{-1} TiO_2, 4: 0.6 mg mL^{-1} TiO_2, 5: 0.8 mg mL^{-1} TiO_2, 6: 1.0 mg mL^{-1} TiO_2

Figure 4.58 showed that adsorption of humic acid onto ascorbic acid modified TiO_2 could also be followed by decreasing FI values at λ_{max}=450 nm for all of the humic acid fractions as well as the raw humic acid. As it could be seen in Figure 4.59, three distinct λ_{max} as 345, 355, 470 nm were recorded revealing a decreasing trend in FI with respect to increasing TiO_2 dose for 100 kDa fractions of humic acid.

Table 4.11. Freundlich coefficients of 100 kDa molecular size fraction of humic acid-ascorbic acid modified TiO_2

	K_f	1/n
UV_{365}, m^{-1}	87.69	0.361
UV_{280}, m^{-1}	110.9	0.450
UV_{254}, m^{-1}	119.0	0.457
TOC, m gL^{-1}	12.65	1.03

The adsorption capacity, K_f, and adsorption strength, 1/n, for 100 kDa filtered humic acid-ascorbic acid modified TiO_2 system were listed in Table 4.11. According to Table 4.11, adsorption capacity constants for both the UV_{280} and UV_{254} centers were found to be very close to each other and higher than UV_{365} groups. 1/n values were found to be lower than one; it indicated that the capacity tended to be independent of concentration. They expressed unfavorable adsorption intensities.

4.3.4. 30 kDa Fractionated Humic Acid Adsorption onto Ascorbic Acid Modified TiO_2

In order to examine the molecular size effect on the adsorption behavior of humic acid, the batch adsorption experiments were also carried out with 30 kDa molecular size fractionated humic acid and ascorbic acid modified TiO_2 as adsorbent. The adsorption isotherms of $Color_{436}$, UV_{254} and TOC were shown in Figures 4.60, Figures 4.61 and Figures 4.62, respectively.

Figure 4.60 showed that the values of C_e varied from 2.46 – 3.75 m^{-1} for $Color_{436}$. The calculated q_A values varied in between 36.8–55 m^{-1} g^{-1}.

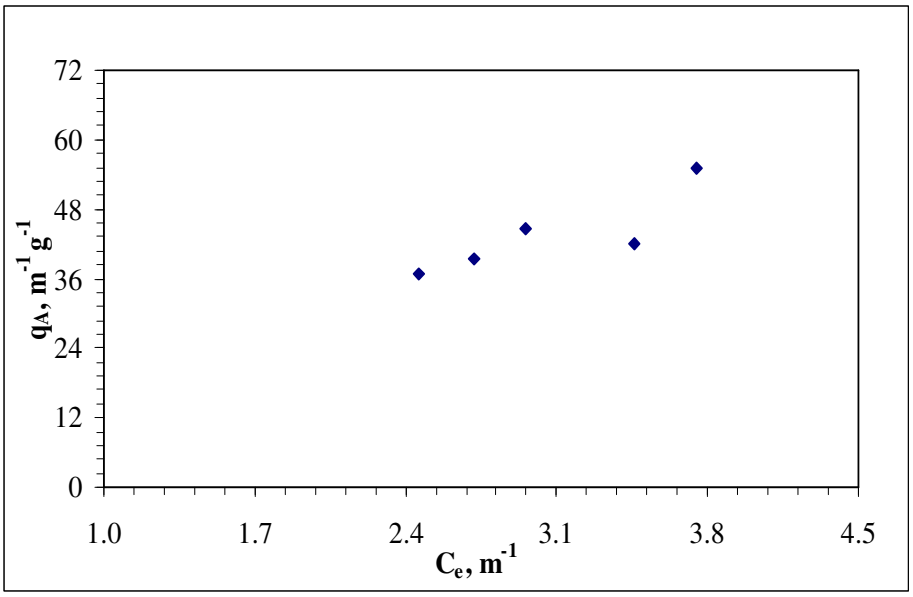

Figure 4.60. $Color_{436}$ adsorption isotherm of 30 kDa humic acid onto ascorbic acid modified TiO_2

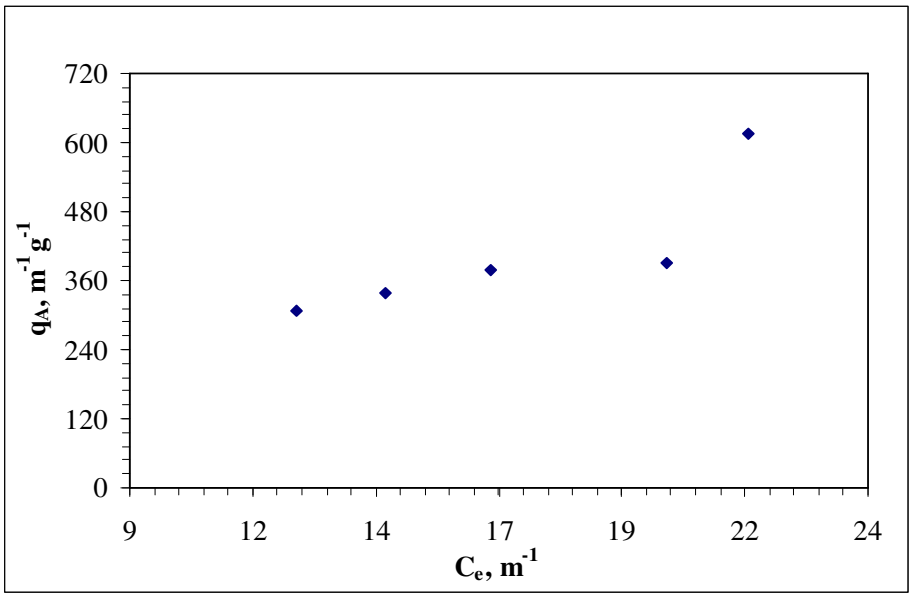

Figure 4.61. UV_{254} adsorption isotherm of 30 kDa humic acid onto ascorbic acid modified TiO_2

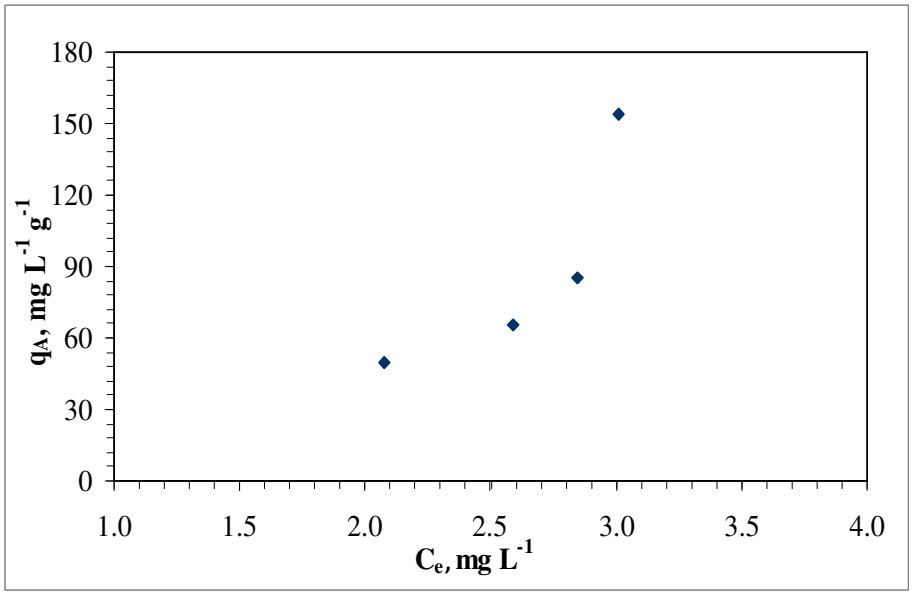

Figure 4.62. TOC adsorption isotherm of 30 kDa humic acid onto ascorbic acid modified TiO_2

As it could be seen in Figure 4.61, C_e values varied between 12.4–21.6 m^{-1} for UV_{254}. The values of q_A calculated to be in the range of 306–615 m^{-1} g^{-1} for the corresponding C_e values.

Figure 4.62 showed that the C_e values varied between 2.07 to 3.01 mg L^{-1} for TOC. The values of q_A calculated to be in the range of 49–154 mg $L^{-1}g^{-1}$.

ΔC_e and Δq_A values for 30 kDa filtered humic acid were 0.71 m^{-1} and 18.2 $m^{-1}g^{-1}$ respectively at $Color_{436}$. ΔC_e and Δq_A for UV_{254} were 9.2 m^{-1} and 309 m^{-1} g^{-1} respectively. Molecular size fractionation of humic acid resulted in steep curves with high Δq_A of 105 mg L^{-1} g^{-1} in a short C_e range of 0.94 mg L^{-1} for TOC isotherm. The type of isotherm for $Color_{436}$ showed a linear isotherm while the isotherms for UV_{254} and TOC exhibited C-type isotherm.

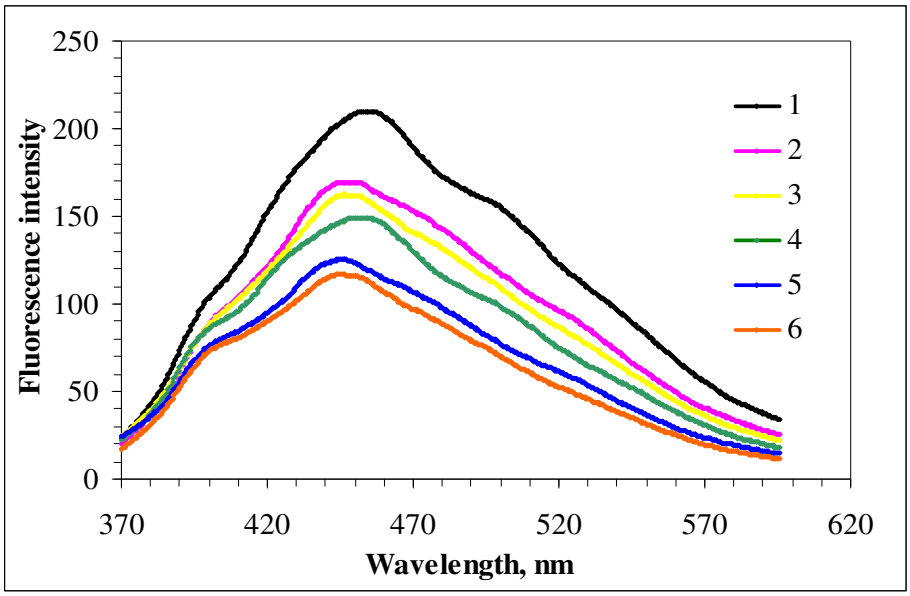

Figure 4.63. Emission scan spectra of 30 kDa humic acid onto ascorbic acid modified TiO_2 Where numbers represent, 1: 30 kDa AHA, 2: 0.2 mg mL^{-1} TiO_2, 3: 0.4 mg mL^{-1} TiO_2, 4: 0.6 mg mL^{-1} TiO_2, 5: 0.8 mg mL^{-1} TiO_2, 6: 1.0 mg mL^{-1} TiO_2

Adsorption of humic acid onto ascorbic acid modified TiO_2 could also be followed by decreasing FI values at λ_{max}=450 nm for all of the humic acid fractions as well as the

raw humic acid as seen in Figure 4.63. However, Figure 4.64 indicated three distinct λ_{max} as 345, 355, 470 nm were recorded revealing a decreasing trend in FI with respect to increasing TiO_2 dose for 30 kDa fractions of humic acid.

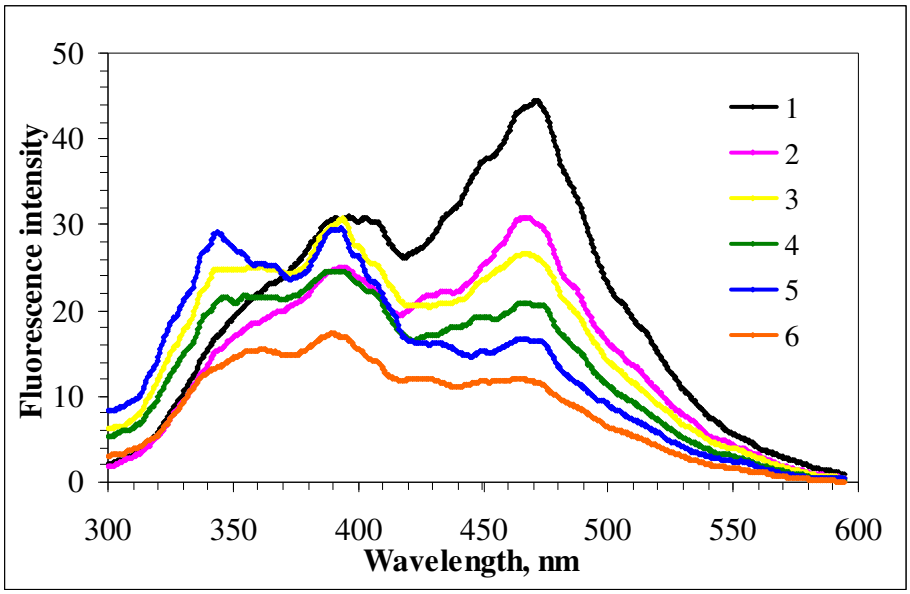

Figure 4.64. Synchronous scan spectra of 30 kDa humic acid onto ascorbic acid modified TiO_2

Where numbers represent, 1: 30 kDa AHA, 2: 0.2 mg mL^{-1} TiO_2, 3: 0.4 mg mL^{-1} TiO_2, 4: 0.6 mg mL^{-1} TiO_2, 5: 0.8 mg mL^{-1} TiO_2, 6: 1.0 mg mL^{-1} TiO_2

For comparison purposes maximum fluorescence emission scan intensity values were displayed for all of the humic acid fractions as well as raw humic acid (Figure4.65). Maximum emission scan FI values displayed a range of 106-154 for raw AHA, 130-192 for 0.45 µm AHA, 149-194 for 100 kDa and 116-209 for 30 kDa. The highest FI was recorded for 209 for 30 kDa AHA. A slightly decreasing trend was observed for 100 kDa and 30 kDa fractions. However an increasing trend in FI values were recorded for 0.45 µm fraction of humic acid and an inconsistent trend was observed for raw humic acid after respective adsorption equilibrium.

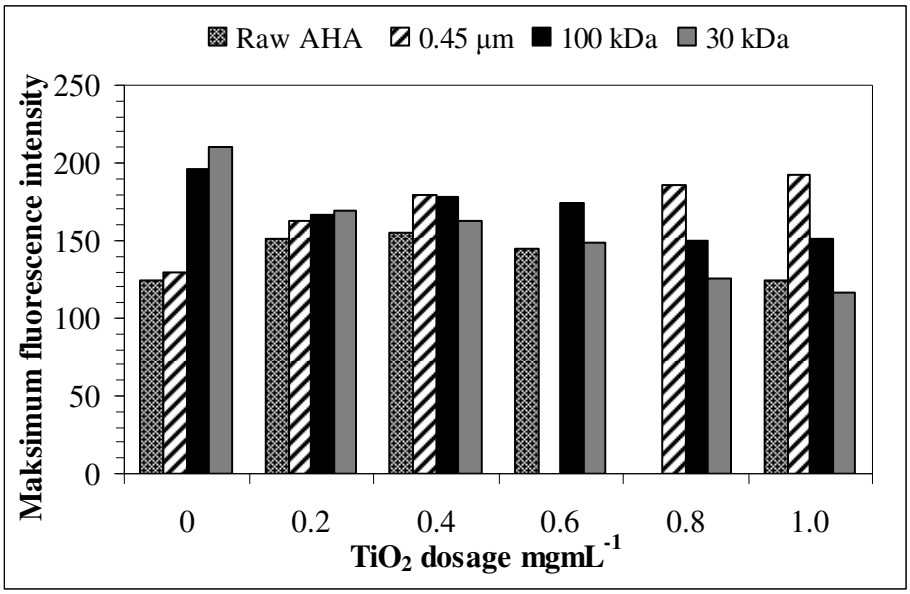

Figure 4.65. Maximum fluorescence intensity of humic acid- ascorbic acid modified TiO_2 emission scan

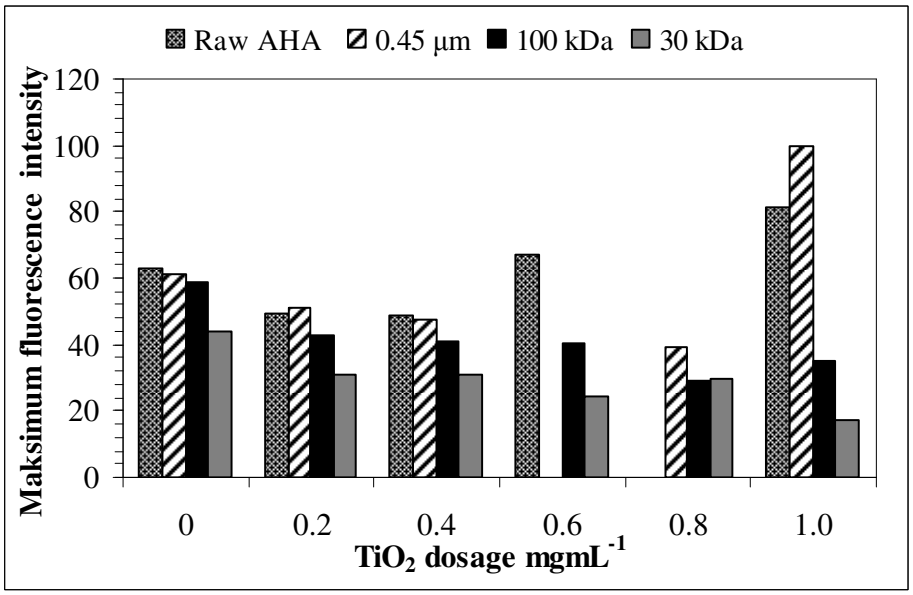

Figure 4.66. Maximum fluorescence intensity of humic acid- ascorbic acid modified TiO_2 synchronous scan

A similar approach was also presented for synchronous scan spectra maximum intensity values (Figure 4.66). Maximum synchronous scan FI values displayed a range of 48-200 for raw AHA, 39-100 for 0.45 μm AHA, 29-58 for 100 kDa and 17-44 for 30 kDa. The highest FI was recorded for 200 for raw humic acid. For lower molecular weight fractions as 100 kDa and 30 kDa a general decreasing trend was attained for all of the adsorbent doses. However a slight decreasing trend was attained for raw humic acid displaying a different behavior for 1.0 mg mL^{-1} TiO_2. For 0.45 μm humic acid fraction and raw humic acid fraction a similar trend was observed.

The Freundlich coefficients for 30 kDa molecular size fraction of humic acid-ascorbic acid modified TiO_2 are listed in Table 4.12.

Table 4.12. Freundlich coefficients of 30 kDa molecular size fraction of humic acid-ascorbic acid modified TiO_2

	K_f	1/n
$Color_{436}$, m^{-1}	18.60	0.758
UV_{365}, m^{-1}	4.679	1.88
UV_{280}, m^{-1}	13.43	1.21
UV_{254}, m^{-1}	23.65	1.00
TOC, mg L^{-1}	6.604	2.22

According to Table 4.12, adsorption capacities, K_f, of $Color_{436}$, UV_{254} and TOC for 30 kDa filtered humic acid-ascorbic acid modified TiO_2 were found to be 18.60, 23.65 and 6.604, respectively. Moreover, the adsorption intensity, 1/n were 0.758, 1.00 and 2.22, respectively. Adsorption intensity for $Color_{436}$ was lower than UV absorbing centers. This indicated the strong concentration dependency and favorable adsorption intensity for UV adsorbing centers because 1/n values were found to be higher than one. On the other hand, isotherm for $Color_{436}$ showed a nonlinear trend because 1/n was lower than one.

CONCLUSION

In this study, the effect of molecular size fractionation on the sorption properties of humic acid onto metal ion TiO_2 (Fe), and TiO_2 modified with an organic substance (ascorbic acid) samples in comparison to TiO_2 Degussa P-25 were investigated. Freundlich adsorption model was adopted for the data evaluation. The main emphasis on working was to judge complex interactions between the surface properties of titanium dioxide and the molecular size dependent fractions of the humic acid on adsorption properties of humic acid.

The adsorption profiles of the selected UV-vis parameters of humic acid and its molecular size fractions onto bare TiO_2 displayed various characteristics that could also be followed by fluorescence properties. K_f values changed as raw HA < 0.45 μm ≅ 100 kDa. No distinct isotherm could be assessed for 30 kDa fraction for $Color_{436}$. UV_{254} parameter K_f values changed as raw HA < 30 kDa <100 kDa <0.45 μm. On the other hand, TOC parameter expressed K_f values as 30 kDa <0.45 μm <100 kDa < raw HA. The overall evaluation of 1/n could be expressed by the range of 0.612-3.10.

The adsorption profiles of the $Color_{436}$ and UV_{254} of humic acid and its molecular size fractions and Fe doped TiO_2 exhibited distinct differences with respect to the conditions of the humic acid and bare TiO_2 system.

Freundlich adsorption model parameters as;

K_f displayed changes for $Color_{436}$ as raw HA < 100 kDa <30 kDa <0.45 μm for UV_{254} as raw HA < 100 kDa < 0.45 μm < 30 kDa. TOC parameter the sequence is the 30 kDa <100 kDa < raw HA <0.45 μm. On the other hand, 1/n values displayed a range of 1.03-13.2 irrespective of the parameter.

The use of ascorbic acid modified TiO_2 expressed comparatively different adsorption patterns respect to bare TiO_2 as well as the Fe doped TiO_2. Raw HA ascorbic acid modified

TiO_2 system could be modeled by Freundlich adsorption model for TOC. Molecular size fractions of humic acid displayed rather high K_f values and lower 1/n values. The observed differences in adsorption behavior of raw HA as well as the molecular size fractions could be explained by the probable diversity of the attraction sites on both of the organic moieties.

REFERENCES

Aiken, G.R., McKnight, D.M., Wershaw, R.L., MacCathy, P. (Eds.), 1985. Humic Substances in Soil, Sediment and Water. John Wiley and Sons, Inc., U.S.A.

Bas, T., 2001. Humic Acid and Oxide Surface Interactions: Adsorption, Desorption and Surface Charge Effects, M.S. Thesis, Boğazici University.

Balzani, V., Scandola, F., 1991. Supramolecular Photochemistry, Horwood, Chichester, England.

Bekbolet, M., Suphandag, A.S., Uyguner, C. S., 2002. An investigation of the photocatalytic efficiencies of TiO2 powders on the decolorisation of humic acids. Journal of Photochemistry and Photobiology A: Chemistry, 148, 121-128.

Bekbolet, M., Cecen, F., Ozkosemen, G., 1996. Photocatalaytic oxidation and subsequent adsorption characteristic of humic acids. Water Science and Technology, 34, 65-72.

Bekbolet, M., Ozkosemen, G., 1996. A preliminary investigation on the photocatalaytic degradation of a model humic acid. Water Science and Technology, 33, 6, 189-194.

Buffle, J., Greter, F., Haerdi, W., 1977. Measurement of complexation properties humic and fulvic acids in natural waters with lead and copper ion-selective electrodes. Analytical Chemistry, 49, 216-222.

Buffle, J., Wilkinson, K. J., Stoll, S., Filella, M., Zhang, J., 1998. A generalized description of aquatic colloidal interactions: The three-colloidal component Approach. Environmental Science and Technology, 32, 19, 2887 -2899.

Burba, P., Aster, B., Nifant'eva, T., Shkinev, V., Spivakov, B.Ya., 1998. Membrane filtration studies of aquatic humic substances and their metal species: a concise

overview Part 1. Analytical fractionation by means of sequential-stage ultrafiltration. Talanta, 45, 977-988.

Cabaniss, S.E., Shuman, M.S., 1988. Copper binding by dissolved organic matter: I. Suwannee river fulvic acid equilibria. Geochimica et Cosmochimica. Acta, 52, 185–193.

Clapp, C. E., Hayes, M. H. B., 1999. Size and shapes of humic substances. Soil Science, 164(11), 777-789

Conte, P., Piccolo, A., 1999. Conformational arrangement of dissolved humic substances: influence of solution composition on association of humic molecules. Environmental Science and Technology, 33, 1682-1690.

Davis, J.A., Gloor, R., 1981. Adsorption of dissolved organics in lake water by aluminium oxide: Effect of molecular weight. Environmental Science and Technology, 15, 1223-1229.

Davis, W.M., Eriekson, C.L., Johnston, C.T., Delfino, J.J., Porter, J.E., 1999. Quantitative Fourier transforms infrared spectroscopic investigation of humic substance functional group composition. Chemosphere 38, 12, 2913–2928.

Giles, C. H., MacEwan, T. H., Nakhwa, S. N., Smith, D., 1960. A system classification of solution adsorption isotherms and its use in diagnosis of adsorption and in measurement of specific surface areas of solids. Journal of Chemical Society, 33, 3973-3993.

Giles, C.H., Smith, D., Huitson, A., 1974a. A general treatment and classification of the solute adsorption isotherm. Journal of Colloid Interface Science, 47, 755–765.

Giles, C.H., D'Silva, A.P., Easton, I.A., 1974b. A general treatment and classification of the solute adsorption isotherm, Part II: Experimental interpretation. Journal of Colloid and Interface Science, 47, 3, 766.

Hautala, K., Peuravuori, J., Pihlaja, K., 2000. Measurement of aquatic humus content by spectroscopic analyses. Water Research, 34, 1, 246–258.

Hoffmann, M.R., Martin, S.T., Choi, W., Bahnemann, D.W., 1995. Environmental applications of semiconductor photocatalysis. Chemical Reviews, 95, 69–96.

Hua, Z., Manping, Z., Zongfeng, X., Low, G.K-C., 1995. Titanium dioxide mediated photocatalytic degradation of monocrotophos. Water Research, 29, 2681-2688.

John, J., Salbu, B., Gjessing, E., and Bjoerrstad, H., 1988. Effect of pH, humus concentration and molecular weight on conditional stability constants of cadmium. Water Research, 22, 1381.

Jones, M.N., Bryan, N.D., 1998. Colloidal properties of humic substances. Advances in Colloid and Interface Science, 78, 1, 1-48.

Kerc, A., Bekbolet, M., Saatci, A.M., 2003a. Effect of partial oxidation by ozonation on the photocatalytic degradation of humic acids. International Journal of Photoenergy, 5, 2, 75-80.

Kerc, A., Bekbolet, M., Saatci, A.M., 2003b. Sequential oxidation of humic acids by ozonation and photocatalysis. Science and Engineering, 25, 6, 497-504.

Khan, E., Babcock, R.W., Suffet, I.H., Stenstorm, M.K., 1998. Biodegradable dissolved organic carbon for indication wastewater reclamation plant performance and treated wastewater quality. Water Environmental Research, 70, 1033–1040.

Kononova M. M., 1966, Soil Organic Matter: Its Nature, Its Role in Soil Formation and Soil Fertility. Pergamon Press Oxford, New York.

Kosanic, M.M., 1998. Photocatalytic Degradation of oxalic acid over TiO2 powder. Journal of Photochemistry and Photobiology A: Chemistry, 119, 119-122.

Leenheer, J.A., 1981. Comprehensive approach to preparative isolation and fractionation of dissolved organic carbon from natural waters and wastewaters. Environmental Science and Technology, 15, 578–587.

Linsebigler, A.L., Lu, G., Yates, J.T., 1995. Photocatalysis on TiO2 surfaces: Principles, mechanisms, and selected results. Chemical Reviews, 95, 735–758.

Ma, H., Kim, S.D., Cha, D.K., Allen, H.E., 1999. Effect of kinetics of complexation by humic acid on toxicity of copper to Ceriodaphnia dubia. Environmental Toxicology and Chemistry, 18, 828–837.

Matthews, R.W., 1991. Photooxidative degradation of coloured organics in water using supported catalysts. Water Research, 25, 1169-1176.

Mert, E. H., Yalcın, Y., Kılıc, M., San, N., Cınar, Z., 2008. surface modification of TiO_2 with ascorbic acid for Heterogeneous photocatalysis: Theory and experiment. Journal of Advanced Oxidation Technologies, 11, 2, 199-207.

Nifant'eva, T.I., Shkinev, V.M., Spivakov, B.Ya., Burba, P., 1999. Membrane filtration studies of aquatic humic substances and their metal species: A concise overview. Part 2. Evaluation of conditional stability constants by using ultrafiltration Talanta, 48, 257.

Perminova, I.V., 1999. Size exclusion chromatography of humic substances: Complexities of data interpretation attributable to nonsize exclusion effects. Soil Science, 164, 834-840.

Peuravuori, J., Koivikko, R., Pihlaja, K., 2002. Characterization, differentiation and classification of aquatic humic matter separated with different sorbents: Synchronous scanning fluorescence spectroscopy. Water Research, 36, 4552–4562.

Piccolo, A., Nardi, S., Concheri, G., 1996. Micelle-like conformation of humic substances as revealed by size exclusion chromatography. Chemosphere, 33, 595-602.

Piccolo, A., Conte, P., Cozzolino, A., 1999. Effects of mineral and monocarboxylic acids on the molecular association of dissolved humic substances. European Journal of Soil Science, 50, 687-694.

Piccolo, A., Conte, P., Trivellone, E., van Lagen, B., Buurman, P., 2002. Reduced heterogeneity of a lignite humic acid by preparative HPSEC following interaction with an organic acid. Characterization of size separates by PYR-GC-MS and 1H NMR spectroscopy. Environmental Science and Technology. 36, 76–84.

Preston, C. M., 1996. Application of NMR to soil organic matter analysis: History and prospects. Soil Science, 161, 144-166.

Rice, J. A., MacCarthy, P., 1990. A model of humin. Environmental Science and Technology, 24, 1875-1877.

Rice, J. A., MacCarthy, P., 1991. Statistical evaluation of the chemical composition of humic substances. Organic Geochemistry 17, 635-648.

Robertson, P.K.J., Lawton, L.A., Munch, B., Rouzade, J., 1997. Destruction of cyanobacterial toxins by semiconductor photocatalysis. Chemical Communications, 393-394.

Sakthivel, S., Shankar, V.M., Palanichamy, M., Arabindoo, B., Bahnemann, D.W., Murugesan, V., 2004. Enhancement of photocatalytic activity by metal deposition: Characterization and photonic efficiency of Pt, Au and Pd deposited on TiO_2 catalyst. Water Research, 38, 3001–3008.

Sawyer, C.N., McCarty P.L., 1978. Chemistry for Environmental Engineering, Third Ed., McGraw-Hill Book Company, New York

Sclafani, A., Palmisano, L., Schiavello, M., 1990. Influence of the Preparation Methods of TiO_2 on the Photocatalytic Degradation of Phenol in Aqueous Dispersion. Journal of Physical Chemistry, 94, 829-832.

Schulten, H. R., Leinweber, P., 2000. New insights into organic-mineral particles: Composition, properties and models of molecular structure. Biology and Fertility of Soils, 30, 399-432.

Selcuk, H., Bekbolet, M., 2008. Photocatalytic and photoelectrocatalytic humic acid removal and selectivity of TiO_2 coated photoanode. Chemosphere, 73, 854-858.

Senesi, N., 1990. Molecular and quantitative aspects of the chemistry of fulvic acid and its interactions with metal ions and organic chemicals Part II: The fluorescence spectroscopy approach. Analytica Chimica Acta, 232, 77-106.

Siddiqui, M.S., Amy, G.L., Murrhy, B.D., 1997. Ozone enhanced removal of natural organic matter from drinking water source. Water Research, 31, 3098–3106.

Silva, S., Zanetti, B., Burzoni, E., Dell'Agnola, G., Nardi, S., 1981. Caratteristiche spettrofuorimetriche e potere complessante di acidi umici a diverso peso molecolare. Agrochimica, 25, 131-141.

Snoeyink, V.L, Summers, R.S., 1999. Adsorption of Organic Compound, Chapter 13. In Letterman, R.D., (Ed.), Water Quality and Treatment, AWWA, Fifth Ed., McGraw Hill, Inc., USA, 13.1-13.76.

Sontheimer, H., J.C. Crittenden, Summers, R. S., 1988. Activated Carbon for Water Treatment, Second Ed., DVGW-Forschungstelle am Engler-Bunte-Institut der Universitat Karlsruhe, Karlsruhe, Germany.

Sposito, G., 1989. The Chemistry of Soils, Oxford University Press, New York.

Stevenson, F.J., 1994. Humus Chemistry: Genesis, Composition, Reactions, Second Ed., John Wiley and Sons, Inc., New York.

Suffet, I.H., MacCarthy, P., (Eds.), 1989. Aquatic Humic Substances: Influence on Fate and Treatment of Pollutants, Advances in Chemistry Series 219, American Chemical Society, Washington DC, USA.

Suphandag, S.A., 1998. Adsorption Capacity of Natural Organic Matter on Semiconductor Powders, M.S. Thesis, Bogazici University.

Suphandag, S.A., 2006. Evaluation of NOM-Metal Oxide Adsorption System under Influential Structural Concepts, Ph.D. Thesis, Bogazici University.

Swift, R.S., 1989. Molecular Weight, Size, Shape, and Charge Characteristics of Humic Substances: Some Basic Considerations. In Hayes, M.H.B., MacCarthy, P. Malcolm, R.L., Swift, R.S. (Eds.), Humic Substances II, 449-465, John Wiley and Sons, Inc., New York.

Tanaka, T., Senoo, M., 1995. Sorption of ^{60}Co, ^{85}Sr, ^{137}Cs, ^{237}Np and ^{241}Am on soil under coexistence of humic acid; effects of molecular size of humic acid. Material Research Society Symposium Proceedings, 353 1013.

Tatsuma, T., Tachibana, S., Miwa, T., Tryk, D.A., Fujishima, A., 1999. Remote bleaching of methylene blue by UV-Irradiated TiO_2 in the gas phase. Journal of Physical Chemistry B, 103, 8033-8035.

Thomsen, M., Lassen, P., Dobel, S., Hansen, P.E., Carlsen, L., Mogensen, B.B., 2002. Characterization of humic materials of different origin: a multivariate approach for quantifying the latent properties of dissolved organic matter. Chemosphere, 49, 1327–1337.

Thurman, E.M., Malcolm, R.L., 1981. Preparative isolation of aquatic humic substances. Environmental Science and Technology, 15, 463–466.

Uyguner, C.S., Bekbolet, M., 2004. Evaluation of humic acid, chromium (VI) and TiO_2 ternary system in relation to adsorptive interactions. Applied Catalysis B: Environmental, 49, 267-275.

Uyguner, C.S., Bekbolet, M., 2005a. Evaluation of humic acid photocatalytic degradation by UV–vis and fluorescence spectroscopy. Catalysis Today, 101, 267–274.

Uyguner, C.S., Bekbolet, M., 2005b. A comparative study on the photocatalytic degradation of humic substances of various origins. Desalination, 176, 167-176.

Uyguner, C.S., Bekbolet, M., 2007. Contribution of metal species to the heterogeneous photocatalytic degradation of natural organic matter. International Journal of Photoenergy, 2007, Article ID 23156, 8 pages.

Uyguner, C.S., Suphandag, S.A., Kerc, A., Bekbolet, M., 2007. Evaluation of adsorption and coagulation characteristics of humic acids preceded by alternative advanced oxidation techniques. Desalination, 210, 183-193.

vanLoon, G. W., Duffy, S.J., 2000. Environmental Chemistry, Oxford University Press Inc., New York.

Vassileva, E., Proinova, I., Hadjiivanov, K., 1996. Solid-phase extraction of heavy metal ions on a high surface area titanium dioxide (Anatase). Analyst, 121, 607-612.

Yazıcı, O., 2006. Aromatic kirleticilerin fotokatalitik degredasyon reaksiyonlarının hızlandırılması. Katekolün Fe^{+3} iyonları ile katkılandırılmış TiO_2 beraberindeki fotokatalitik degredasyon kinetiğinin incelenmesi. Yüksek Lisans Tezi, Yıldız Teknik Üniversitesi, Fen Bilimleri enstitüsü.

Wang, H., Adesina, A.A., 1997. Photocatalytic Causticization of Sodium Oxalate Using Commercial TiO_2 Particles. Applied Catalysis B: Environmental, 14, 241-247.

Weber, J. W., 1972. Physicochemical Processes for Water Quality Control. John Wiley and Sons, Inc., U.S.A, 199-259.

APPENDIX A

Adsorption Profiles of Humic Acid onto TiO_2-Degussa P-25

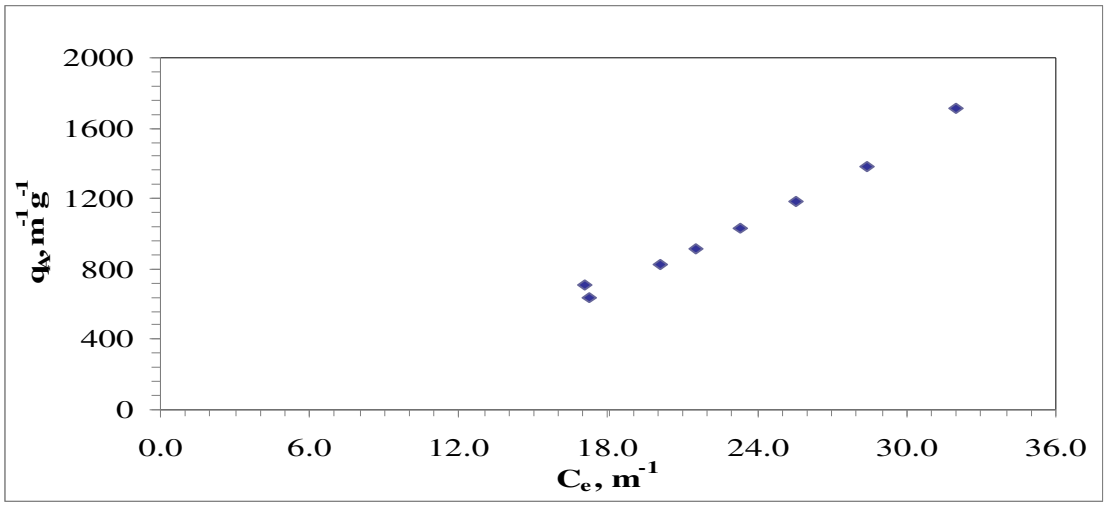

Figure A.1. UV_{365} Adsorption isotherm of humic acid on Degussa P-25

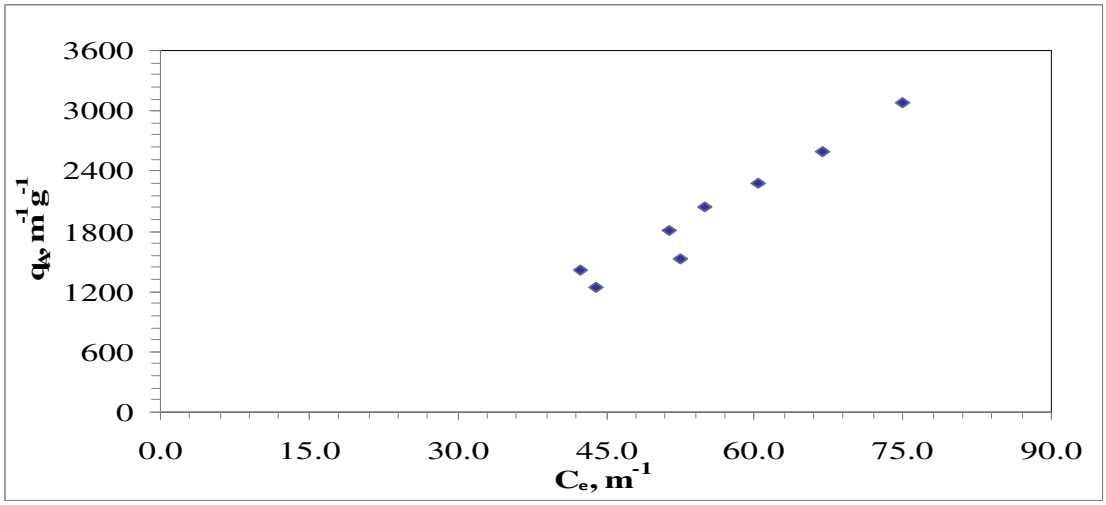

Figure A.2. UV_{280} Adsorption isotherm of humic acid on Degussa P-25

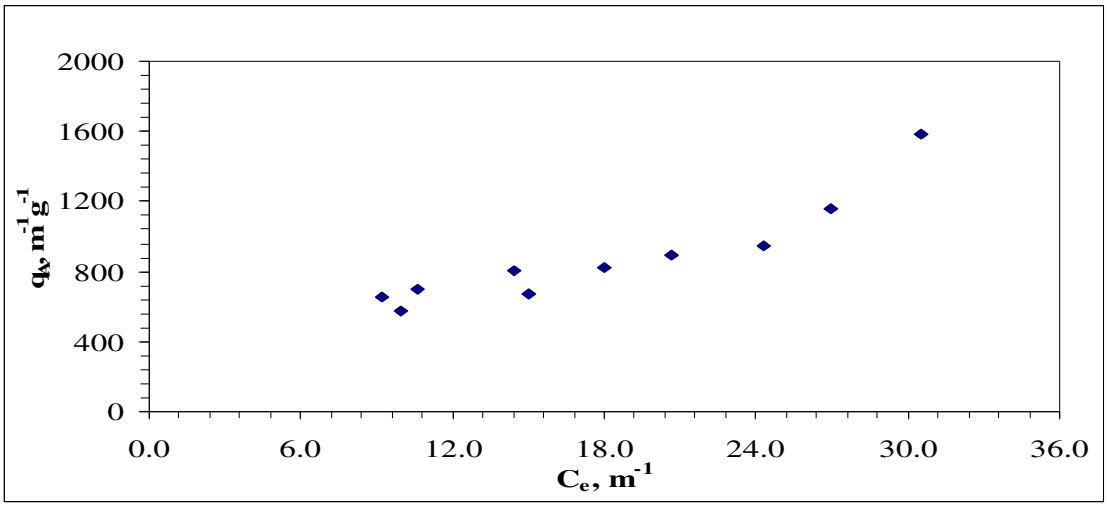

Figure A.3. UV_{365} Adsorption isotherm of 0.45 µm humic acid on Degussa P-25

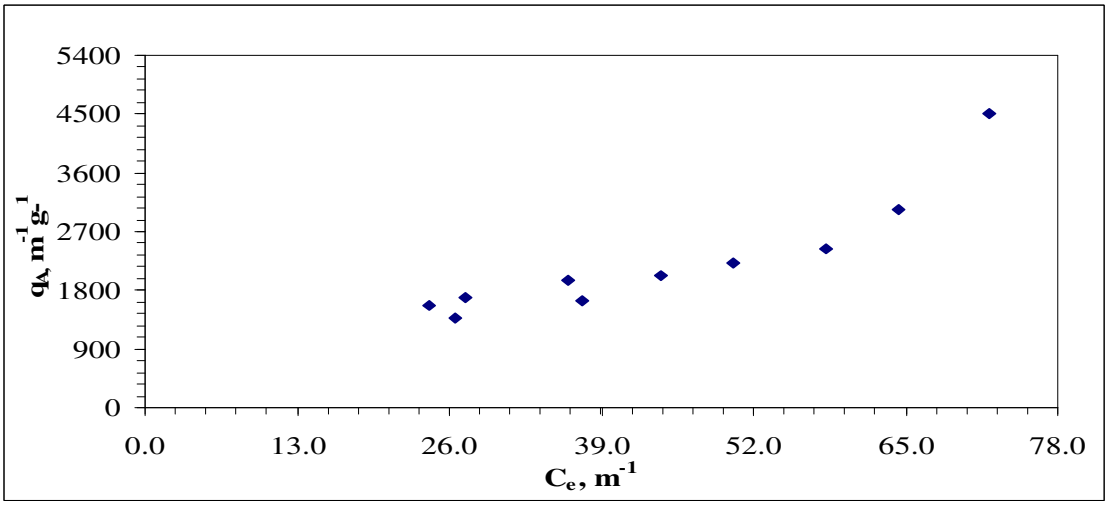

Figure A.4. UV_{280} Adsorption isotherm of 0.45 µm humic acid on Degussa P-25

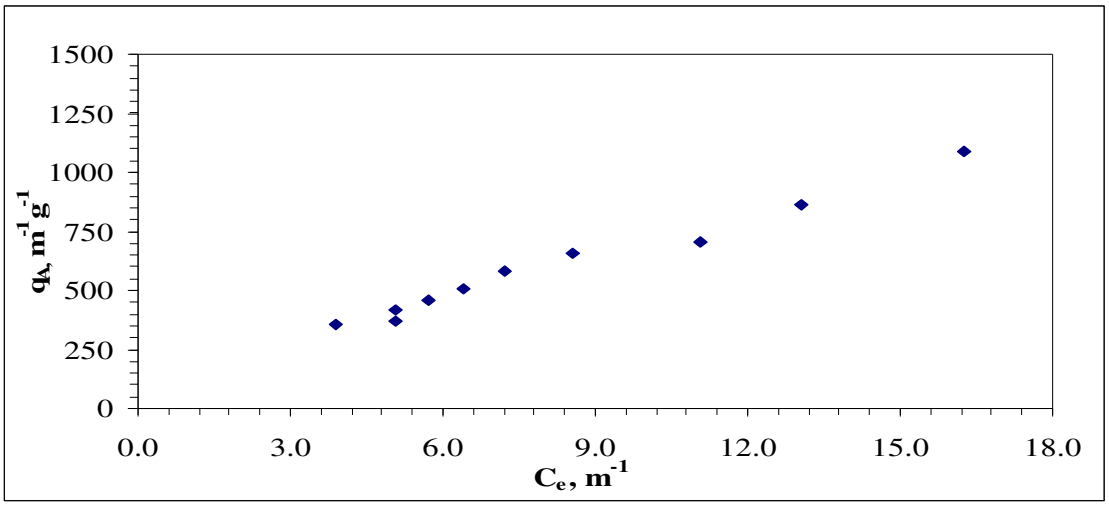

Figure A.5. UV_{365} Adsorption isotherm of 100 kDa humic acid on Degussa P-25

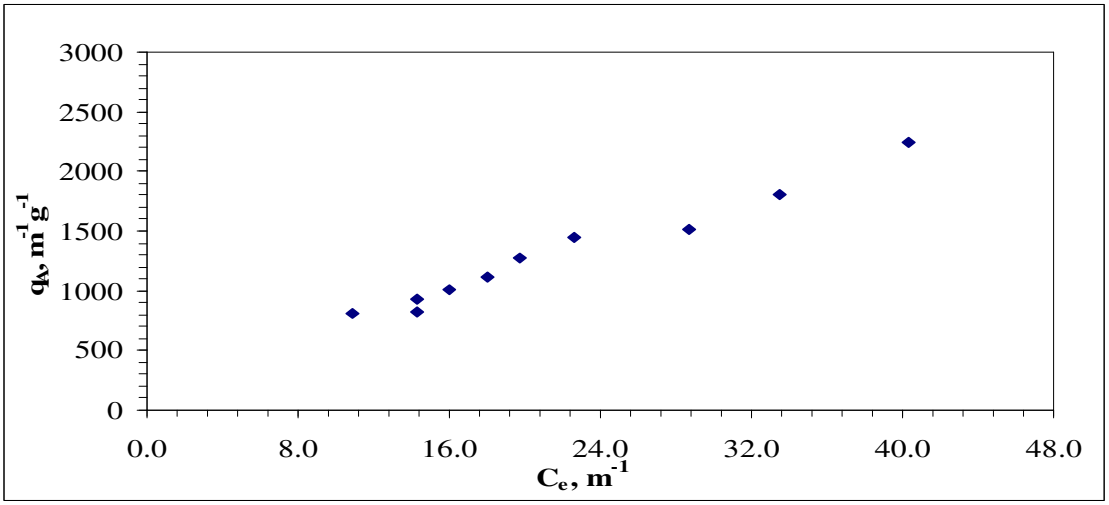

Figure A.6. UV_{280} Adsorption isotherm of 100 kDa humic acid on Degussa P-25

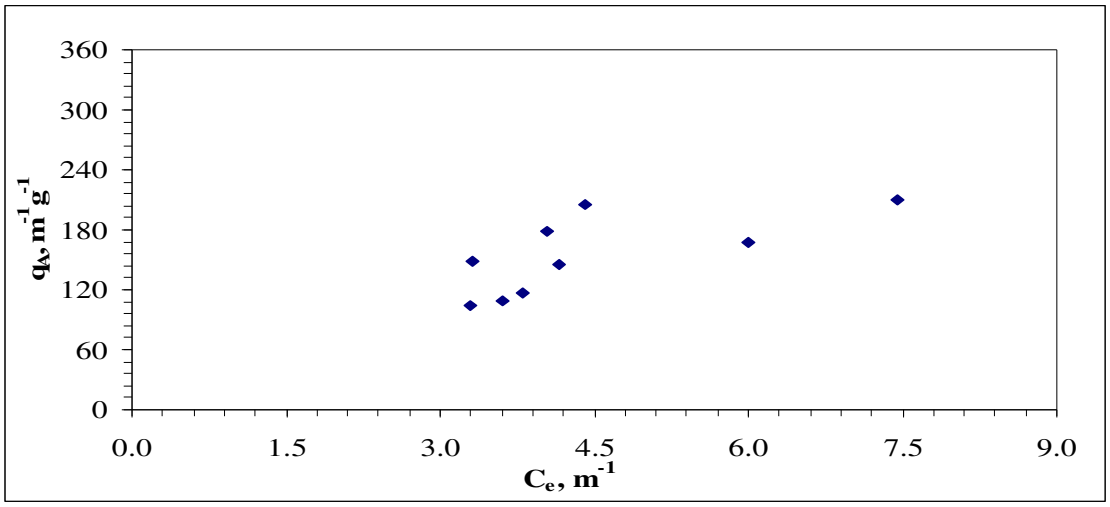

Figure A.7. UV_{365} Adsorption isotherm of 30 kDa humic acid on Degussa P-25

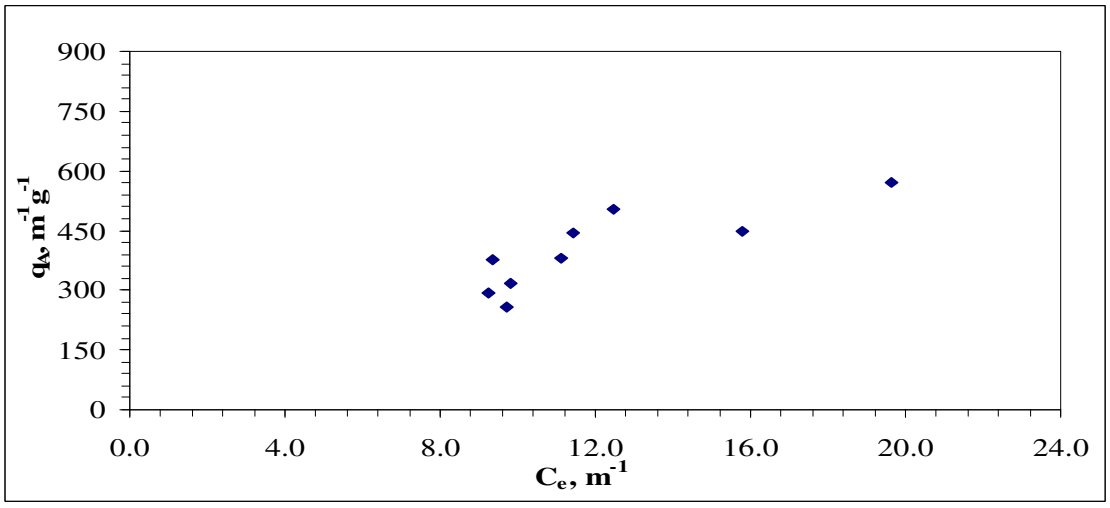

Figure A.8. UV_{280} Adsorption isotherm of 30 kDa humic acid on Degussa P-25

APPENDIX B

Adsorption Profiles of Humic Acid onto Fe Doped TiO_2 Degussa P-25

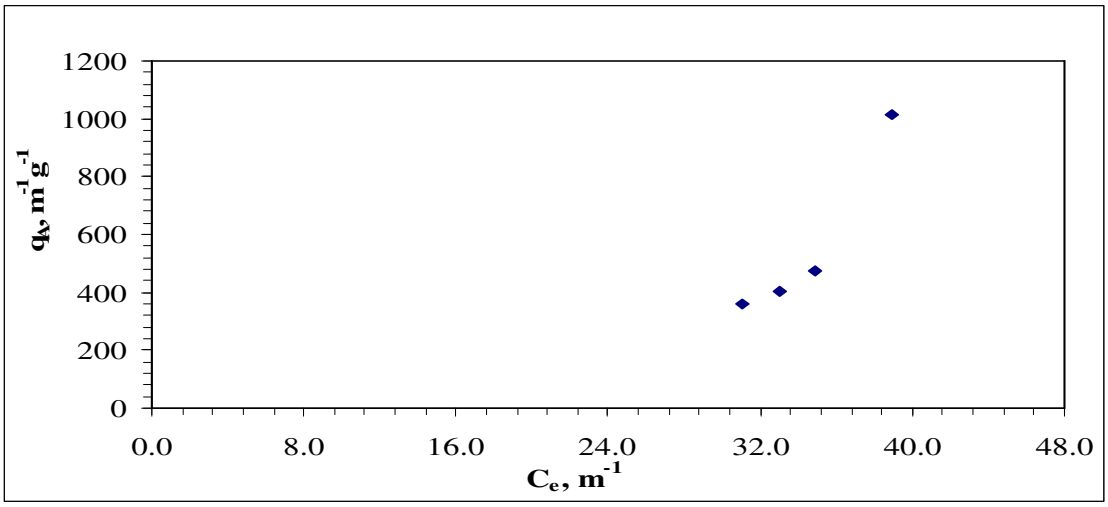

Figure B.1. UV_{365} Adsorption isotherm of humic acid onto Fe doped TiO_2

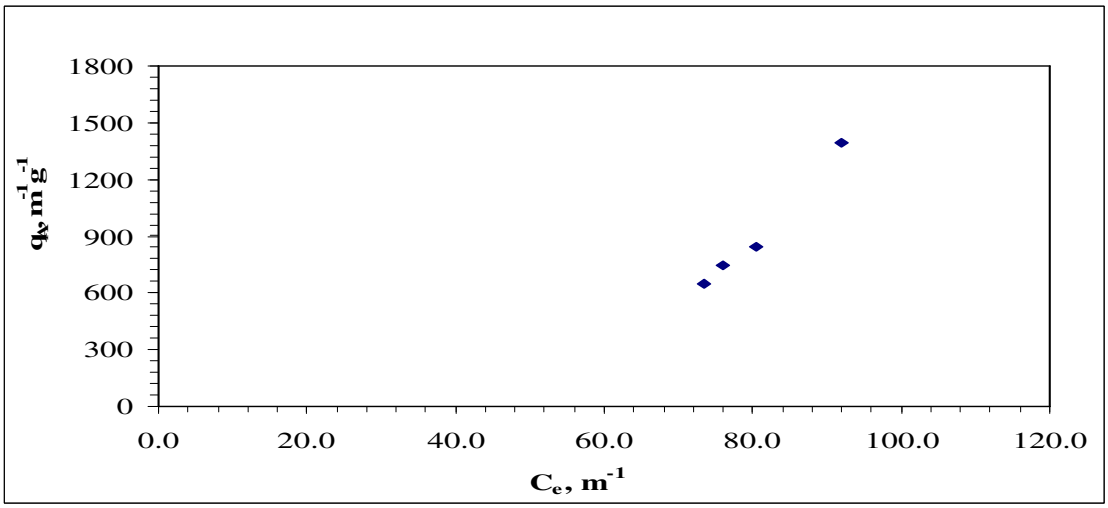

Figure B.2. UV_{280} Adsorption isotherm of humic acid onto Fe doped TiO_2

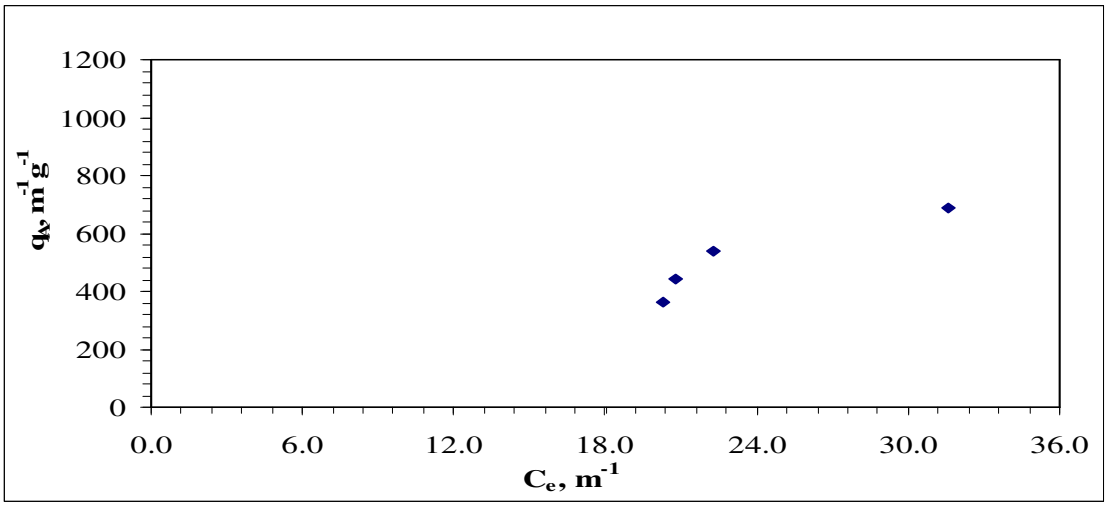

Figure B.3. UV_{365} Adsorption isotherm of 0.45 µm humic acid onto Fe doped TiO_2

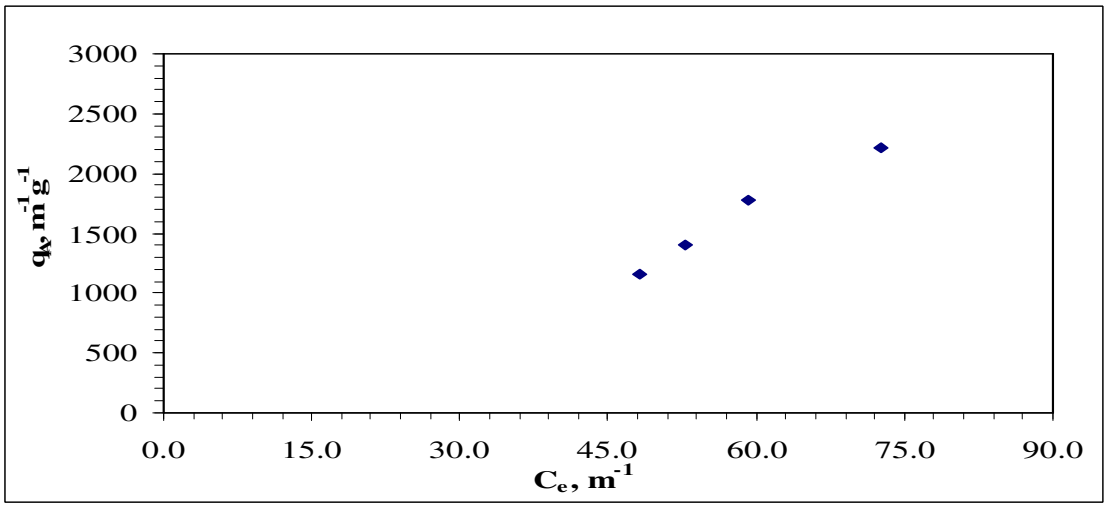

Figure B.4. UV_{280} Adsorption isotherm of 0.45 µm humic acid onto Fe doped TiO_2

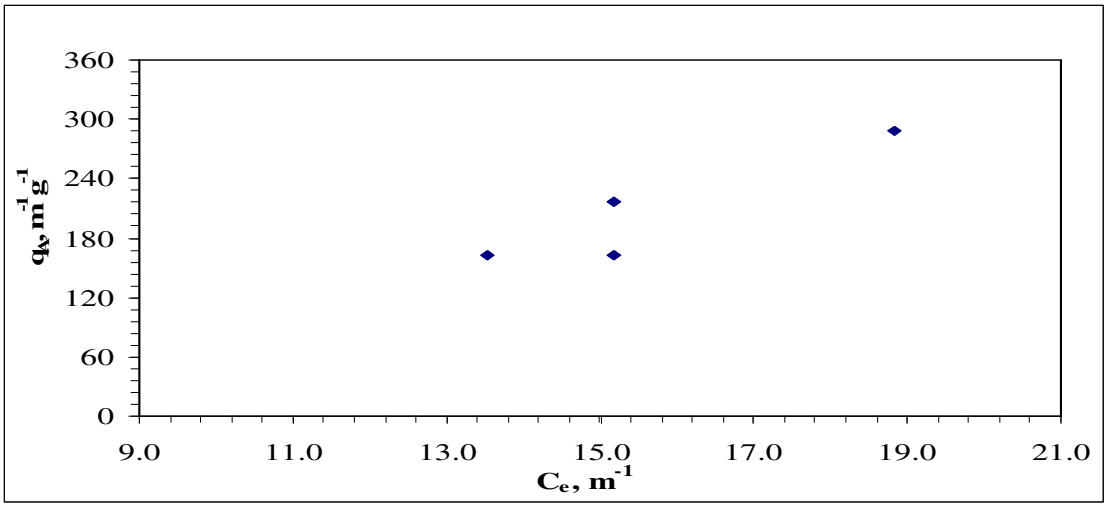

Figure B.5. UV_{365} Adsorption isotherm of 100 kDa humic acid onto Fe doped TiO_2

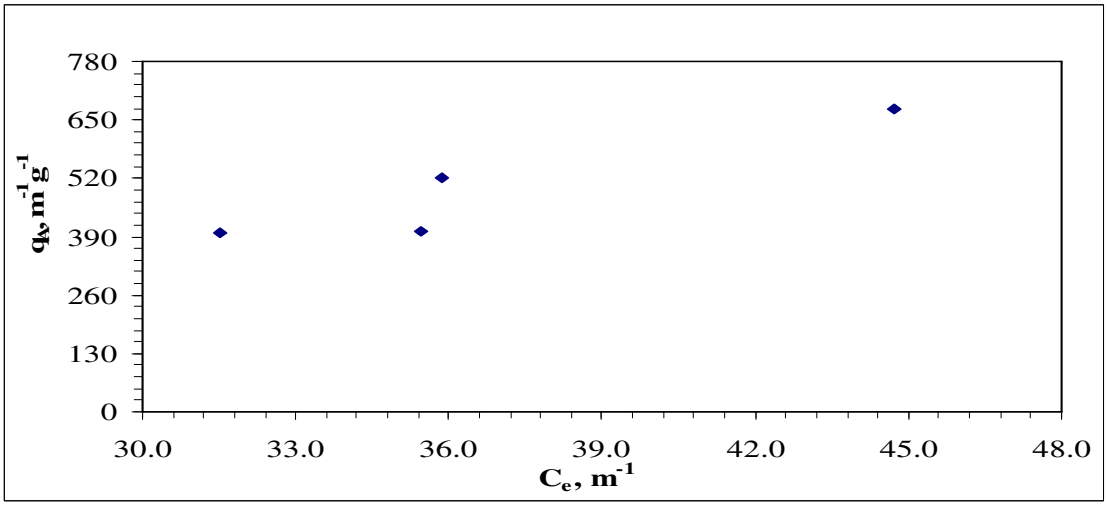

Figure B.6. UV_{280} Adsorption isotherm of 100 kDa humic acid onto Fe doped TiO_2

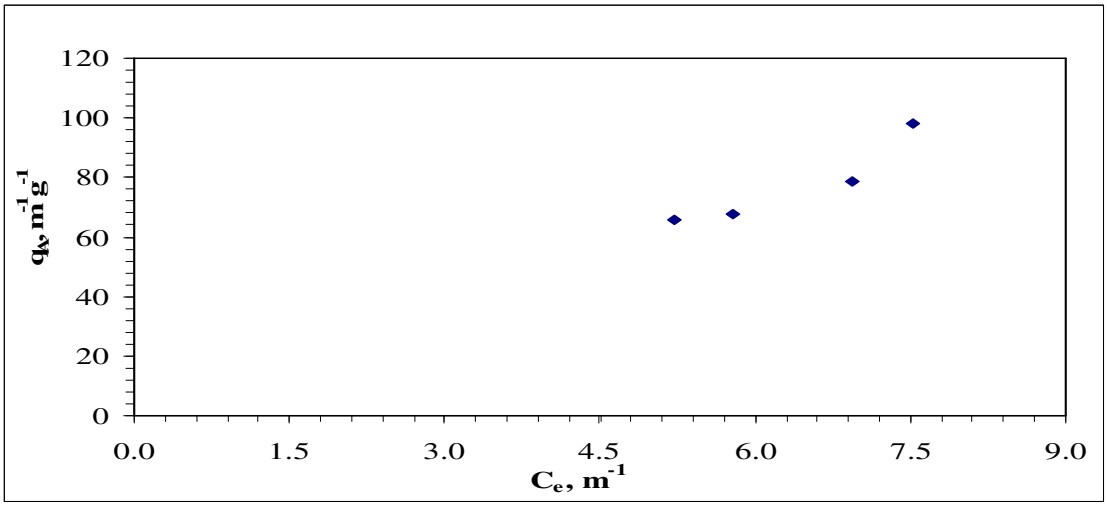

Figure B.7. UV_{365} Adsorption isotherm of 30 kDa humic acid onto Fe doped TiO_2

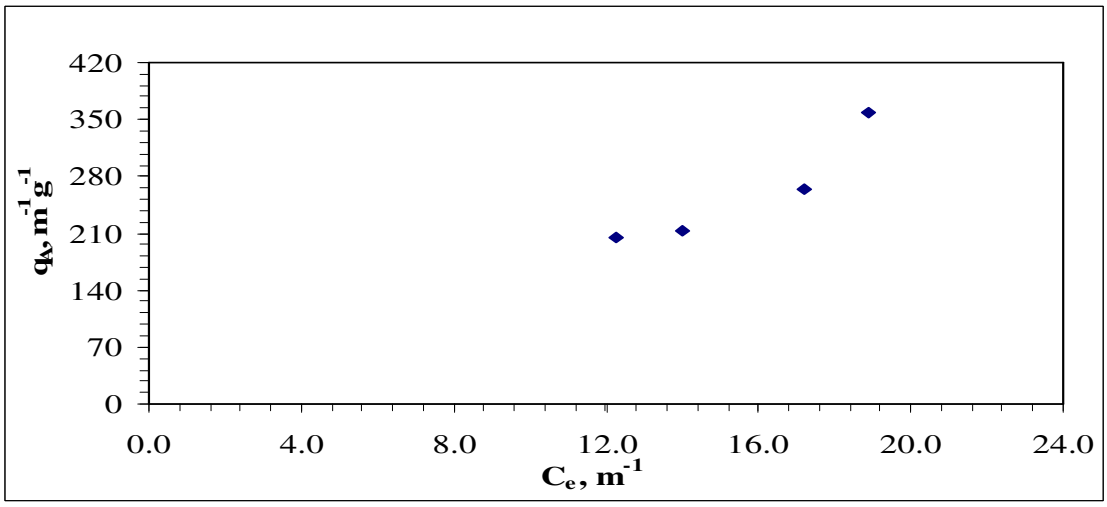

Figure B.8. UV_{280} Adsorption isotherm of 30 kDa humic acid onto Fe doped TiO_2

APPENDIX C

Adsorption Profiles of Humic Acid onto Ascorbic Acid Modified-TiO_2 Degussa P-25

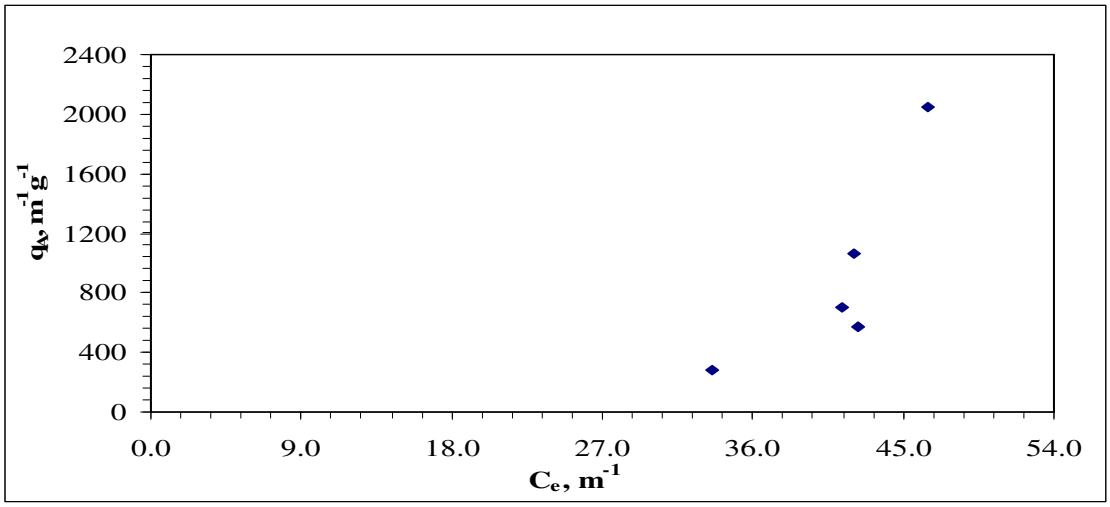

Figure C.1. UV_{365} Adsorption isotherm of humic acid onto ascorbic acid modified TiO_2

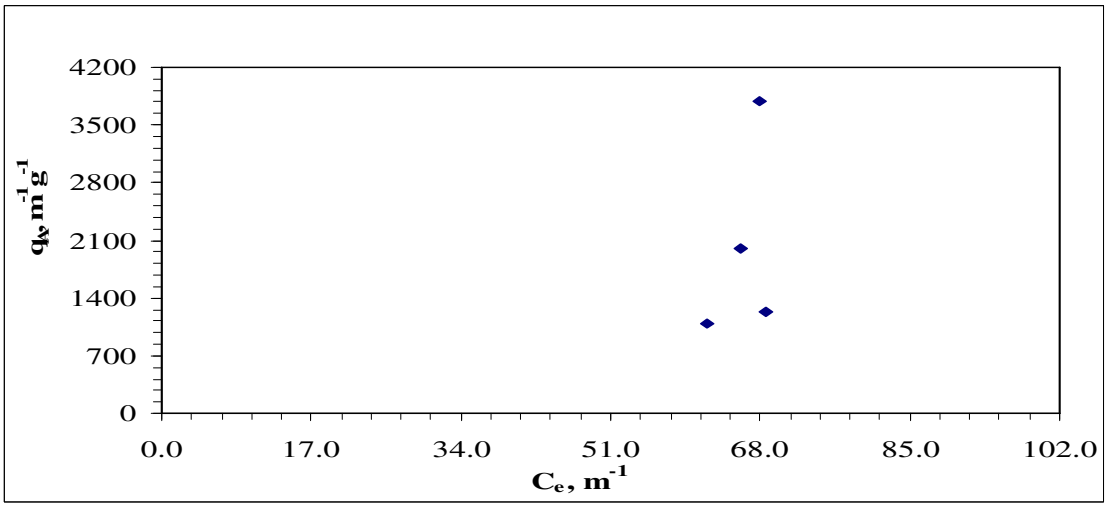

Figure C.2. UV_{280} Adsorption isotherm of humic acid onto ascorbic acid modified TiO_2

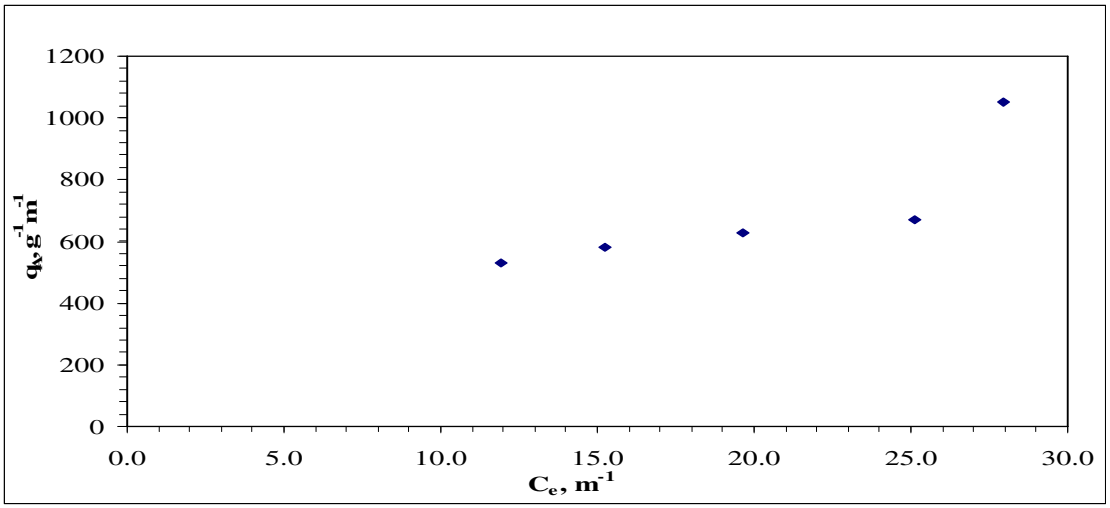

Figure C.3. UV_{365} Adsorption isotherm of 0.45 µm humic acid onto ascorbic acid modified TiO_2

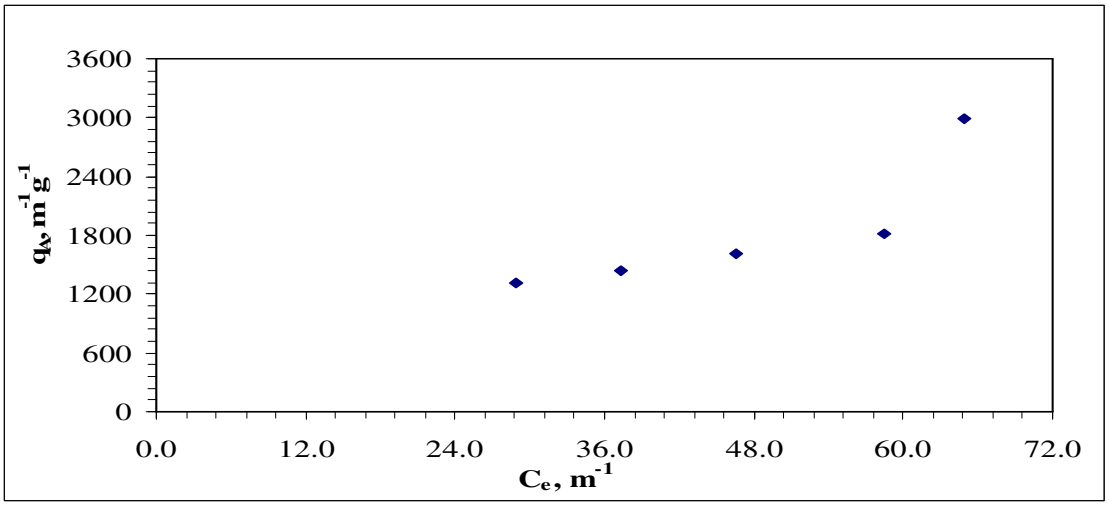

Figure C.4. UV_{280} Adsorption isotherm of 0.45 µm humic acid onto ascorbic acid modified TiO_2

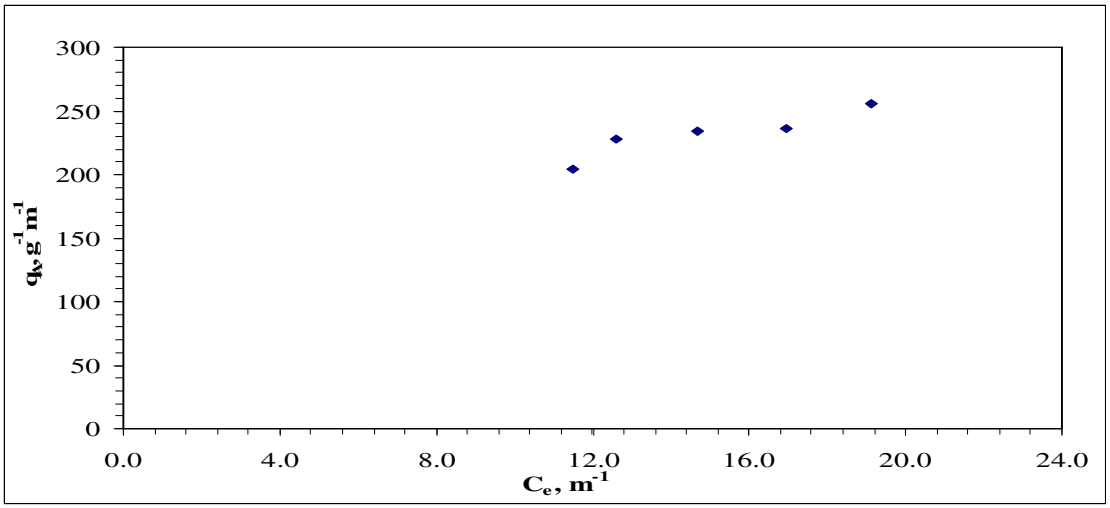

Figure C.5. UV_{365} Adsorption isotherm of 100 kDa humic acid onto ascorbic acid modified TiO_2

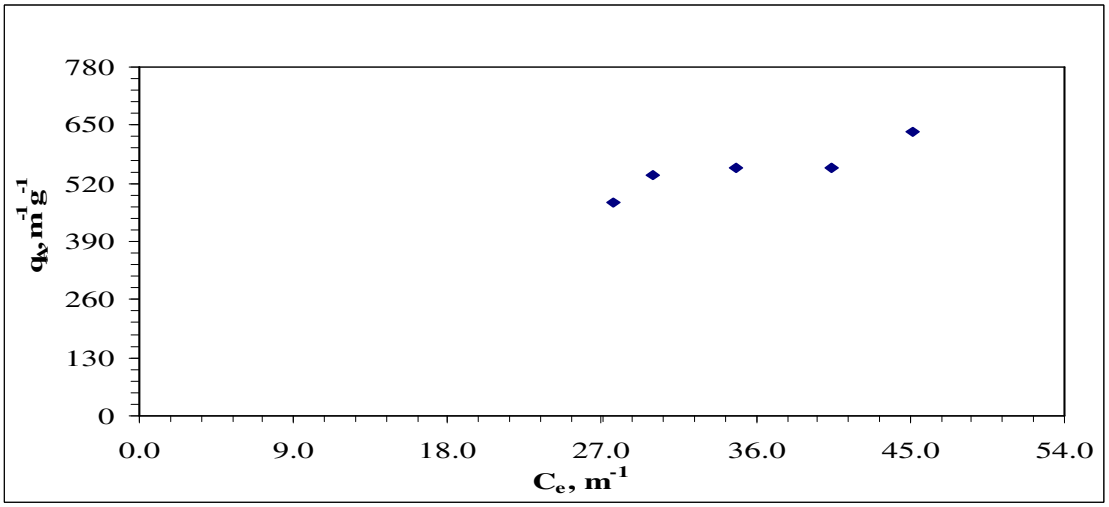

Figure C.6. UV_{280} Adsorption isotherm of 100 kDa humic acid onto ascorbic acid modified TiO_2

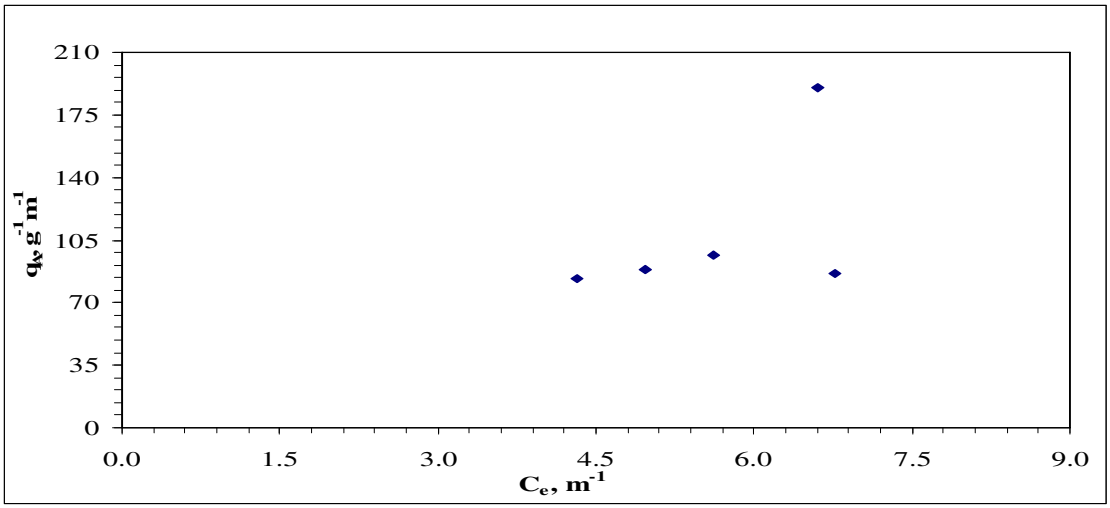

Figure C.7. UV_{365} Adsorption isotherm of 30 kDa humic acid onto ascorbic acid modified TiO_2

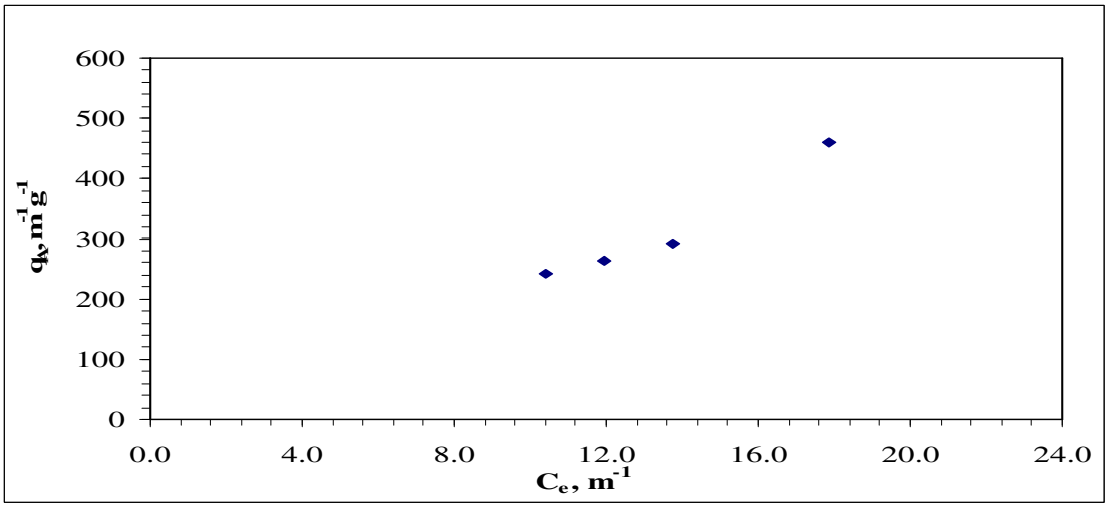

Figure C.8. UV_{280} Adsorption isotherm of 30 kDa humic acid onto ascorbic acid modified TiO_2